Universitat Autònoma de Barcelona

Carbon nanotubes and metal nanoparticles as electrode platform for sensors and biosensors

Andrea Cipri

Doctoral Thesis

Doctoral Studies in Chemistry

Director: Manel del Valle Zafra

Departament de Química

Facultat de Ciències

2015

-

Thesis submitted to aspire for the Doctor Degree

Andrea Cipri

Director's Approval:

Dr. Manel del Valle Zafra Professor of Analytical Chemistry

Bellaterra (Cerdanyola del Vallès), 20 October 2015

-

Funding Acknowledgments

-

The present dissertation has been carried out at the laboratories of the Grup de Sensors i Biosensors of the Departament de Química from Universitat Autònoma de Barcelona, with the support of the Marie Curie Actions fellowship FP7-PEOPLE-2010-ITN-264772 and the financial support of the Ministry of Economy and Innovation (MINECO) Project " Electronic tongue fingerprinting: aplicaciones en el campo alimentario y de seguridad" (MCINN, CTQ2013-41577-P).

Grup de Sensors i Biosensors

Unitat de Química Analítica

Departament de Química Universitat Autónoma de Barcelona

Edifici Cn, 08193, Bellaterra.

-

“To my parents,
for their help and support.”

INDEX

INDEX

ABBREVIATIONS

Abbreviations

AA	Ascorbic Acid
AE	Auxiliar Electrode
ANN	Artificial Neural Network
AOs	Atomic Orbitals
CB	Conductive Band
CDH	Cellobiose dehydrogenase
CNF	Carbon nanofiber
CNTs	Carbon nanotubes
CPE	Carbon Paste Electrode
*Ct*CDHC291Y	Mutant of *Corynascus thermophilus* CDH
CV	Cyclic Voltammetry
CVD	Chemical Vapour Deposition
CYT_{CDH}	Cytochrome domain in CDH
DA	Dopamine
DET	Direct Electron Transfer
DMF	N-N-Dimethylformamide

DOS	Electroni Density Of States
DPV	Differential Pulse Voltammetry
EA	Electron Affinity
EC	European Commission
EDS	Energy Dispersion Spectroscopy
ET	Electronic Tongue
FAD	Flavin Adenin Dinucleotide
GC or GCE	Glassy Carbon electrode
GEC	Graphite – Epoxy Composite electrode
HOMO	Highest Occupied Molecular Orbital
HPLC	High – Performance Liquid Chromatography
I-T	Chronoamperometry technique
LED	Light Emitting Diode
LOD	Limit of Detection
LOQ	Limit of Quantification
LUMO	Lowest Unoccupied Molecular Orbital
MBE	Molecular Beam Epitaxy
MOCVD	Metallorganic CVD
MOMBE	Metallorganic MBE
MOPS	3-(N-morpholino)propanesulfonic acid
MOs	Molecular Orbitals
*Mt*CDH	*Myriococcum thermophilum* CDH
MWCNTs	Multi Wall Carbon Nanotubes
*Nc*CDH	*Neurospora crassa* CDH
Nd:YAG	Laser Neodimium – doped Yttrium Aluminium Garnet ($Nd:Y_3Al_5O_{12}$)
NNI	US National Nanotechnology Initiative
NPs	Nanoparticles
PCA	Principal Component Analysis
PDADMAC	Poly(diallyldimethylammonium)chloride
PSS	Poly Styrene Sulfonate
PVD	Physical Vapour Deposition
RE	Reference Electrode
RSD	Relative Standard Deviation
S/N	Signal to Noise ratio

SAM	Self Assembled Monolayer
SCE	Saturated Calomel Electrode
SEE	Standard Error of Estimate
SEED	Substrate – Enhanced Electroless Deposition
SEM	Scanning Electron Microscopy
SPE	Screen Printed Electrode
SWCNTs	Single Wall Carbon Nanotubes
SWSV	Square Wave Stripping Voltammetry
TEM	Transmission Electron Microscopy
UA	Uric Acid
VB	Valence Band
VLS	Vapour – Liquid – Solid method
WE	Working Electrode

SUMMARY

Summary

This work is mainly focused on the improvement of the properties of sensors and/or biosensors using carbon nanotubes and metal nanoparticles as electrode platform. After having gone through a good amount of literature examples, to reach this goal it has been decided to embed the metal nanoparticles on the carbon nanotubes surface to be able to take advantage of both material properties; for this reason, various synthetic procedures from the literature has been tested, modifying and optimizing them. This first step of the work was aimed to find a facile and quick synthetic protocol to generate a nano-hybrid material and it ended with an effective *one-pot* synthetic protocol that allows having the final desired material without intermediate purification steps. Of course the protocol has to be slightly modified depending on the desired metal nanoparticles. The obtained nano-hybrid materials have been characterised, especially through transmission electron microscopy (TEM) but also some time with scanning electron microscopy (SEM), after every synthesis to verify if the protocol was working.

The next step has been a test of the nano-hybrid material, applying it to the surface of an epoxy graphite electrode (largely used in our lab) or a screen-printed electrode (SPE) for the detection of a biomolecule, Tyrosine. This test showed remarkable results (Article 1) with a clear improvement of the detection ability and sensitivity of the nano-hybrid material against the bare screen-printed

electrode or the modification with only carbon nanotubes (without metal nanoparticles). After this success few different nano-hybrid materials have been prepared with different metal nanoparticles with the objective to try them in an electrode array system commonly used in our lab, the electronic tongue system, used for the resolution of mixtures of analytes.

An electronic tongue system is not just an array of sensors (this would be better explained in the Introduction of this work), but it also needs a step of data processing since the analytes involved in the process supply very similar results; for this, an advanced chemometric treatment is needed, (in our case using Artificial Neural Networks). With the aim of gathering new variants, in this case the use of enzymatic biosensors, part of this work has been carried out at the Lund University (Sweden) in collaboration with the group of Prof. Lo Gorton; in this way, the computer processing part could be applied without having to worry also of the electrode optimization, since in that group they already had optimized biosensors that could be used for our purpose. This collaboration resulted in an interesting outcome (Article 3 – manuscript) where we have been able to build as a proof-of-concept a novel bio-electronic tongue with variation of a specific enzyme (cellobiose dehydrogenase – CDH), a sensing element never used before in this manner.

The last step of this work has been the integration of the synthesised nano-hybrid materials in the sensors for the electronic tongue used in our lab. The targets of the electronic tongue have been the sugars present in sugarcane bagasse used for the production of bio-fuels. The results collected and the goodness of prediction of the electronic tongue system have been satisfactory and they have been recently published (Article 2), showing a proof-of-concept of a working system for sugar mixtures resolution.

RESUMEN

Resumen

Este trabajo se centra principalmente en la mejora de las propiedades de los sensores y/o biosensores utilizando nanotubos de carbono y nanopartículas metálicas como plataformas de electrodo. Después de haber considerado varios ejemplos de la literatura, para alcanzar este objetivo se ha decidido integrar las nanopartículas metálicas en la superficie de los nanotubos de carbono para conseguir las ventajas de las propiedades de los dos materiales; por esta razón se han ensayado diversos procedimientos de síntesis de la literatura, y éstos han sido adaptados y optimizados. Esta primera etapa del trabajo tuvo como objetivo encontrar un protocolo sintético fácil y rápido para generar un material nano-híbrido y ha terminado con un protocolo de síntesis eficaz que calificaríamos "*one-pot*" ya que permite tener el material final deseado sin etapas de purificación intermedias. Por supuesto, el protocolo tiene que modificarse ligeramente dependiendo de las nanopartículas metálicas deseadas. Los materiales nano-híbridos obtenidos se han caracterizado, especialmente a través de microscopía electrónica de transmisión (TEM), pero también a veces con microscopía electrónica de barrido (SEM), después de cada síntesis para verificar si el protocolo estaba funcionando.

El siguiente paso ha sido la prueba del material nano-híbrido, aplicándolo a la superficie de un electrodo de epoxy-grafito (mayormente utilizado en nuestro laboratorio) o un electrodo

serigrafiado (SPE) para la detección de una biomolécula, tirosina. La prueba mostró resultados notables (Artículo 1), con una clara mejora de la capacidad de detección y la sensibilidad del material nano-híbrido contra el electrodo serigrafiado sin modificación o la modificación con sólo los nanotubos de carbono (sin nanopartículas metálicas). Después de este éxito se prepararon otros materiales nano-híbridos con diferentes nanopartículas metálicas; el objetivo era experimentar en un sistema multi electrodos utilizado en nuestro laboratorio, la lengua electrónica, que se utiliza para la resolución de mezclas de analitos.

Un sistema de lengua electrónica no es sólo un conjunto de sensores (que se explicará mejor en la introducción de este trabajo), sino que también necesita una etapa de procesamiento de datos ya que los analitos que participan en el proceso suministran señales similares, por lo que se necesita una interpretación quimiométrica avanzada (en nuestro caso con redes neuronales artificiales). Con el objeto de recoger nuevas variantes, en este caso la utilización de biosensores enzimáticos, parte de este trabajo se ha llevado a cabo en la Universidad de Lund (Suecia), en colaboración con el grupo del Prof. Lo Gorton; de esta manera se ha podido aplicar la parte de procesamiento informático sin tener que preocuparse también de la optimización de los electrodos, ya que en ese grupo ya se habían optimizado los biosensores que podrían ser utilizados para nuestro propósito. Esta colaboración dio lugar a un resultado interesante (Artículo 3 - manuscrito) en los que hemos sido capaces de construir una *proof-of-concept* de una innovadora lengua bio-electrónica usando variaciones de una enzima específica (celobiosa deshidrogenasa - CDH) como elemento de detección que nunca se había construido antes.

El último paso de este trabajo ha sido la integración de los materiales nano-híbridos sintetizados en los sensores para la lengua electrónica utilizada en nuestro laboratorio. Los objetivos de la lengua electrónica han sido los azúcares presentes en bagazo de caña utilizado para la producción de biocombustibles. Los resultados recogidos y la buena predicción del sistema de lengua electrónica han sido excelentes y han sido publicados recientemente (artículo 2), y enseñan una *proof-of-concept* de un sistema de trabajo para la resolución de mezclas de azúcares.

CHAPTER 1 – INTRODUCTION

1. Introduction

The aim of this PhD work was to test a new nanomaterial to be used as platform or sensing element in electrochemical sensors, capable of providing customizable response properties as to be the base of electronic tongue sensor system. To achieve this goal was necessary to select a nanomaterial and find an easy and fast way to synthesise it. After a literature search the choice felt on two promising nanomaterials, carbon nanotubes (CNTs) and metal nanoparticles (NPs), so the challenge became to join them to take advantage of the properties from both nanomaterials and test if they were exploitable as sensing element in electrochemical sensors, for example in some application already developed in our lab with different materials.

Why nanomaterials? The major excitement about nanomaterials and therefore Nanoscience and Nanotechnology, come from the potential of these materials to lead to an incredible variety of applications (e.g. solar energy conversion, biomedical applications, nanoelectronics, smart catalysts, etc.). The main feature of nanomaterials is that their physical and chemical properties unique, and in some case size dependent (nanoparticles), allowing so the possibility not only to engineer their chemical composition, but also tune their size and shape of the nanostructure [1-3]. But what are nanomaterials and which is the definition?

The answer to this question has always been not clear, only recently has been reached an agreement on the definition due to health and safety reasons and marketing purpose. There are two

slightly different definitions, one a bit vague and the other probably too fussy and elaborated. The first one has been proposed in 2004 from the US National Nanotechnology Initiative (NNI) *"Nanomaterials: materials with dimensions of roughly 1-100 nm, where unique phenomena enable novel applications"* [4] and the second comes from the European Commission (EC) in 2011 *"Nanomaterial means a natural, incidental or manufactured material containing particles, in an unbound state or as an aggregate or as an agglomerate and where, for 50% or more of the particles in the number size distribution, one or more external dimensions is in the size range 1-100 nm; and/or has a specific surface area by volume greater than 60 m^2 cm^{-3}, excluding materials consisting of particles with a size smaller than 1 nm"* [5]. In any case both definitions definitely agree on one rule, *"Size does matter, but only if it changes an intrinsic material property"*, in other words nanoscale size is a necessary but not sufficient condition to fully define a nanomaterial. Therefore the definition of nanomaterials tends to include a wide variety of compounds. There is a concept that can help understanding and classifying nanomaterials, the concept of dimensionality. The compounds can be organized in *three-dimensional* (3-D), which are the classic bulk compounds with all three dimensions above 100 nm, then *two-dimensional* (2-D), where only the thickness dimension is below 100 nm and the other two are above (thin films, graphene), *one-dimensional* (1-D), with only one dimension bigger then 100 nm and the other two below (nanowires, nanotubes), and in the end the *zero-dimensional* (0-D), which are those materials with all three dimensions below 100 nm, such as quantum dots, nanopores and nanoparticles (Figure 1). In our case, we will combine as hybrid new material, 1-D carbon nanotubes with 0-D metal nanoparticles, as descibed below.

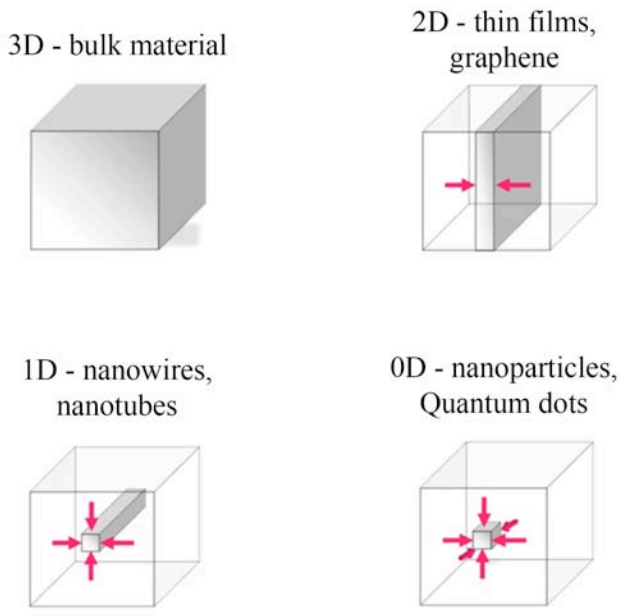

Figure 1- Schematic representation of the dimensionality concept; from bulk material to nanomaterial.

1.1 Carbon Nanotubes

1.1.1 A general view

Since their discovery in 1991 by Iijima [6] carbon nanotubes (CNTs), with their outstanding mechanical and extraordinary electronic properties, have gathered much attention every year. Although at the beginning research was focused on growth and characterization, their interesting properties have led to an increasing number of investigations focused on the application and development of the material. Their broad range of applications which can go from nanoelectronics to microscopy including composites, nanoelectro mechanical systems, chemical sensors, biosensors and many more [7-9]; still there are rather few products on the market, with consumer demand, made with carbon nanotubes, but some are there even if for now with mainly professional demand. This increased the motivation of the scientific community to move beyond basic properties and explore the real issues associated with CNT-based applications, to convert a material into a device, a device into a system, and so on.

Carbon nanotubes show one of the most unsophisticated chemical compositions and atomic bonding configurations; with this in mind it is important to underline the main aspect of the carbon hybridization when looking at the properties of the resulting materials. Considering simple carbon structures we have on one hand diamond, that has a sp^3 hybridization that provide a rigid and almost isotropic structure, on the other hand graphite, that has a sp^2 hybridization that shows planar bonds, three-fold coordinated in the planes with weak bonding between planes and anisotropic physical properties [7, 10]. Carbon nanotubes have sp^2 carbon units as graphite and show an hexagonal honeycomb lattices and a seamless structure, they are hollow and can present between few and several tens of nanometres in diameter and several to many microns in length [11, 12]

1.1.2 Structure and properties

As mentioned in the previous Section CNTs are characterized from an sp^2 hybridization, their *tubular* structure give them a slightly different hybridization compared to the graphene, where the sp^2 orbitals are oriented all on the same plane, the orbitals on the carbon atoms of CNTs are a bit distorted due to the curvature of the carbon sheet to form the nanotube generating a different σ - π

hybridization. Furthermore CNTs are not open but closed structures with two caps at both ends of the tube. It is possible to define two different domains with different properties, the tube and the caps [13]. The caps can be considered as half of fullerene-like molecule and define the diameter of the nanotube. These formations are allowed by topological defects in the carbon sheet, which in this case are pentagons. Most of the times CNTs are used after opening the caps and this can be possible thanks to different purification or oxidative treatments.

CNTs can be divided in two big groups, multi-wall (MWCNTs) and single-wall (SWCNTs) carbon nanotubes [14, 15]. As shown in Figure 2, MWCNTs can be represented as different graphenes sheet forming a roll and organized in multiple and concentric layers defining a hole with a typical diameter from 2 to 25 nm and a layer distance around 0.34 nm [6, 10] and arrive to an outer diameter up to 100 nm. SWCNTs, instead, are made from a single graphene sheet rolled seamlessly, generating a tube with diameter around 0.4-2 nm.

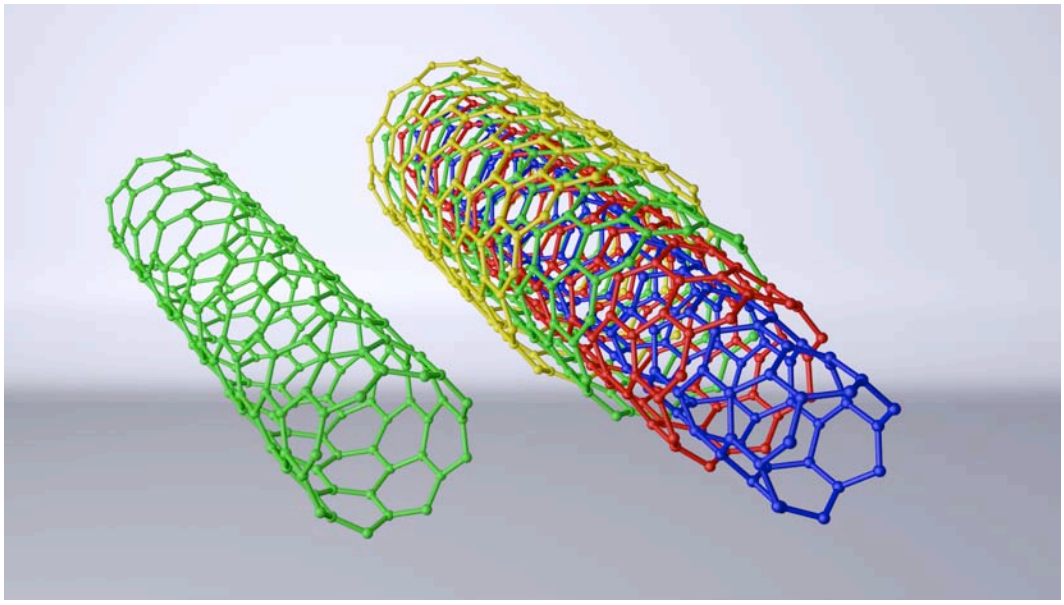

Figure 2 – Schematic representation of SWCNT (left) and MWCNT (right).

To explain the different structures of CNTs it is common to use as example a SWCNT due to its single graphene sheet formation, and to better understand these structures of the nanotubes is important the definition of chiral vector C_h and chiral angle θ. The chiral vector is a vector that gives us the rolling orientation of the graphene sheet and it is given by the following formula:

$$C_h = n\bar{a}_1 + m\bar{a}_2$$

Where a_1 and a_2 are the unit vectors in the two-dimensional hexagonal lattice, and n and m are the integers (Figure 3). The diameter of the nanotube is given from the length of the chiral vector divided by 1/4. The chiral angle θ is the angle between the chiral vector C_h and a_1.

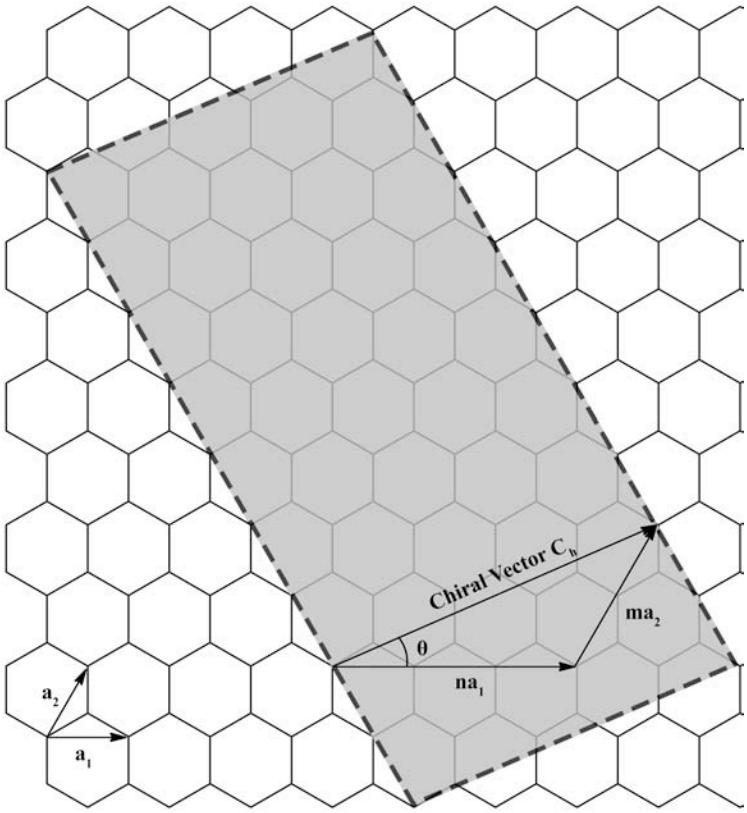

Figure 3 – Schematic diagram of a hexagonal sheet of graphite and the parameters that define the structure of a nanotube when the sheet is rolled (chiral vector, chiral angle, basis vectors a_1 and a_2)

The chiral vector allows the understanding of another structure subdivision of CNTs. The ends of the chiral vector join together when the graphene sheet is rolled up to create a cylinder. Considering this, it is possible to form tubes with different diameters and different helical arrangements of hexagons when the values of *n* and *m* change, therefore generating different nanotube structures [16]. There are three ways on how the graphene sheet can be rolled up and these ways generate three types of carbon nanotubes commonly named *Armchair*, *Zig-zag* and *Chiral*.

Armchair nanotubes are formed when $n = m$ and the chiral angle is 30°. *Zig-zag* nanotubes are formed when *n* or *m* is zero and the chiral angle is 0°. All the structures in between are known as *Chiral* nanotubes and show chiral angles between 0° and 30° [16]. A representation of all the three structures is shown in Figure 4.

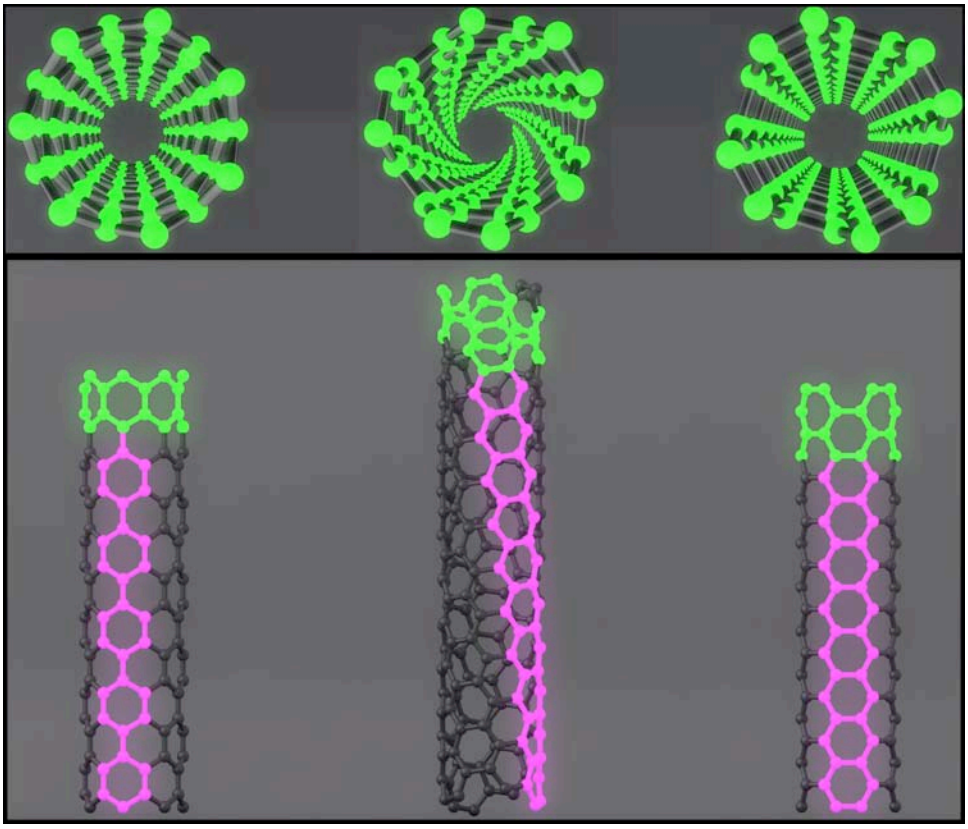

Figure 4 – Schematic representation of the atomic structure of Zigzag (left), Chiral (centre) and Armchair (right) nanotubes; top view with only atoms highlighted and side view.

So far to explain the principal structures of the CNTs was used the SWCNT, but as mentioned before exist another form of nanotubes that can generate other structure variations, the MWCNTs.

MWCNTs being like several SWCNTs one inside the other can be subjected to variations on the walls all along the longitude of the tube, these variations can generate a change in the morphology of the nanotube.

There are three kinds of MWCNTs, *hollow*, *bamboo-like* and *Herringbone* (Figure 5). The *hollow* nanotubes are the classical ones, a series of concentric SWCNTs with an even hole all along the length. The *bamboo-like* instead present a series of cross planes due to the bending of some of the walls forming caps, generating in this way periodic hollow sections like in a bamboo stick. The last form is the *Herringbone* shape, which shows the walls of the nanotube forming angles along the axis narrowing the central cavity, and so differing for this reason from the *bamboo-like* not having caps formation along the tube. The main morphology difference between the *hollow* MWCNTs and the *bamboo-like* and *Herringbone* MWCNTs is the high density of terminating edge planes contained in the last two.

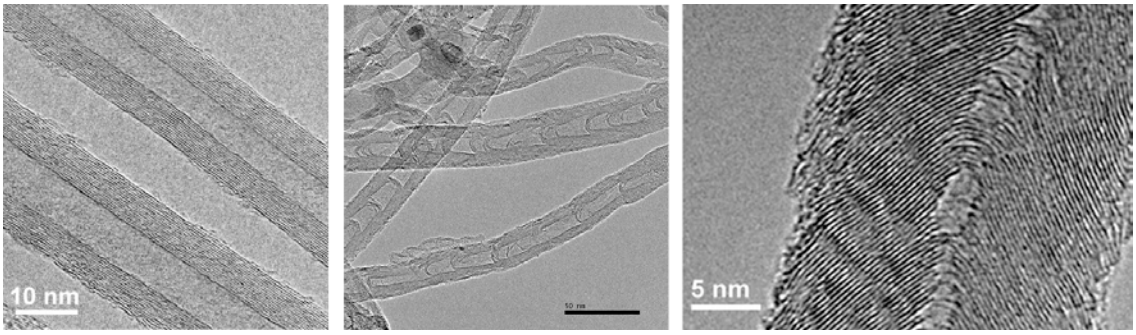

Figure 5 – Example of different carbon nanotube morphologies. TEM images of (from left to right) *hollow*, *bamboo-like* and *Herringbone* MWCNTs.

These structure characteristics combined with their morphology and size give to the nanotubes exceptional mechanical properties such as:

- High stability and low density;
- Strength and stiffness, showing an impressive Young's modulus[1] up to 1.2 TPa for the best MWCNT [17-19], higher than other known materials;
- Elastic deformability higher than hard materials, being able to bear up to a 15% of tensile strain before fail with a unique behaviour of elastic buckling to release the stress (Figure 6) [20, 21];
- Interesting surface properties (selectivity, surface chemistry);

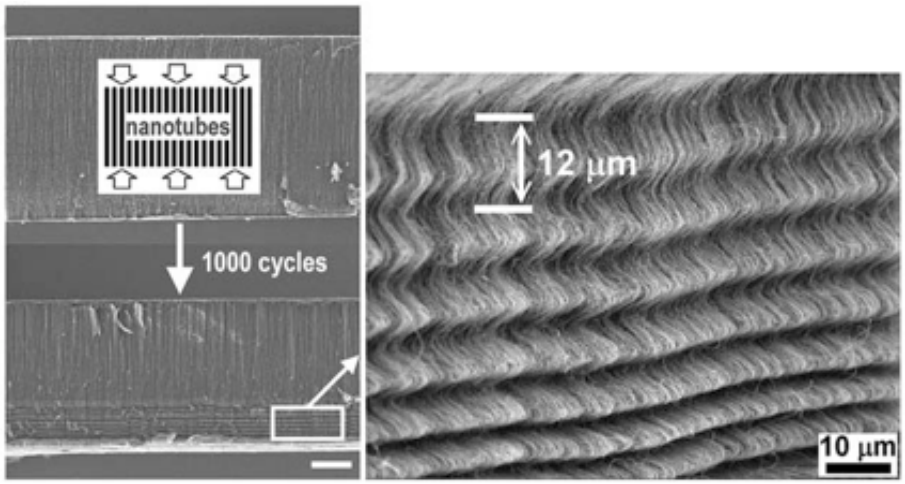

Figure 6 – A SEM micrograph showing a buckled array of aligned MWCNTs after 1000 cycles of compression at 85% strain. From reference [21].

The exceptionality of these properties is related to the strength of the carbon bond, displaying in CNTs mechanical characteristic superior to other known materials. In fact they are extremely

[1] Young's modulus is a measure of the fitness of an elastic material and a quantity used to characterise materials.

flexible; CNTs can be twisted, bent and flattened for example in small circles without breaking, or compressed without fracturing [7, 11].

In addition to these mechanical properties, the helicity and diameter of the nanotubes introduces interesting changes in the electronic density of states (DOS)[2]. These changes give to the nanotubes unique electronic properties, such as Quantum confinement[3], allowing them to behave as metal or semiconducting material. As mentioned the DOS change between the two behaviours and it is possible to see it in Figure 7, where can be noted the presence of a small band gap in the semiconductor DOS graph and the absence of it in the metal DOS graph. Has been proved that this metallic or semiconducting behaviour depend on the *n* and *m* integers which define the CNT structure [22] and allow to predict it, so when a nanotube has a value of $n - m$ equal to zero or to a multiple of 3 it has metal characteristics, the remains values define semiconducting nanotubes. Since these behaviours are also related to the diameter with the formula

$$E_g = 2d_{cc}\gamma/D$$

Where $2d_{cc}$ is the band gap and D the diameter, therefore the wider the diameter the more metallic the behaviour [23]

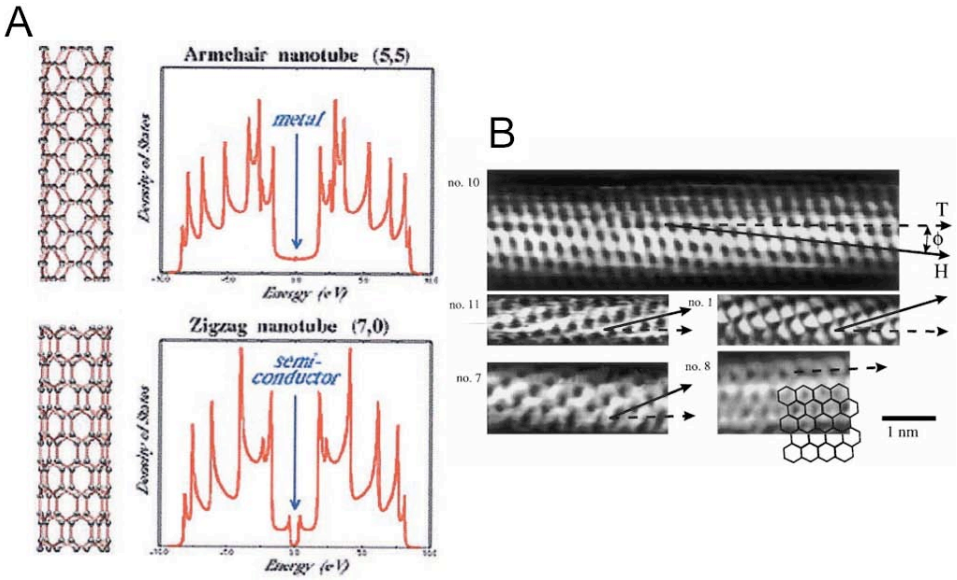

Figure 7 – A) Electronic properties of two different CNTs. The Armchair (5,5) nanotube (upper) exhibits a metallic behaviour (finite value of charge carriers in the DOS at the Fermi energy). In the Zigzag (7,0) nanotube (lower) there is a small gap and so behave as a semiconductor (no charge carriers in the DOS at the Fermi energy). From reference [22]; B) Atomically resolved STM images of individual single-walled CNTs. The lattice on the surface of the cylinders allows a clear identification of the tube chirality. The dashed arrows represent the tube axis **T**, the solid arrows indicate the direction of the nearest-neighbour hexagon rows **H** and ϕ is the chiral angle. From reference [23]

[2] The density of states (DOS) of a system describes the number of electron states per volume unit and per energy unit that are available to be occupied

[3] Quantum confinement can be observed when the diameter of a material has the same size of the wavelength of the electron wave function; therefore the electronic and optical properties are substantially deviated from the ones of the bulk material.

These electronic properties give to the carbon nanotubes a wide range of interesting applications for electronic devices, such as nanotube-based field emitters, optoelectronic memories [24], nanoscale light-emitting diodes (LEDs) [25, 26], nanoprobes in biological and chemical investigation [7].

Both electrical and mechanical properties are affected from topological defects on the nanotubes surface, as for example pentagons or heptagons instead of hexagons, making them for example mechanically weaker than nanotubes without defects. In this sense the perturbation to the electronic structure in closed nanotubes shows a more metallic behaviour on the caps than on the cylinders. So on one hand we have these topological defects that can affect some property weakening it, but on the other hand these defects enhances the chemical reactivity at the ends and defects giving the possibility to open the nanotubes, fill them with other molecules/materials and functionalise the ends [27-29]. This characteristic, mainly due to the σ - π hybridization, makes CNTs very attractive in chemical and biological applications because of their high sensitivity to environmental and chemical interactions. The most common chemical groups that can be found at the ends or defects along the carbon nanotubes are hydroxyl-, carboxyl- or carbonyl-functionalization, like the groups shown in Figure 8.

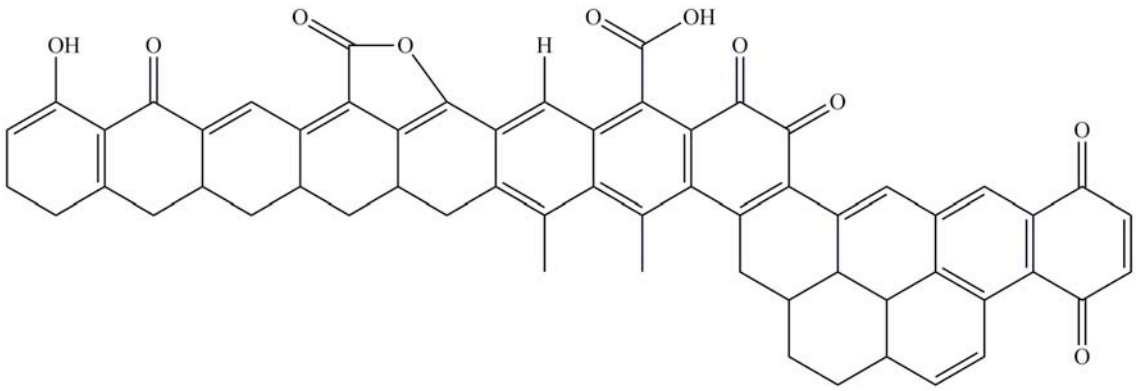

Figure 8 – Chemical groups at nanotube ends

So the chemical properties raised a good interest among the scientific community, interest that include different kind of reaction, such as wetting, opening, filling, absorption, doping, charge transfer, etc. and also the chemical and biological applications like separation, purification, detection and sensing systems. As said the chemical properties provide, for example, the easy opening of the nanotubes since their ends presents defect and are more reactive than the sidewalls, and this step is useful for all the further chemical and biological applications. There are many ways to open the CNTs for instance plasma etching, vapour phase oxidation or with acid solutions such as HNO_3 [28, 30]. Other important features concerning the chemical properties are the charge

transfer and the chemical doping, where especially the charge transfer can be improvable with chemical or electrochemical pre-treatments, which can occur at the same time of the carbon nanotubes purification. Usually CNTs can be doped with intercalation of B and N to make them p- or n-type material even if it is possible to have the same results with a non-covalent approach as the molecular absorption, but on the other hand these intercalations, with i.e. alkali metals or halogens, are used for enhance the metallic conductivity or for charge- energy-storage applications. There are experimental observations that these intercalating agents mainly enter intertube spaces or defects enhancing the electrochemical capability of the nanotubes for charge transfer and storage. Indeed, nanotube has shown an interesting enhancement on the electrochemical capability when used as sensor electrode material [31-34]. The red-ox reaction that occur at the electrode develop an electron flow that generate and store energy. Staying in the electrochemical properties of the nanotubes, several works have observed their electroactivity due to the reactive groups present on the CNTs surface [14, 30, 35, 36]. The small dimensions allow the CNTs to generate a high current density on the surface of the electrode, and ab-initio calculations have demonstrated that this enhancement on the electron transfer is due to the curvature of the tubes generating changes in the energy bands close to the Fermi level. Therefore the presence of pentagonal defects produce regions with a higher charge density compared to the hexagonal regions, demonstrating a connection between the electroactivity and the presence of defects [35]. CNTs showed also an interesting electrocatalytic activity, with lower peak potential separations and higher peak currents in voltammetric analysis of several molecules, linked to their dimensions, topological defects on the surface and electronic structure [7, 15, 35, 36]

1.1.3 Synthesis of carbon nanotubes

The synthesis technique has a key role to obtain carbon nanotubes highly pure and without morphological defects. In the process it is also important to control the diameter and other features like for example the number of walls in MWCNTs. For this reason the synthesis of carbon nanotubes received a significant attention especially to find a protocol able to move from lab-scale to large-scale production keeping the same yields and purity of carbon nanotubes. Commonly the synthesis is based on three different methods, which are the basic procedures used to produce CNTs, both SWCNTs and MWCNTs. The methods are: Chemical Vapour Deposition (CVD), also known as catalytic decomposition of hydrocarbons, Electric Arc Discharge and Laser Ablation or vaporization [7, 37-39].

Chemical Vapour Deposition (CVD)

This chemical process involve the pyrolysis of an high carbon content gas at high temperature and in presence of a catalyst [38]. The most followed protocol for CVD is the supported growth process and it use a catalyst deposited on a substrate or support medium that is inside a flow apparatus (a tube at atmospheric pressure in a furnace with a controlled temperature where is injected a gas with an high carbon content) and exposed to high temperatures (500-1100 °C) for a given time. There is also another process called floating-catalyst growth, where the catalyst and the carbon source are injected in the system at the same time, as aerosol or gas phase. Therefore, the carbon source decomposition and the following reaction can occur following a self-deposition onto a surface in the reactor or suspended in the gas flow. Usually the substrates are metallic Si, SiO_2 based materials or silicon wafers, and the catalysts are Fe, Ni or Co, which have resulted to be successful. With these methods is possible to tune the diameter of the nanotubes because it is proportional to the catalyst particle size, therefore the tuning can be made controlling the catalyst deposition. The most used carbon source is acetylene, but has been also employed methane, ethylene and propylene. Between the two processes the floating-catalyst one is used to grow SWCNTs and the other to grow mainly MWCNTs.

Electric Arc Discharge

This method was the first used to obtain carbon nanotubes and it consists of an electric arc between two graphite electrodes separated by ≈1 mm and under inert helium atmosphere. The potential applied between the two electrodes is 10-35 V to generate a current of 60-100 A and the crucial factor is to get a stable discharge plasma. The reaction that occur is simple, high temperature are achieved and the anode material start sublimating and ends depositing on the cathode surface and surrounding walls. The inner part of the deposits is mainly composed by MWCNTs and graphite nanoparticles, instead the outer part is mainly made of SWCNTs and fused graphite powder [40]. To favour the generation of SWCNTs has been reported the use of electrodes with single or bi-metal mixtures of Co, Y, Fe and Ni, and the most efficient have been the bi-metal Co/Y and Ni/Y [41, 42]. The typical production rates for this method are around 20-100 mg/min, but there are different parameters that can affect the nanotubes production, such as the pressure and flow rate, the electrode materials and dimensions, the electric field strength, and the gas type beside variables as instrument size and geometry or thermal gradient [38].

Laser Ablation

The Laser Ablation method works with a quartz tube with a solid graphite target inside and the tube is positioned inside a thermostated oven. The graphite target is vaporized with a pulsed Nd:YAG laser obtaining a formation of a carbon-based soot that contains the nanotubes. To reach mainly the production of SWCNTs is necessary to dope the graphite target with transition metal catalysts. This method was later modified adding a second laser Nd:YAG slightly delayed from the first [43]. With this method it has been produced SWCNTs at a production rate of 1.5 g/h using a 1.7 kW subpicosecond free electron laser (FEL) [44].

1.1.4 Carbon nanotubes as sensor material

Among all the unique properties of CNTs, if we bear in mind the electrical capabilities and charge transfer characteristic, it is clear how they can be useful and suitable for sensors. For this reason CNTs have generated an enormous attention for the preparation of electrochemical sensors [45]. As mentioned in Section 1.1.2 a pre-treatment of the CNTs is usually necessary to have an improvement on their electron transfer properties and to enhance their chemical reactivity that can allow further functionalization. The typical protocols used as pre-treatment are based on the oxidation of the nanotubes, and these protocols can go from light procedures till drastic treatments. So depending on the strength of the treatment it is possible to not only break the CNTs but also to shorten them. In any case the pre-treatment provide ends and sidewalls with a high concentration of different oxygenated groups, mainly carboxyl groups. The protocols used can be divided in two main groups, chemical and electrochemical, and in three steps, oxidation, washing and drying, to make easier the understanding of the techniques involved.

One of the chemical pre-treatments firstly used is the oxidation in air, and this is due to its role as purification methods for CNTs. Therefore, with the oxidation in air is possible to join the purification and pre-treatment/activation in a single process. Have been proposed different oxidation methods in air that shift, for example, from 400 °C under air flow for 1 hour to 600 °C under air flow for 5 minutes [46, 47], only to cite two among the big numbers of air oxidation. Another way frequently used to obtain the activated nanotubes after purification is to use acidic solutions. Typical solutions are sulphuric acid, nitric acid and hydrochloric acid, either used

individually, in concentrated or diluted solutions, or in mixtures of them, concentrated or diluted in different ratios, at room temperatures or mildly heating or under reflux and with or without sonication, all these combinations kept for different times [48-50]. Figure 9 shows an example of acidic treatment.

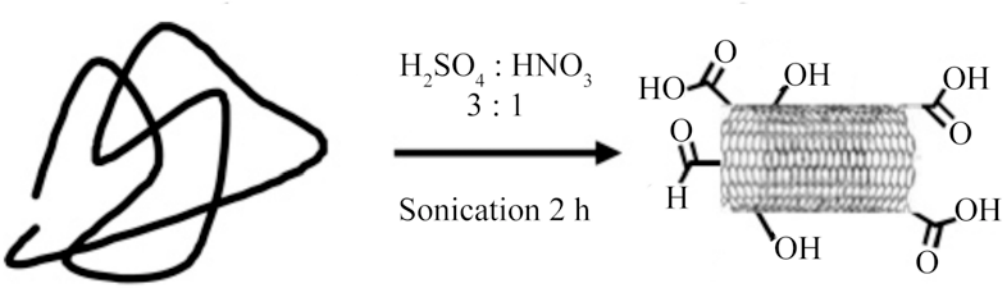

Figure 9 – Example of nanotubes activation with acidic treatment.

Generally after the oxidation the next step is to wash the nanotubes with ultrapure water until a neutral or close to neutral pH value and then the drying step. This last step can be carried on at room temperature leaving the nanotubes exposed to the air, or under an IR lamp, or under vacuum at a given temperature. More drastic or combined pre-treatment protocols has been proposed, such as a protocol with a mixture of nitric (65%) and sulphuric (98%) acid with a 3:1 ratio, for 8 h at 40 °C, washed with ultrapure water and dried at 100 °C overnight [46], which provide not only the functionalization of the ends of the nanotubes but also their shortening in fragments of different length. A combined air-acidic pre-treatment was proposed by Palleschi et al. [47], after the air flow oxidation an additional step in a 6.0 M HCl solution for 4 h with ultrasonic agitation, and then washing and drying step.

The effect of the chemical pre-treatment has been evaluated from Hu et al. [51]; in their work they reported that there is an increase in resistivity when nanotubes were pre-treated with acids or mixture of acids for longer times.

The electrochemical pre-treatments are also often used and various protocols have been proposed. These kinds of pre-treatments are generally used after immobilizing the nanotubes on the electrode surface and then applying a potential, which usually depend on the investigated system. For instance, only to cite some protocol, it is possible to go from 18 cycles between -1.00 V and 1.50 V at 1.0 V/s in 50 mM phosphate buffer (pH 7.40) [52] to 75 cycles with the same voltammetric conditions [53], respectively used to enhance the detection of dopamine and amitrole. Electrochemical pre-treatments have been used also in combination with chemical pre-treatments,

hence applying firstly the chemical oxidation and then the electrochemical step using a wide range of potentials depending on the target molecule. Usually, for the electrochemical pre-treatment, the solution where the oxidation of the nanotubes is carried out is the buffer also used for the analysis, or sometimes a sodium hydroxide/sulphate solution at different concentrations.

The preparation of the CNTs-modified electrodes is another important step in the use of nanotubes as electrode material for sensors. Considering the low solubility of nanotubes in most usual solvents, different strategies have been proposed. It is possible to have modifications that go from casting the electrode surface with a solution containing the CNTs to directly include in a composite material that goes inside the electrode cavity. The immobilization of the nanotubes on the electrode surface can be displayed in a brief overview as follow.

As described before, one of the strategies used to immobilize CNTs on the electrode surface is the dispersion in a solution, which can be of a variety of origin, and the making of the electrode, normally a gold electrode or a glassy carbon electrode (GCE), is usually based on casting it on its surface with a drop of the given dispersion and then drying it at room temperature or under controlled temperature. For instance, acidic solutions are often used to disperse CNTs, and one of the infinite protocols proposed provide the preparation of a MWCNT-GCE by well polishing first the GCE and then casting it with 20 μL of a concentrated nitric acid solution with a content of 2 mg/mL MWCNTs and drying at room temperature for 30 min [54]. Only to cite one more protocol, and show how different they can be even if always in an acidic solution, the dispersion can be made in concentrated sulphuric acid with a concentration of 1 mg/mL and a drop of 10 μL casted on the surface of a well polished GCE [55]. Other media used to disperse the nanotubes are chitosan, nafion and N,N-dimethylformamide (DMF) [56-58].

The second strategy, also mentioned, to use CNTs as sensor platform, is to include the nanotubes in a bulk composite matrix and use the composite to fill the electrode cavity creating a solid CNT electrode and not only covering the surface. CNTs can be mixed with Teflon [59], epoxy resin [60] or generate a carbon nanotubes paste electrode [52] using mineral oil. Usually these composites have different ratios between CNTs and the binding material (60/40% w/w or 55/45% w/w for mineral oil; 80/20% w/w for epoxy resin), different curing times or drying temperatures (i.e. 40 °C for 1 week for epoxy resin) and different ways to polish them. At the end, both strategies have pros and cons, for instance in the covering dispersion method the strength of the bonding between the nanotubes and the electrode surface is not so strong, allowing a lower number of different measures compared to the composite ones. On the other hand the CNTs-composite electrodes are more stable and reusable compared to the covering dispersion ones, but the amount

of nanotubes at the surface is usually smaller giving so a bit lower activity than the others. Another interesting strategy that can be placed between the composite and the covering dispersion is to use the CNTs as an ink [61]. In other words this strategy provide the dispersion of the nanotubes in ink, in a similar way to that of screen-printed electrode preparation (SPE). The most efficient protocol was the one used to produce the classic graphite SPE only substituting the graphite with CNTs, obtaining a good combination of the advantages of thick films sensors and the electrochemical properties of the CNTs. This ink technique can be applied not only to the SPE but also to classic electrodes, such as glassy carbon or gold, dropping the ink on the electrode surface and letting it dry.

The electrical properties and their effect on the electron transfer and electrochemical characteristics of carbon nanotubes let us understand how advantageous and exploitable are CNTs in sensor and biosensor field, since they present an high catalytic effect and also a good perspective for modifications due to their high functionalization of the ends and walls of the tube.

1.2 Metal Nanoparticles

1.2.1 A general view

Nanoparticles (NPs), compared to CNTs, have a much longer history. They are not necessary produced in a lab with modern techniques, but have existed in nature for a long time and it is possible to see their use going back to ancient times. Metal nanoparticles were used as colour pigments in lustre and glass technology [62, 63]. Glazed ceramics with metallic lustre decorations appeared in Mesopotamia during the 9th century, in these decorations were present silver and/or copper nanoparticles, origin of the incredible optical properties of the decorated objects [64]. Metal nanoparticles are also able to colour glass in an amazing way, for example gold has been used to include an eye-catching red colour to glass. One of the most beautiful examples of this red and use of metal nanoparticles in glass is the Lycurgus Cup in the British Museum (Figure 10). This cup was made by Romans in the 4th century and has the characteristic to appear with a green jade colour when the glass reflect the light, for example in daylight, or with a red colour when the light goes through the glass, for example with internal illumination [65, 66].

Figure 10 – The Lycurgus Cup, at the British Museum of London, coloured in green in reflected light (left) and coloured in red in transmitted light (right). These two colours are due to the presence of gold and silver nanoparticles in the glass.

Scientifically speaking, a big step in the knowledge and study about nanoparticles was made by Michael Faraday approximately 160 years ago, with his work *"Experimental Relations of Gold (and other Metals) to Light"* presented to the Royal Society of London [67]. His study on the interaction between light and metal nanoparticles can be regarded as the emergence of Nanoscience and Nanotechnology, besides the beginning of modern colloid chemistry. Therefore, nanoparticles have gathered interest since a long time for their optical properties; instead recently they raised again the interest of the scientific community for their electrical and catalytic properties.

1.2.2 Structure and properties

Being a 0-D nanomaterial, there is not so much to talk about the structure of nanoparticles; the size in every direction is below 100 nm, so all the considerations are usually about the morphology and properties that are closely related. Nanoparticles properties are strongly size dependent. Their morphology can cover a wide range of shapes, from spheres to cubes, going through hexagons/polyhedra, pyramids, nanostars, nanorods (if the length is below 100 nm), etc. This characteristic can be tuned following different synthetic protocols, using for example surfactant agents or supporting materials, as will be described in the following Section.

As mentioned before, nanoparticles are, like CNTs, part of the wide family of nanomaterials and their properties have not such a big difference. Nanoparticles are also divided in two main classes as CNTs, semiconductor and metal NPs. Despite being part of the same family of materials, nanoparticles properties are more size dependent compared to nanotubes. CNTs are classified as 1-D nanomaterial and nanoparticles as 0-D, both materials show a characteristic that is called Quantum Confinement, which generate a difference in the organization of the electronic levels and the density of electronic states. Figure 11 shows a schematic representation of this difference, nanoparticles displays their DOS as a non-continuous function of the energy, with spikes as straight lines that uniformly come to zero and then increase again, compared to the 1-D (i.e. nanotubes or nanorods longer than 100 nm) that displays the same kind of spikes but that discontinuously descend and then increase.

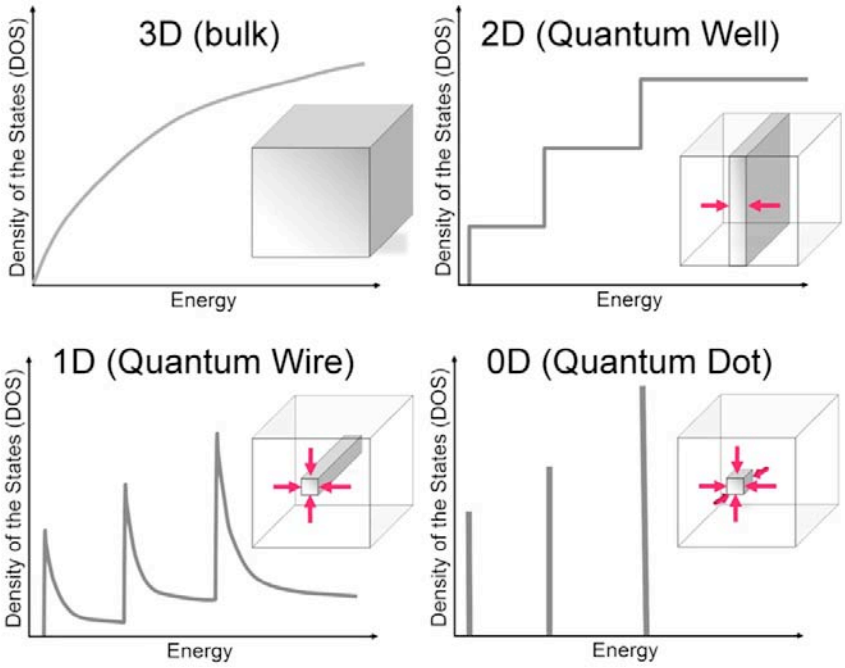

Figure 11 – Electronic DOS for a bulk 3D crystalline material, a 2D quantum well, a 1D quantum wire and a 0D quantum dot. The insets report a cartoon showing the corresponding spatial confinement: arrows define confinements directions. From reference [68]

In CNTs the quantum confinement appears only along the diameter direction, while in the NPs it appears along all directions generating a difference about the same property.

This kind of approach about the explanation of nanoparticles properties can be defined as top-down, since it starts from the bulk properties to go, scaling down the size of one direction at the time, to the NPs properties. Another approach is the bottom-up. In this approach NPs are treated as molecules or clusters. Therefore, their electrical properties are described using the model of atomic and molecular orbitals (AOs and MOs) [1]. The easiest way to arrive to this approach is to considering a simple example, the diatomic hydrogen (H_2). In the H_2 there are two atomic orbitals that combine together resulting in two molecular orbitals, bonding and anti-bonding MOs, spread along the hydrogen molecule. The two electrons, one from each hydrogen atom, are set to minimize the molecule potential energy, so they occupy in the bonding molecular orbital that has the lowest energy and leave unoccupied the anti-bonding MO. The highest occupied molecular orbital is called HOMO and the lowest unoccupied molecular orbital, LUMO. So thinking about the H_2 molecule, it is possible to use the same approach with larger molecules, clusters or bulk materials. Figure 12 shows that as the molecule increase its size, the number of atoms and therefore the number of atomic orbitals joining to form MOs increase, this lead to a proportional increasing of the number of energy levels and to a decrease of the band gap (HOMO-LUMO energy difference) [69].

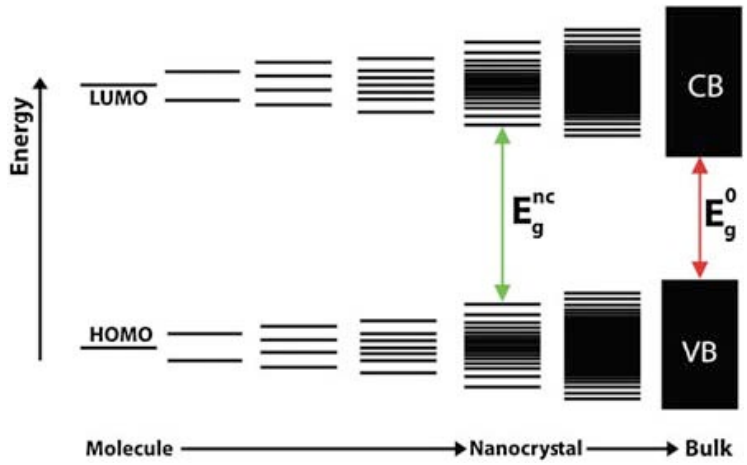

Figure 12 – Scheme of the evolution of the energy level structure from a theoretical diatomic molecule (extreme left) to a bulk semiconductor (extreme right). E^{nc}_g and E^0_g indicate the energy gap between the highest occupied molecular orbital (HOMO) and the lowest unoccupied molecular orbital (LUMO), for a nanocrystal and a bulk; CB and VB means respectively conduction band and valence band. From reference [69]

This means that the density of molecular orbital states is highest at intermediate energy values and lower at the extremes of the energy values. If the number of AOs to be combined is sufficiently large the number of energy levels is so high and the levels are so close that a quasi-continuum is generated, forming bands as described in Figure 12 where the conduction and valence bands (CB and VB) are depicted. The HOMO level is at the top of the VB and the LUMO is at the bottom of the CB. Nanoparticles can be regarded as a large molecule or a cluster of molecules, hence the size dependence of the NPs properties, since the energy gap is tuneable changing the NPs size. This tuneability corresponds to a variation of the optical properties of the nanoparticles due to the quantum confinement, as shown in Figure 13. These two ways to explain nanoparticles properties, bottom-up and top-down, are mainly referred to the semiconductor nanoparticles.

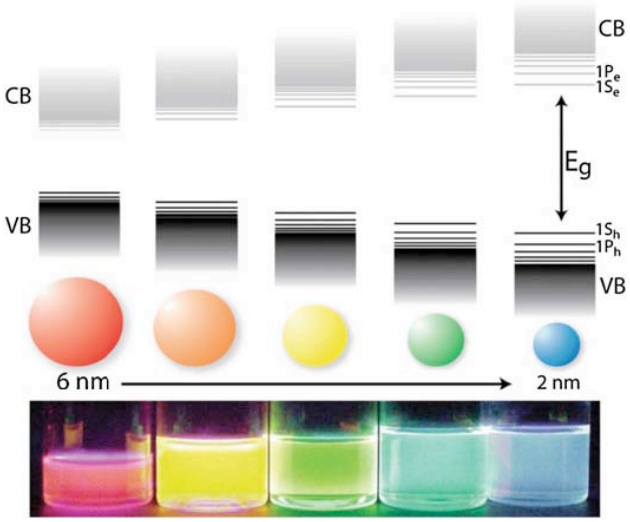

Figure 13 – Schematic representation of CdSe quantum dots and their size-dependent optical properties. From left to right: as the size decrease the band gap increase and the emission/fluorescence under UV excitation (lower panel) shift from red to blue. From reference [2].

As already mentioned the properties of NPs are, in a general wide concept, close to the CNTs properties. NPs may not have the same mechanical properties as CNTs, but in any case they possess really interesting and impressive characteristics, electrical properties in general, then optical properties mainly for semiconductor NPs, and chemical properties mainly for metal NPs. One of the most studied properties for metal NPs is the catalytic activity, and to understand how this property change from metal bulk to metal nanoparticles, the most common example is about gold. For example, gold has always been selected in jewellery for being a noble metal and because it does not tarnish, but another reason is its catalytic inactivity. However, at the end of the 20th century, was found that small gold particles have incredible catalytic properties [70]. From that time on, gold NPs have generated a high interest for fine chemistry and have already found some application as catalyst, such as "odour eater" for bathroom products or in low-temperature oxidation of CO to CO_2. Even if the shift from bulk to nanoparticles increase the catalytic activity of transition metals, this property depends not only on the size but also on the support on which they are dispersed or connected. The interface between the metal nanoparticles and the support material (semiconductor or insulator) can be considered as a *Schottky barrier*[4], polarised due to a partial charge transfer between the metal NP and the support material, an important role in this charge transfer can be played by the defects at the interface or on the support surface [1]. An example of the connection between size and variability of the chemical behaviour can be also taken from the comparison of Au and Pt electron affinity (EA). The Au nanoclusters changes the EA value from *ca.* 2 eV to 4 eV in a small to bigger cluster direction, whereas Pt has an electron affinity value of 9 eV for a single atom and 5.3 eV for the bulk material. The gold nanoparticles catalytic activity and the EA variation according to the size, show that chemical properties can be tuned over a wide range modifying the cluster size [1]. Of course even metal nanoparticles show some optical properties, for example the colour of their colloidal suspensions change accordingly with the particles size, but they are mostly studied for their catalytic properties.

1.2.3 Synthesis of nanoparticles

Nanoparticles synthesis can be carried out in a wide variety of methods, these methods are divided in two broad categories like the ones used to explain NPs properties, *top-down* and *bottom-up* processes [71].

[4] A Schottky barrier is a potential energy barrier for electrons formed at some metal-semiconductor junction. Schottky barriers have rectifying characteristics, suitable for use as a diode.

Top-down processes consist in removing material from a larger scale object in order to create nanostructures; the commonly used techniques for top-down processes are milling and lithography. This last technique is the most used in semiconductor processing industry for the fabrication of integrated circuits; the milling technique, instead, is used to produce nanomaterials in powder form.

Bottom-up processes consist in assembling the nanomaterial using atoms as building blocks, until the desired size and shape is reached. This method allows a more fine control on size and shape of nanoparticles, allowing a higher tuneability of the material. Some of the most used *bottom-up* processes are: Vapour phase deposition methods, as chemical or physical vapour deposition (CVD and PVD respectively), Vapour-Liquid-Solid methods (VLS) and Liquid-phase methods, inside which is possible to classify colloidal, sol-gel and template methods [71].
As mentioned the *Bottom-Up* process allows a higher tuneability, and this is the reason why we will see only some of these processes to have a little example about how they works.

Vapour phase deposition methods

These methods can be used to generate for example nanowires, nanoparticles, films or multilayers and the most common is called Chemical Vapour Deposition (CVD) [71]. As in the case of carbon nanotubes, CVD involves precursor materials in gas phase and their thermal decomposition at high temperatures (500-1000 °C) with a following deposition on a substrate. A variation of the CVD is the Molecular Beam Epitaxy (MBE), used mostly for the generation of thin-films or multilayers. In this technique the precursors are directly deposited on the substrate, allowing the growth of single atomic layers, this means that thin-films can be generated with the deposition of subsequent layers and their thickness can be controlled with atomic precision. Moreover the composition of subsequent layers can be changed, reaching the next level of tuneability giving for example the opportunity to create multicomponent nanostructured thin-films or semiconductor nanoparticles like quantum dots [72]. The name of this technique can change according to the precursors used, for example if the precursors are metallorganic compounds the process is usually called Metallorganic MBE or CVD (MOMBE or MOCVD respectively).

Colloidal Methods

These methods are considered part of the Liquid-phase methods and are based on the chemical precipitation reaction in solution [71]. In a solvent a chemical reaction lead to the nucleation and growth of NPs forming a colloidal solution. The advantage of these methods is in their easiness to be scaled and carried out, and they are relatively cheap. With these methods is possible to synthesise NPs with different composition, such as single compound NPs (i.e. metals, Au or Pd; semiconductors, CdSe; insulators, SiO_2) and alloys [2], doped materials (i.e. ZnSe:Mn) [73, 74] and combination of two or more materials connected by one or more interfaces (i.e. CdSe core and ZnS shell) [2]. Compared to the vapour phase deposition methods, colloidal methods give a higher control on size and shape of the NPs since the other method can only reach the weak quantum confinement regime due to one of the dimension bigger than 10 nm. Another advantage of colloidal methods is the possibility of easy post-synthesis procedures, like size-selection, surface functionalization and generation of nanocomposites (i.e. incorporation in polymers [75]) showing one more time the high versatility of the process.

1.2.4 Nanoparticles in sensors and biosensors

As mentioned in Section 1.2.2 nanoparticles have unique chemical, electronic and physical properties, which sometimes can be the opposite of the bulk material (see gold). These properties make nanoparticles suitable for the assembling of sensing devices, such as electrochemical sensors and biosensors. NPs role is often to enhance the electron transfer, or catalyse electrochemical reactions, and immobilize or labelling biomolecules. A wide variety of NPs have been used in electrochemical sensors and biosensors, such as metal nanoparticles (as catalysts or electron transfer enhancers), semiconductor nanoparticles (as optical labels for biomolecules) and oxide nanoparticles (as immobilization platform for biomolecules) [76, 77]. The most common way to build electrochemical sensors with NPs is their deposition or immobilization on the electrode surface through a NPs solution/ink or sometimes generating the NPs *in-situ* at the electrode surface through electrochemical reaction. Here will be shown only few examples about metal NPs application in electrochemical sensors, as catalysts or electron transfer enhancers, since in this PhD work mainly metal nanoparticles have been used.

One of the advantages gained when nanoparticles with catalytic properties are embedded in

sensors and biosensors, is the possibility to decrease the overpotential of electrochemical reactions subject to study or also to make some previously irreversible redox reaction at unmodified electrodes to a reversible one. For example gold NPs have shown great catalytic properties; they have been used as modifiers in a nitric oxide (NO) microsensor, consisting in a platinum microelectrode modified with gold NPs, considerably decreasing the overpotential for the NO oxidation [78]. It is known that nanoparticles may demonstrate selective catalysis against certain compounds, as shown from Ohsaka and co-workers that developed an electrochemical sensor for dopamine detection in presence of ascorbic acid [79]. To achieve this result the electrode was modified with gold NPs. As shown in Figure 14 the ascorbic acid (AA) reduction potential was shifted at a lower voltage compared to dopamine (DA) and the electron transfer in the redox reaction of dopamine was enhanced having a smaller potential gap between reduction and oxidation peak, so allowing the electrochemical discrimination.

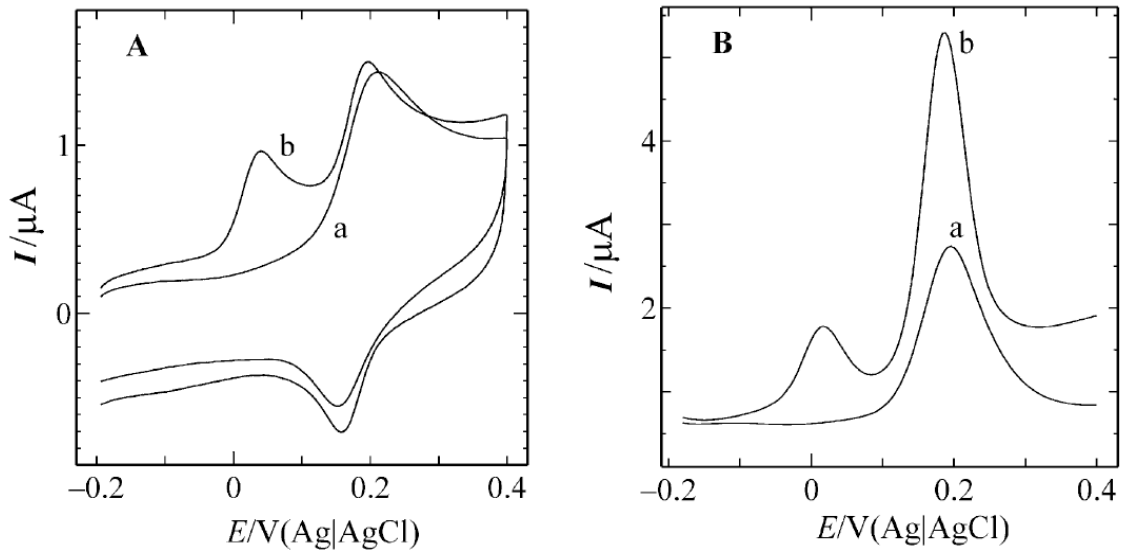

Figure 14 – Cyclic voltammograms (A) and Square Wave voltammograms (B) of a bare Au electrode (a) and a nano-Au modified electrode (b) in presence of a binary mixture of DA (50 μM) and AA (50 μM) in PBS (pH 7.2) at a scan rate of 100 mV/s. From reference [79]

Another metal that shows catalytic properties, and is used in electrochemical sensors, is platinum. An example on the use of Pt nanoparticles can be the H_2O_2 sensor developed from Niwa and co-workers [80]. Their sensor, compared to the Pt bulk electrode, showed a sensitive response to H_2O_2 having a lowering of the overpotential of *ca.* 200 mV. To demonstrate how different nanoparticles can interact differently with molecules, the same group replacing metal source for the NPs, developed a sensor for sugar determination made by Ni NPs dispersed in a carbon-film electrode [81]. Catalytic properties can be found also in some non-metal nanoparticles, an example can be given from copper oxide (CuO) NPs [82].

The electron transfer-enhancing feature of the NPs can be quite useful when these are used in electrochemical sensor involving enzymes. Most of the time enzymes are poor in direct electrical communication with the electrode, and this is due to their typical morphology. The active centres of the enzymes are usually surrounded by protein shells, which are a kind of insulating layer, and the electron transfer between the electrode surface and active centres is blocked or considerably low. Metal nanoparticles are suitable for the enhancing enzyme's direct electron transfer, taking the role of mediators or electrical wires. An example of the co-operation between NPs and enzymes is the work of Willner's group [83], where a gold nanoparticle has been functionalized with a FAD group, then completed with apo-glucose oxidase and finally assembled on the surface of a gold electrode. This configuration showed a very fast electron transfer between enzyme and electrode, that has been reported to be 7 times faster than the one with glucose oxidase natural substrate, oxygen. The mentioned sensor was used to detect glucose without interference, thanks to its fast electron transfer that made it insensitive to oxygen or other interfering species as ascorbic acid [83]. Even other redox proteins can benefit from the use of NPs to enhance their electron transfer. Always gold nanoparticles have been used from Wang et al. [84] in a gold electrode modified with a silica gel network to obtain direct electrochemistry from cytochrome C. As for the catalytic activity, some non-metal (oxide or semiconductor) nanoparticle act as electron transfer enhancer. For example ZrO_2 nanoparticles have been used to immobilize haemoglobin giving direct electrochemistry at a glassy carbon electrode, this combination haemoglobin-ZrO_2 NPs could be used to build a mediator-free biosensor [85].

The features brought from NPs, as the enhancement of the electron transfer, catalytic activity, immobilization support and optical labellers for biomolecules show how this nanomaterial is helpful in the construction of sensors and biosensors. These size dependent properties of the NPs are highly desired in the field of sensors and biosensors.

1.3 CNTs-NPs a hybrid nanomaterial

1.3.1 Advantages from the two nanomaterials

As described in Sections 1.1 and 1.2, both carbon nanotubes and nanoparticles have a wide range of unique properties, starting with the main difference with the bulk material (carbon/graphite for CNTs and various metals or non-metals for NPs) to go to the chemical and electrochemical size dependent properties of the NPs or the morphology related properties in CNTs and so on. The combination of the two materials together was a natural consequence, leading to a new class of hybrid nanomaterials, CNTs-NPs. These new hybrid nanomaterials are basically carbon nanotubes modified with nanoparticles from different sources, but nowadays the most loved term to call this modification seems to be *decoration*, and it has all the potential to integrate and display the unique properties of both precursors. Recently, carbon nanotubes *decorated* with nanoparticles have gathered much interest inside the nanoscience and nanotechnology field, and have been presented as building blocks for a wide range of applications like fuel cells [86, 87], hydrogen storage [88, 89], solar cells [90, 91], gas sensors [92, 93], transparent electrodes [94] and Li-ion batteries [95].
The combination of material properties in CNTs-NPs can be seen for example in the small junction area (< 10 nm^2) at the interface between NP and CNT surface, which allow the size, shape and chemistry tuning, that in the end is the tuning of the material properties. For example in fuel cells NPs size, support and preparation of the catalyst are strongly involved in the electro-oxidation of the fuel compound, CNTs are considered a good support material due to their high surface-to-volume ratio, stability and mechanical properties [96, 97], therefore generating a good combination in the construction of fuel cells proving that CNTs-NPs are effective in the catalysis of redox reaction, due to the increased electrocatalytic activity and surface area [86]. In solar cells CNTs and semiconductor NPs (as CdSe and CdS) have displayed promising perspectives, in these applications the semiconductor NPs act as a photoreceptor and the CNTs act as connection for the electron conduction [98]. Regarding fuel cells and surface area, has been proven that CNTs are an impressive support for Pd NPs due not only to the surface area but also to the possible spreading of H_2 from Pd to CNTs [99]. From Kong et al. [94] has also been demonstrated that metal NPs can increase the electrical conductivity of SWCNTs, due to what Kong and co-workers call doping-induced electron depletion mechanism. Usually CNTs surface act as template where NPs are absorbed or, if functional groups are present, linked (covalently or not); this linking can be carried out either modifying NPs surface (mostly covalent link, but also π-stacking) or with bare NPs (non-

covalent or electrostatic link). All these examples have been showed to explain how the integration of CNTs and NPs leads to an increasing of both material properties, displaying an important characteristic of this new hybrid material, the synergetic effect. In any case, the most critical step in the generation of this hybrid nanomaterial is the synthesis, since a very large amount of different synthesis is possible and a reliable and controllable one is needed.

1.3.2 CNTs/NPs synthesis

The synthesis of CNTs-NPs has gathered much attention in recent years, due to the outstanding outcome of this new hybrid nanomaterial. It is plenty of different strategies adopted to fabricate CNTs-NPs, but those strategies can be mainly grouped in two big classes (Figure 15). The first approach consists in a previous synthesis of the nanoparticles and then connects them to functionalised carbon nanotubes in two ways, non-covalent interactions (i.e. electrostatic, hydrophobic or π-stacking) or covalent interactions (i.e. organic or biomolecular linkers). A second approach, instead, provide a direct deposition of nanoparticles on the carbon nanotubes surface. As in the first approach, also in this case there are different ways to carry out the deposition, through an *in situ* formation of the NPs, a reduction reaction or an electrodeposition process.

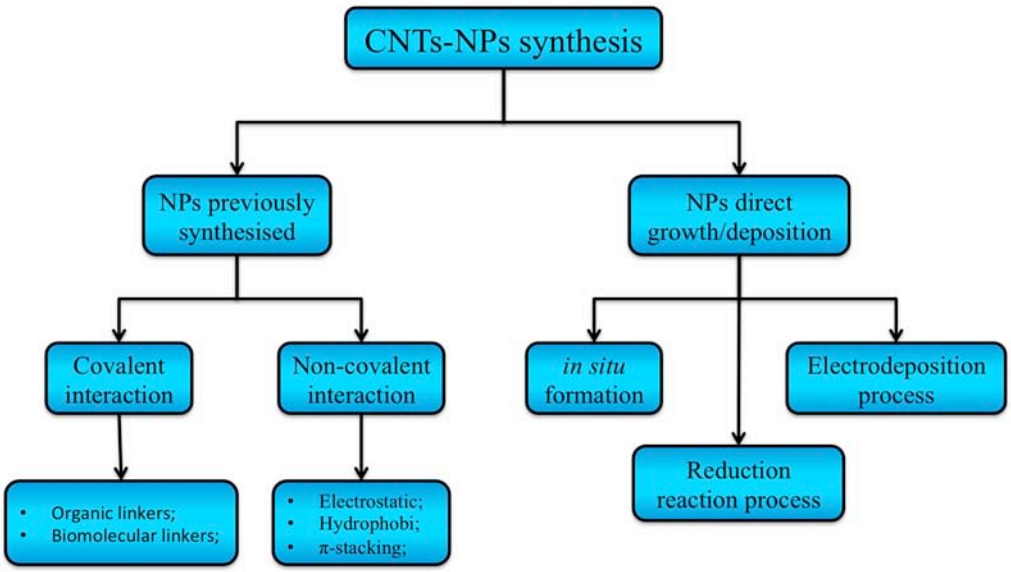

Figure 15 – Scheme of the mainly used reactions for CNTs-NPs synthesis

A popular process to create CNTs-NPs hybrid nanomaterial has been modifying the CNTs surface with desired functional groups. There are some advantages in this technique, for example covalent bonding makes the connection between nanotubes and nanoparticles stronger giving more reliability and robustness; size and shape of the nanoparticles can be easily tuned with specific synthetic methods being separately generated from the nanotubes; controlling the functionalization of the carbon nanotubes is possible to have the control on where and how many NPs are attached (oxidation treatments and/or chemical reaction conditions). Covalent linkers can be organic molecules, like ethylenediamine, used to generate an amide or ester bond between acid functionalised CNTs and acid functionalised NPs. For example a similar protocol has been showed from Banerjee and Wong [100] in the modification of SWCNTs with CdSe nanoparticles, as shown in Figure 16.

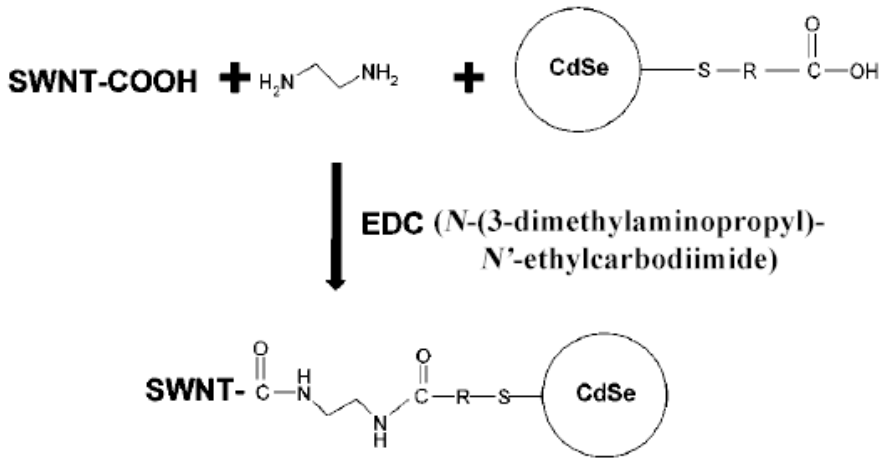

Figure 16 – Reaction scheme of the SWNT/CdSe synthesis, where a linker (ethylendiamine) has been used to couple CdSe NPs with oxidised nanotubes using a carbodiimide mediator as the EDC. From reference [100].

This kind of approach is usually followed to connect semiconductor nanoparticles (as CdSe, CdTe or other quantum dots in general) to the nanotubes; but one characteristic that seems to be important in this kind of reactions is the length of the nanotube, that can affect the position of where the NPs will bind, if at the ends or on the sidewall [101]. Always regarding the covalent interaction, a more recent approach to this kind of linkage is the use of biomolecules, like for example DNA. It has been proved that DNA can act as frame for the organization of gold NPs [102] and an example of this capability has been given with the synthesis of DNA-wrapped SWCNTs modified with gold nanoparticles [103]. Another biomolecule largely used is the streptavidin-biotin combination. The reaction is usually carried out between biotin-modified CNTs and streptavidin-modified NPs in a self-assembly process [104]. Meanwhile on the non-covalent interaction side of the CNTs-NPs synthesis few processes with this approach have gathered much attention, due to their easiness and

less aggressive reactions. One of these processes involves electrostatic interaction between nanoparticles and nanotubes. One of the most used techniques is the *polymer-wrapping*, the nanotubes surface is coated with a polyelectrolyte shell that provide a charged layer where to attach the NPs. The polymer coating can be positively or negatively charged and therefore the NPs will bring an opposite charge. For example SWCNTs can be *decorated* with CdSe-ZnS (core-shell) nanoparticles with the help of sodium dodecyl sulphate (SDS) surfactant [105]. The SDS acts as coating layer on the nanotube surface allowing then an electrostatic interaction between the Zn in the nanoparticle shell (ZnS) and the sulphate of the SDS itself and a dispersion of the NPs along the nanotube surface. Polyelectrolytes are rich in terminal functionalities of different nature therefore the possibilities of tuning the nanotube surface are widely increased for either positively or negatively charged polyelectrolytes. Moreover the thickness of the coating layer can be controlled not only by adding different polymer layers, but also following different assembly reaction condition playing on some parameter, such as pH or ionic strength values. CNTs modified with Pt NPs have been synthesised following a "self-assembly electrostatic layer-by-layer" process [106] allowing a control on the amount of Pt nanoparticles loaded on the nanotube surface and an enhanced catalytic activity on the dioxygen reduction. An example of how to play with the charge of the polyelectrolyte and nanoparticles is given from the use of a positively charged polymer, poly(diallyldimethylammonium)chloride (PDADMAC), and negatively charged Au nanoparticles [107] or the other way around, using a negatively charged polymer, as poly styrene sulfonate (PSS), and positively charged Au NPs [108], Figure 17. In both reactions nanotubes were pre-treated with acidic solutions, to increase the number of carboxylic groups on the surface and ends, beside to help the solubility.

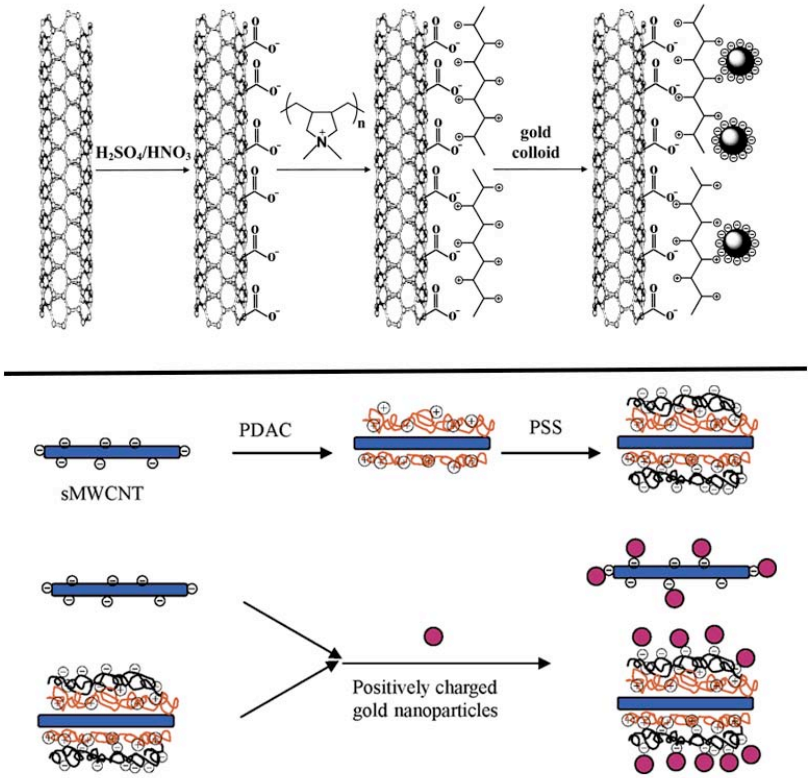

Figure 17 – Scheme of two different CNTs-NPs synthesis with a non-covalent approach playing on the polyelectrolyte and nanoparticle charge. Top, positive polyelectrolyte and negative Au NPs, from reference [107]. Bottom, negative polyelectrolyte and positive Au NPs, from reference [108]

Non-covalent approach does not means only electrostatic interactions, and an alternative way to follow this pathway is the hydrophobic interaction. According to the given definition this approach is based on the interaction between shell-modified nanoparticles and only purified nanotubes, taking advantage of the combination of hydrophobic and hydrogen-bonding interactions. This process has been developed to try to avoid the sometime complicated and more often boring modification of CNTs. An example of this kind of process can be given from the work of Zhong group, they have used hydrophobic interactions to synthesise CNT-Au NPs with simply mixing the two nanomaterials in the same flask [109]. The NPs were modified on the surface to help the hydrophobic and hydrogen-bonding interactions using an alkyl capping shell and nanotubes were just purified with an acid treatment that, as mentioned in Section 1.1.4, not only remove the metal residues from catalysts but also forms carboxyl groups on the sidewalls and ends. Of course another way is to modify the nanotubes with some alkyl chain and keep the nanoparticles surrounded with a stabilizer (like a surfactant) to increase the hydrophobic interaction through a larger contact area to make the composite more stable. In this case has been proved that a crucial factor is involved in the average coverage of the CNTs from the gold NPs, the length of the alkyl chain [110]. In Figure 18 is shown a scheme of the comparison made from Sainsbury and co-workers using alkyl- and

alkylthiol-modified MWCNTs with different chain length. It is possible to notice that with alkyl chains the coverage of gold nanoparticles decrease as the chain length increase, instead with alkylthiol chains the coverage is almost independent from the length. This effect is due to the steric issues associated with chain movements [110].

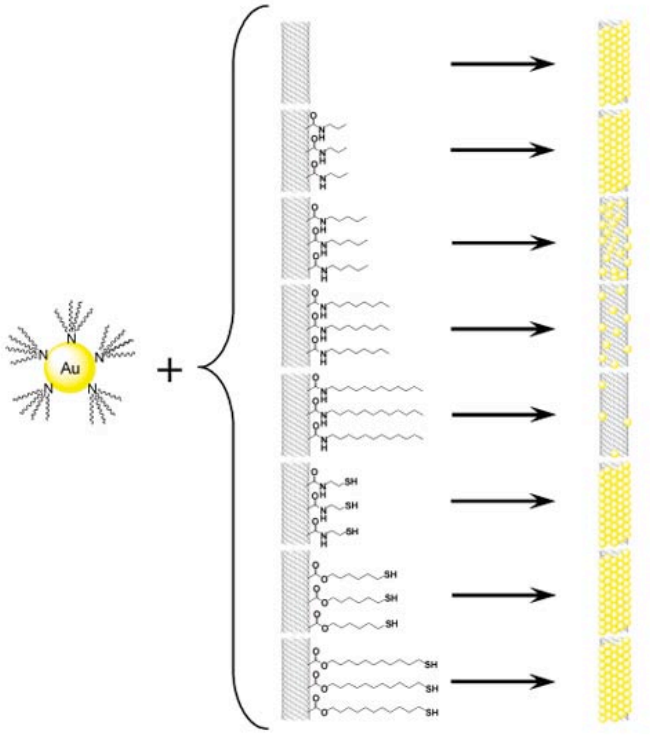

Figure 18 – Schematic representation of the MWCNTs/Au NPs assembly ratio related to the nanotube surface functionalization. From reference [110]

A relatively newer technique used to modify nanotubes with nanoparticles is to take advantage of the π-π stacking interaction, which can be seen as an electrostatic interaction that instead of involving the charge of the parts in the hybrid material, involve the interaction between the π-electrons of an aromatic species and the π-electrons delocalised on the nanotube surface. This interaction is stronger then it seems, for example can withstand temperatures of >400 °C still stable [111]. The singularity of this technique is that while the interaction between the aromatic linker and the nanotube is only π-π stacking, on the nanoparticle side, usually a thiol- or amino-terminated aromatic linker bind them, presenting in this way both covalent and non-covalent interaction within the same modification.

Therefore, the first approach of generating the nanoparticles separately from the nanotubes and then connecting them in a further reaction shows that there is some advantage from covalent interactions, like for example the robustness of the nanomaterial and the high control on where nanoparticles are

linked to the nanotubes, but on the other hand these modifications change the surface of the nanotubes, adding defects and switching the sp^2-hibridization into an sp^3-hybridization breaking the 1-D periodicity. Non-covalent modifications, instead, take advantage of their protocols easiness and non-destructive interactions preserving the electronic and optical properties of CNTs. Another characteristic of the non-covalent modification is the opportunity to have a uniform coating of NPs.

As previously mentioned, the second approach to generate CNTs-NPs hybrid nanomaterial is the direct growth/deposition of NPs on the CNTs surface. Recently this approach has gathered more interest than the pre-synthesised NPs. Some of the reasons for this growing attention are for example the absence of degradability for some electrical property due to the presence of a dielectric shell layer (linker between CNT and NP), the lower cost and the less procedure steps in the synthesis. Commonly the direct growth/deposition of NPs consist in a first step where the nanotubes walls are functionalized with hydroxyl-, carbonyl- and carboxyl- groups thorough reactions with strong acids or microwave irradiation or ultrasonication, to enrich their reactivity. In the end this step is very close to the purification step after the CNTs synthesis. The second step consists in the growth/deposition of the NPs, which can be carried out with chemical reduction, *in situ* growth or electrodeposition.

Chemical reduction deposition, for example, consist in a reaction of functionalized CNTs with a metal salt in presence of a reducing compound, like $NaBH_4$ or citric acid, or performing the reaction in H_2 atmosphere at high temperature. The most used reducing agent still remains $NaBH_4$, even if are present in literature example of use of H_2 and citric acid [112-114], especially for noble metal nanoparticles as gold but also for palladium, platinum, copper and other metals [115-117]. As most of the procedures that follow the direct growth/deposition approach, the chemical reduction deposition is a *one-pot* reaction that means all the reaction steps about the assembly of the nanotubes and nanoparticles take place in the same flask without intermediate processes Figure 19. Some example of the chemical reduction deposition can be given from the work of Zhang *et al.* [118] or Hu et al. [119]. Both works use $NaBH_4$ as reducing agent to generate Au NPs, for example Zhang and his co-workers used a surfactant to enhance the solubility of the CNTs and to act as a template site for the growth of the NPs. Hu and his co-workers, instead, used thiol-modified CNTs and then added $HAuCl_4$ and $NaBH_4$ for the generation of Au NPs, this result was then compared with the same thiol-modified CNTs used in a reaction with pre-synthesized Au NPs simply stirred together with the thiol-CNTs to obtain the final hybrid nanomaterial. This comparison resulted in a better size dispersion for the direct grown nanoparticles than the pre-synthesized ones, both onto thiol-modified CNTs.

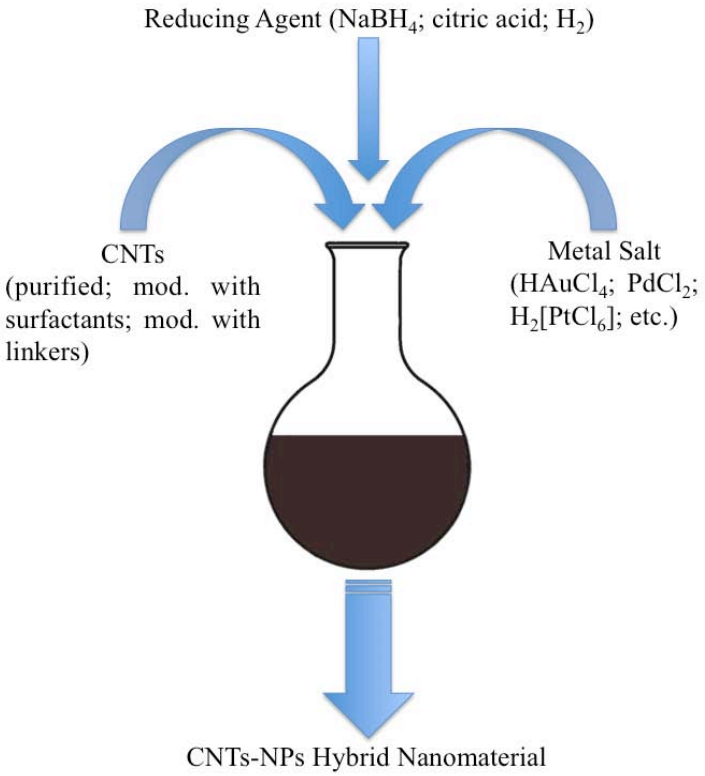

Figure 19 – Scheme of a one-pot synthesis, all the precursors are added one by one in the same flask, allowing the formation of the product in one single step instead of having to prepare separately the NPs, purify them and then add to the CNTs and purify again.

A similar procedure to the chemical reduction reaction can be the *in situ* growth of nanoparticles previously mentioned. Also this procedure is fundamentally a one-pot reaction, but there is no need of a reducing agent for the metal salt. Inside an *in situ* reaction the carboxylic acid groups on the nanotube surface, due to an oxidative pre-treatment, act not only as enhancer for the solubility of CNTs but also as preferred nucleation site for the NPs, due to their tendency towards a coordinative complexation with metal ions. In this kind of synthesis, not being involved a proper reducing compound, the reduction of metal occur, presumably, for the direct redox reaction between the metal ions and the CNTs [120]. The procedure consists in simply add the purified nanotubes to a metal solution of interest and after few minute the nanoparticles start forming. However the *in situ* reaction seems to be really easy and quite fast, there is a limitation in its mechanism, not all the metals can be reduced by the CNTs. The limitation consists in the fact that the reducing agent, in this case the CNTs, has to have a redox potential lower than the redox potential of the metal ions of interest, to allow the metal to be transformed in nanoparticles. Therefore Cu^{2+} and Ag^{+}, for example, cannot be reduced into nanoparticles because of their lower redox potential compared to CNTs. For this reason has been developed a technique named SEED (Substrate-Enhanced Electroless Deposition) that consist in blocking CNTs on a metal support and then immersing the

nanotubes and support in the metal solution of our interest [121]. In this case the metal chosen as support material has to have a redox potential lower than the redox potential of the CNTs and the metal we want to use for nanoparticles generation. The *in situ* growth reaction is based on the same principles (redox reactions) of the electrodeposition technique, just without the electrode. The electrodeposition technique is considered a facile method to generate nanoparticles, due to some characteristic as the high purity of the metal nanoparticles obtainable [122, 123] and the possibility to control size and dispersion of the particles by playing with the deposition condition (such as applied potential and deposition time). An advantage of this technique is that commonly the nanoparticles deposition lasts from few seconds to several minutes, making of this a fast synthesis. A little limitation, instead, is that it seems to be often restricted to the use of noble metals as Pt, Au, Ag and Pd to obtain pure metallic nanoparticles [124, 125], but anyway it is possible to obtain metal oxides nanoparticles [126]. An example of a general experiment for the electrodeposition of metal NPs can be given from the work of Guo and co-workers [123], the nanotubes are involved in a soft oxidation step and then they receive an electrochemical treatment to form the NPs. In the work reported by Guo Pt nanoparticles are formed through cyclic voltammetry, where previously the metal forms complexes with the carboxylate groups on the surface of the CNTs and then transforms in well-dispersed nanoparticles all along the CNTs surface.

This direct growth/deposition approach demonstrated in the last years its efficiency in generating CNTs-NPs nanomaterials, with either metal or semiconducting nanoparticles. One of the biggest advantages of the strategies using this approach is that for both materials, NPs and CNTs, the properties and structures remains practically untouched, fully preserved, compared to other procedures where the surface of the nanotubes receive more defects from the treatments losing some electrical property, or where nanoparticles surfaces are modified to allow some interaction to be connected to the CNTs and lowering so their optical properties (i.e. semiconductor nanoparticles). The disadvantage of these strategies is that not always is easy to have control on the dispersion or size of the NPs, since the mechanism is not always well known. Moreover the protocols sometimes require toxic, unstable or highly reactive precursor, making of these strategies not always the first choice, but potentially they are the easiest way to obtain a CNTs-NPs hybrid nanomaterial with inside the untouched properties of each sides, nanotubes and nanoparticles.

1.3.3 CNTs/NPs applications

Since its *"discovery"* the hybrid nanomaterial, CNTs/NPs, have been used in a really wide range of applications. Usually this material has been and is generated modifying carbon nanotubes with transition metals as for example Pd, Au, Pt and Ag, therefore is not surprising that one of the most common applications is in the catalysis field. For example hydrogenation catalysts are really important in the petrochemical and fine chemical industries, and Pd *decorated* CNTs have showed interesting catalytic properties on the hydrogenation of cinnamaldehyde to hydrocinnamaldehyde [127]. Comparing the CNTs/Pd catalyst to the commercial Pd catalyst the hydrogenation rate was only slightly increased, but what moved the authors attention was the selectivity towards the hydrogenation of the C=C double bond instead of the C=O double bond, both present in the cinnamaldehyde molecule [127]. Another studied application is the hydrogen storage, where Ni and Pt NPs modified CNTs have been used [128, 129] and CNTs/Ni showed a much higher reversible chemical adsorption compared to CNTs alone. Inside the wide range of applications possible for CNTs/NPs hybrid nanomaterial, Dong and co-workers show in their work [130] the development of a thin film with CNTs and Pt NPs that could be exploited as electrode in a fuel cell due to its oxygen reduction reaction. Moving from metal NPs to semiconducting NPs *decoration* of CNTs the applications turn more into photovoltaic devices due to the band gap they possess. In this case CNTs are usually modified with quantum dots like CdSe, CdS, CdTe and PbSe. As example Willner and co-workers [131] fabricated a hybrid nanomaterial of CNTs/CdS that has shown a photon-to-electron conversion efficiency of 25% compared to the 1.5% of only CNTs. A less common, but still potential, application is the use of CNTs/NPs for drug delivery or fluorescence labelling modifying for example the NPs or quantum dots with streptavidin or other biomolecules or proteins, connect to the CNTs and then follow the path of the eventual drug [132, 133].

Among the wide range of possible applications for this hybrid nanomaterial, a well known one is the use of it as material for sensors in general. These applications can be for chemical or electrochemical sensors. In the chemical sensors field, CNTs/NPs material has been used to detect molecules that usually are hard to easily detect with other materials, for example methane (CH_4). Pd *decorated* CNTs have shown a sensitivity 10 times higher than conventional sensors for CH_4 detection [134] or for example in another work CNTs with electrodoposited Pd NPs was used to fabricate a flexible H_2 sensor with high performance [135].

About the electrochemical sensors, CNTs/NPs hybrid nanomaterial can be almost seen as a nano-electrochemical sensor itself Figure 20, since the NPs can act as sensing element to catalyse redox reactions and CNTs as transducer to bring the electrical signal to the instrument.

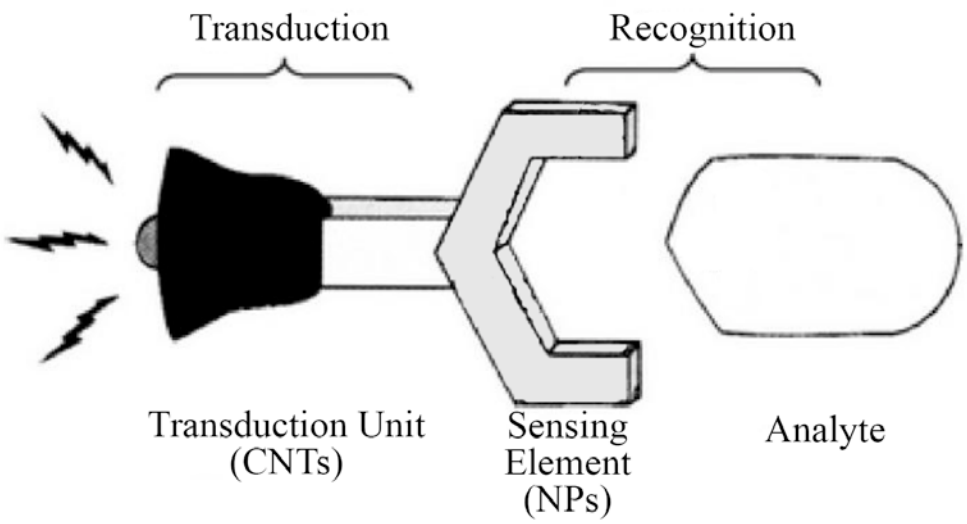

Figure 20 – Schematic representation of a sensor composition in all its typical parts.

This is the reason why it has been used as sensing material in different electrochemical sensors and biosensors, for example for the detection of H_2O_2, dopamine, hydrazine, glucose and many other targets [136-140]. The preparation of CNTs/NPs modified electrochemical sensors is generally carried out casting the electrode surface with a previously prepared solution of the hybrid nanomaterial, other ways used depend on how the CNTs/NPs have been synthesised, for example if the electrodeposition method is used to generate the NPs onto the CNTs surface, which means that the nanotubes are already on the electrode surface, is a way to directly modify the electrode without a further step of surface casting. The most common solvents used to make the hybrid nanomaterial solution are H_2O, DMF or methanol, paying attention to obtain a well-dispersed suspension. Another way to include the CNTs/NPs material in the electrode is to make with this material an ink-like composite, similar to the ink used to fabricate the screen printed electrode, and then or manually cast a classic gold, glassy carbon or platinum electrode, or also directly fabricate a screen printed electrode with the ink containing CNTs/NPs hybrid nanomaterial. The ink casting, compared to the solution casting, has the advantage to be easier to deposit on the electrode surface but on the other hand there is an optimization work to do for finding the right thickness of the ink to be used. The process usually does not need any technological instruments; either solution or ink is firstly deposited on the electrode surface and than dried. The drying step can be carried out at room temperature or with a vacuum desiccator.

As previously mentioned CNTs/NPs hybrid nanomaterial has been used in a wide range of electrochemical sensors, but one unclear thing is its selectivity towards different targets, most of the works are all with just one analyte. In other words CNTs/NPs hybrid nanomaterial even showing a good sensitivity is not often as selective as other electrodes, like for example ion selective

electrodes, or enzyme, protein, DNA based sensors or biosensors. Usually those kinds of sensors have a specific site where the target analyte can react, giving so a good selectivity, the CNTs/NPs sensors instead do not have such sites, the NPs act as catalyst for the redox reaction of the target analyte and they cannot select which analyte to react with. At this point to clarify this concept, it is probably better to make an example; in case of a three compounds mixture (A, B and C) with a high selective sensor it is possible to detect only one of the compounds and do not have a reaction with the other two, while with a CNTs/NPs sensor all the three compounds react at the electrode surface, even if differently, giving a response that is a combination of the three. This of course shows a low selectivity for the hybrid nanomaterial, but if the compounds A, B and C are for example one target and two interferents, the selective sensors have more difficulties to detect only one compound since the interferents have a similar structure to the target, while in this case the CNTs/NPs sensors have a better behaviour, being able to detect all the three compounds but with different responses. This behaviour is due to the properties of CNTs/NPs hybrid nanomaterial, which consist in the combination of the catalytic and electronic properties of both NPs and CNTs. In the example of mixture with one target and two interferents usually these three compounds have their redox potential really close to each other, and it can result in a not clear electrochemical signal for example overlapping peaks in a voltammetry analysis. This can happen with common sensors as Pt, Au or glassy carbon electrodes, but even with selective biosensors that cannot distinguish really well between target and interferents. NPs in CNTs/NPs nanomaterial, instead, are able to differently catalyse the redox reaction of the compounds, shifting so the redox potentials of the molecules in different ways and at slightly different potentials being able to overcome the overlapping of the peaks and giving a cross-response. An example of this behaviour can be seen in the work of Huang and co-workers [136] where they were detecting dopamine (DA) in presence of two interferents, uric acid (UA) and ascorbic acid (AA). In Figure 21, reported form Huang work, is possible to see the signal generated from a carbon paste electrode (CPE), bare and modified with Pd NPs *decorated* carbon nanofibers (CNF/Pd-CPE), which are very similar to CNTs, against single targets (left column) and the mixture (right column) with a clear improvement given from the CNF/Pd-CPE (B and D graph) compared to the CPE sensor.

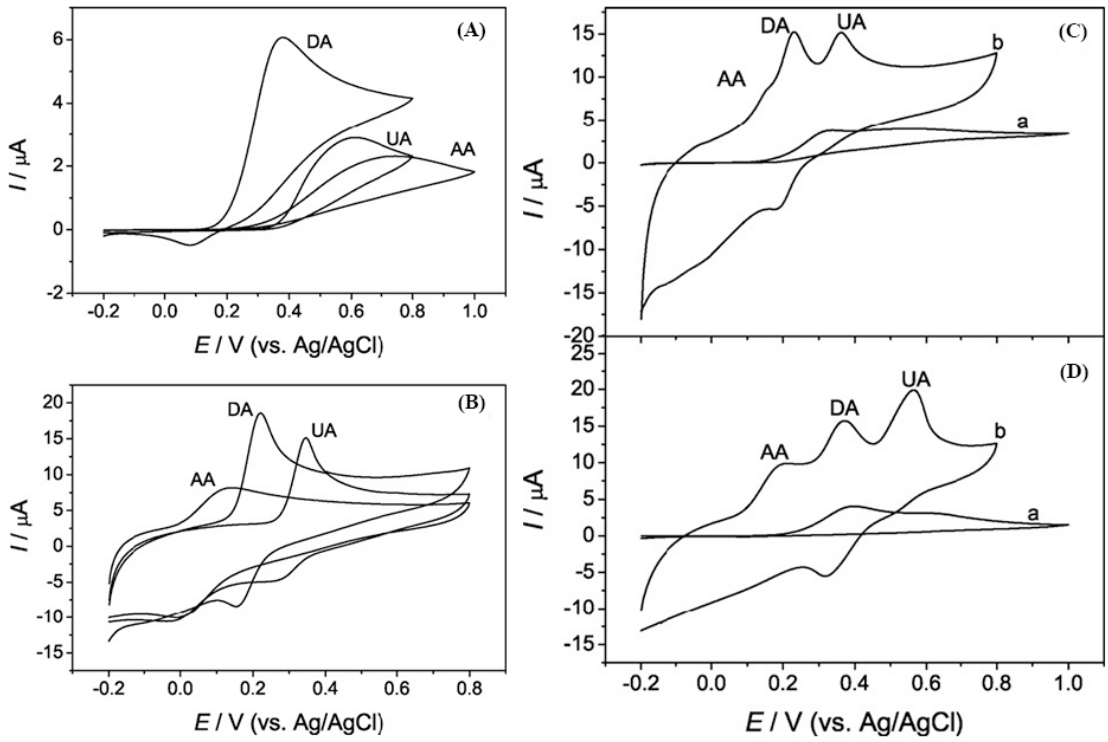

Figure 21 – Left column: Cyclic voltammetries of DA (2mM), UA (2mM) and AA (2mM) at the surface of bare CPE (A) and CNF/Pd-CPE (B) in PBS (0.1M), pH 7 and scan rate of 50 mV/s; Right column: Cyclic voltammograms of a mixture of DA, UA and AA (1mM, 1mM and 2mM respectively) at bare CPE (C) and CNF/Pd-CPE (D) in PBS (0.1M), pH 7 and scan rate of 50 mV/s; from reference [136]

Obviously the behaviour is dependent on the metal loaded on the CNTs, because every metal catalyse in different ways, being for example more efficient with some compound and less with some other. So CNTs/NPs hybrid nanomaterial has a cross-response ability as electrochemical sensor, making it exploitable for example in an array of sensors or biosensors, where it could means different electrodes with different modifications. The sensors or biosensors can take the advantage of having different metals or metal oxides NPs loaded on the CNTs or NPs modified with biomolecules and then loaded on the CNTs, making this new hybrid nanomaterial perfectly suitable to be included in the so called Electronic Tongue systems.

Electronic Tongue systems

The IUPAC definition for an Electronic Tongue (ET) [141] defines it as "a multisensor system, which consist of a number of nonspecific and low-selective sensors and uses advanced mathematical procedure for signal processing based on Pattern Recognition or Multivariate data analysis, as Artificial Neural Networks (ANN), Principal Component Analysis (PCA), etc." and it is thought as a system for analysis of liquids. The ET is a bio-inspired system or device, which recall the human tongue for how it works and how it is made. Of course the first thought behind the ET

was to reproduce the sense of taste, but the idea to artificially reproduce the natural response of a human being to environmental stimuli was first published in 1943 [142], probably one of the first steps and/or attempts to build an "artificial brain", and then it was followed in 1982 and 1995 by the first examples of related devices, respectively an electronic nose for gas analysis [143] and an ET for liquid analysis [144]. As mentioned in the IUPAC definition an ET consists of low-selective and nonspecific sensors and at a first sight this can be seen as really far from what a real human tongue is, when actually they are quite similar. The common concept of a human tongue is that it has specific zones where the flavours can be tasted, like sweet on the tip salty and sour on the sides and bitter on the back (Figure 22a); well according to the U.S. National Library of Medicine, this is a misconception because actually has been demonstrated that the flavours can be tasted in all the tongue (Figure 22b) [145, 146], and that the most sensitive parts are the edges, the tip and the back more than the middle, the only exception is about the back part that is actually more sensitive for bitter flavour but this is probably more to protect our body from swallowing poisonous or spoiled food since the back of the tongue is the last barrier before the throat.

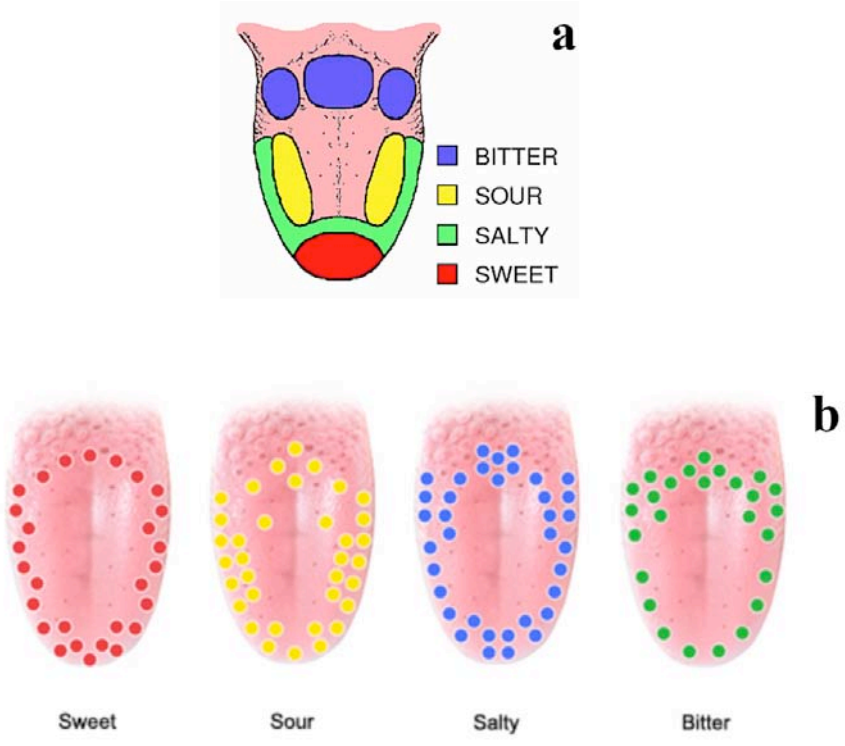

Figure 22 – a) Typical representation of flavour zones in a tongue; **b**) more accurate representation of the flavour zones in a tongue, all the flavours can be perceived on the whole tongue. From U.S. National Library of Medicine.

So the human tongue actually is made of nonspecific and low-selective "sensors" since all the tongue can taste all the flavours. This means that imaging the tongue as a device it would have sensors with cross-response, as the ET system. In the end the two systems, biological and artificial,

are really close on how they are made, while on how they work there is some difference.

Of course after tasting or analysing a sample, the data collected have to be processed to understand what that sample contains. The human tongue whether the sample is complex or not, will send all the data to the brain that, thanks to the experience and the learning process through the years, is able to understand the information. An ET system, instead, depending on the complexity of the sample can generate from a small to a huge amount of data, like for example when a mixture of compounds is present. As from definition an ET system use advanced mathematical procedures to understand the collected data, these procedures are usually based on Pattern Recognition techniques like for example ANN and/or PCA. A scheme comparison between an ET system and a "biological tongue system" analysis is shown in Figure 23, aiming to compare the steps inside the analysis made through the two methods, in this case as an example is shown a comparison of a wine test.

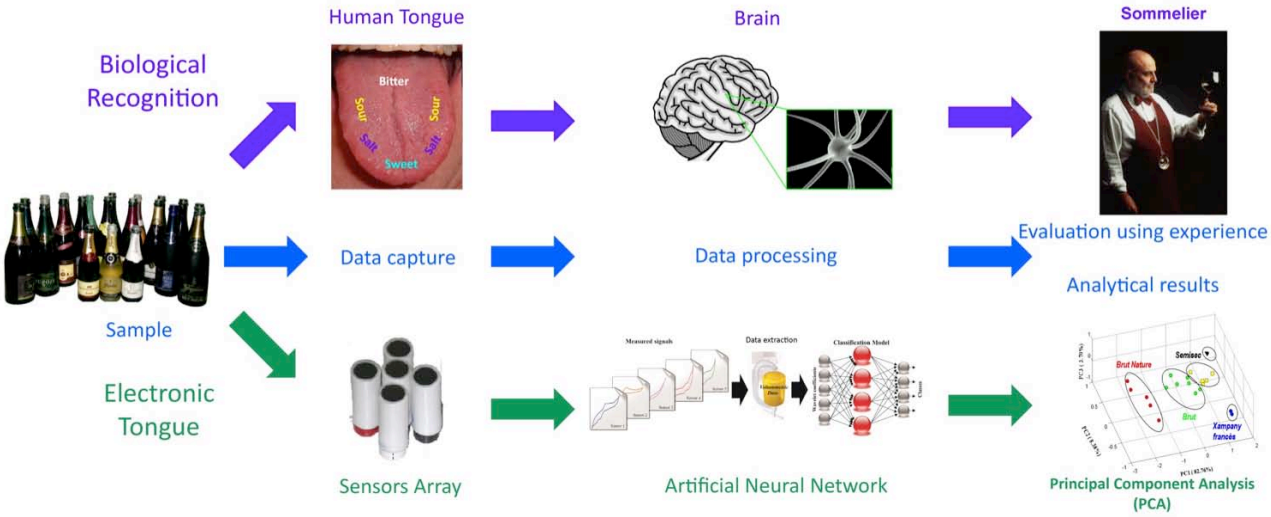

Figure 23 – Schematic comparison of the involved steps between an ET system and a "biological tongue system" (a sommelier) in a wine test. From reference [147]

For an ET the closest mathematical process to reproduce a human brain-like to analyse all the collected data is the ANN, since it is capable of managing a huge amount of information. Of course it is not always necessary to use this chemometric tool, but it can have advantages due to its ability to learn from internal errors and adjust the prediction to the best result. Well, what is an ANN? An ANN is a statistical learning model inspired by biological networks, like the brain, and is used to predict or approximate functions that can depend on a large number of inputs and are generally unknown. As in a brain an ANN is generally presented as a system of interconnected "neurons" which send messages to each other. In an ANN these connections have a numeric weights that can be tuned based on experience, making so neural networks adaptive to inputs and capable of learning [148]. Basically they consist in three layers, input layer, hidden layer and output layer, inside every

layer there is a number of "neurons", in the input layer it is decided by the number of data used by the ANN, in the hidden layer it is decided by the user and in the output layer depends on how many results we want, for example for a three compounds mixture, three neurons (Figure 24). A frequently used ANN model, with the capability of learning, in ET systems is what is called "back-propagation algorithm" that is part of the so-called Feed-forward Neural Networks [148] learning process. Not being the intent of this PhD work to explain in detail the math and reasons that are behind ANNs and ETs, but being just a possible application of the hybrid nanomaterial developed during this work, all the explanations about ANNs and ETs are at an entry-level and not deeply detailed to ease the understanding. As mentioned an ANN is a learning model, but it needs a basic level of "knowledge" that is given trough a training process. In other words the ANN needs that someone teaches it what to look for with known inputs, then it is able to process unknown inputs of the same kind and this step is strictly necessary especially for ET systems.

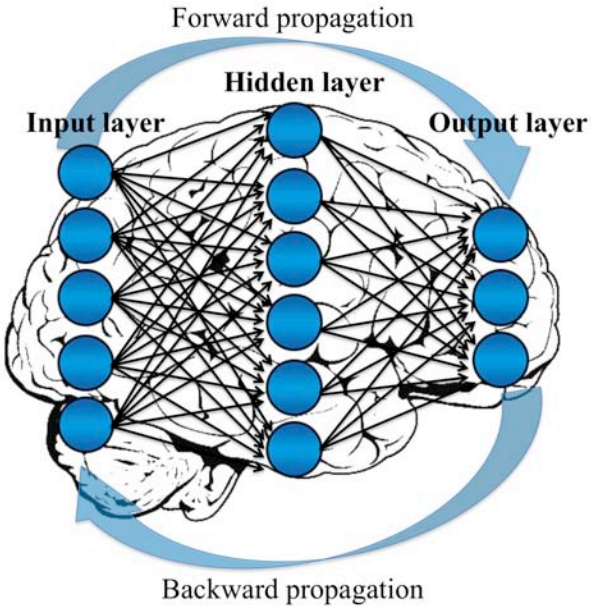

Figure 24 – Schematic representation of a simple ANN model for three target analytes with a "back-propagation algorithm", which consist in a first forward propagation of the inputs assigning them a numeric weight, and a backward propagation of the errors allowing the inputs to be re-weighted and start the loop again until, for example in a training step, the predicted values become closest to the known values, allowing in this way the learning process.

Briefly in practice, the training step to resolve, as an example, a three compounds mixture is carried out using a prepared set of standard solution containing different concentrations of the three compounds, usually the lowest, the middle and the highest concentrations in the range needed for the analysis considering a simple model; all these samples have known concentrations, forming so the training of the ANN. After this step, the further one is to test the ANN with some sample with a mixture of randomly chosen, but still known, concentration from the range needed for the analysis, to verify if the ANN is working properly. If the results are good is possible to apply that ANN

model also to unknown samples, having back for example the right concentration prediction for the compounds we trained the ANN for and which we want to analyse. The learning process is inside every step of the use of an ANN, as mentioned the frequently used algorithm for it is the "back-propagation algorithm", that is actually the most similar example of how the brain works. In few words, for example considering the training step, this algorithm consists in propagating forward the data inputs, i.e. collected from cyclic voltammetries, through the ANN then check with the known concentrations, consider the error and propagate it backward to adjust the prediction changing the numeric weight given for each data, and so on until it reaches the desired level of error. This learning process is tuneable thanks to the possibility of changing the number of "neurons" in the hidden layer or in the input layer, which is tuneable for example with a pre-step of data compression to reduce a bit the complexity of the data used for the input layer, and/or changing the transform functions that connect the layers and give back as a result the numeric weight of the data, allowing in this way a full control from the user and an adaptability to almost any kind of situation.

So the ET system could be a powerful instrument to analyse complex matrixes with cost-effective resources, if we consider the cost in money and time of high performance instruments (HPLC and similar), chemicals for preliminary resolution of mixtures to low the level of interferents or complexity and so on, and also could be applied for having a constant monitoring in production lines without having to manually take samples to the analysis lab, since the system can be automated. A big help to the ET system can be given from the CNTs/NPs hybrid nanomaterial, since the system needs low-selective sensors with a cross-response behaviour and sensors made with the CNTs/NPs material showed this potential beside a high sensitivity, a possibility to be integrated in many ways in the sensors devices and to be tuneable according to the field of use.

1.4 References

1. Roduner, E., *Size matters: why nanomaterials are different.* Chemical Society Reviews, 2006. **35**(7): p. 583-592.
2. Donega, C.d.M., *Synthesis and properties of colloidal heteronanocrystals.* Chemical Society Reviews, 2011. **40**(3): p. 1512-1546.
3. Alivisatos, A.P., *Perspectives on the physical chemistry of semiconductor nanocrystals.* Journal of Physical Chemistry, 1996. **100**(31): p. 13226-13239.
4. T.N.N. Initiative, Strategic Plan, 2004.
5. European Commission: Reccomendation on the definition of nanomaterials, Official Journal of the European Union, 2011. **L275**, 38-40
6. Iijima, S., *HELICAL MICROTUBULES OF GRAPHITIC CARBON.* Nature, 1991. **354**(6348): p. 56-58.
7. Ajayan, P.M. and O.Z. Zhou, *Applications of Carbon Nanotubes*, in *Carbon Nanotubes*, M. Dresselhaus, G. Dresselhaus, and P. Avouris, Editors. 2001, Springer Berlin Heidelberg. p. 391-425.
8. Harris, P.J.F., *Carbon Nanotube Science - Synthesis, Properties and Applications*. 2009, Cambridge Press.
9. Meyyappan, M., J. Han, and e. al., *Carbon Nanotubes - Science and Applications*. 2005, CRC Press.
10. Cohen, M.L., *Nanotubes, nanoscience, and nanotechnology.* Materials Science & Engineering C-Biomimetic and Supramolecular Systems, 2001. **15**(1-2): p. 1-11.
11. Ajayan, P.M., *Nanotubes from carbon.* Chemical Reviews, 1999. **99**(7): p. 1787-1799.
12. Zhao, Q., Z.H. Gan, and Q.K. Zhuang, *Electrochemical sensors based on carbon nanotubes.* Electroanalysis, 2002. **14**(23): p. 1609-1613.
13. Ajayan, P.M. and T.W. Ebbesen, *Nanometre-size tubes of carbon.* Reports on Progress in Physics, 1997. **60**(10): p. 1025-1062.
14. Dresselhaus, M.S., et al., *Nanowires and nanotubes.* Materials Science & Engineering C-Biomimetic and Supramolecular Systems, 2003. **23**(1-2): p. 129-140.
15. Balasubramanian, K. and M. Burghard, *Chemically functionalized carbon nanotubes.* Small, 2005. **1**(2): p. 180-192.
16. Thostenson, E.T., Z.F. Ren, and T.W. Chou, *Advances in the science and technology of carbon nanotubes and their composites: a review.* Composites Science and Technology, 2001. **61**(13): p. 1899-1912.
17. Lu, J.P., *Elastic Properties of Carbon Nanotubes and Nanoropes.* Physical Review Letters, 1997. **79**(7): p. 1297-1300.
18. Salvetat, J.P., et al., *Mechanical properties of carbon nanotubes.* Applied Physics A, 1999. **69**(3): p. 255-260.
19. Ebbesen, T.W., et al., *Electrical conductivity of individual carbon nanotubes.* Nature, 1996. **382**(6586): p. 54-56.
20. Lu, J.P. and J.I.E. Han, *Carbon nanotubes and nanotube-based nano devices.* International Journal of High Speed Electronics and Systems, 1998. **09**(01): p. 101-123.
21. Cao, A.Y., et al., *Super-compressible foamlike carbon nanotube films.* Science, 2005. **310**(5752): p. 1307-1310.
22. Ajayan, P.M., J.C. Charlier, and A.G. Rinzler, *Carbon nanotubes: From macromolecules to nanotechnology.* Proceedings of the National Academy of Sciences of the United States of America, 1999. **96**(25): p. 14199-14200.
23. Wildoer, J.W.G., et al., *Electronic structure of atomically resolved carbon nanotubes.* Nature, 1998. **391**(6662): p. 59-62.
24. Star, A., et al., *Nanotube optoelectronic memory devices.* Nano Letters, 2004. **4**(9): p. 1587-1591.
25. Chen, J., et al., *Bright infrared emission from electrically induced excitons in carbon nanotubes.* Science, 2005. **310**(5751): p. 1171-1174.
26. Misewich, J.A., et al., *Electrically induced optical emission from a carbon nanotube FET.* Science, 2003. **300**(5620): p. 783-786.
27. Zhou, C.W., J. Kong, and H.J. Dai, *Intrinsic electrical properties of individual single-walled carbon nanotubes with small band gaps.* Physical Review Letters, 2000. **84**(24): p. 5604-5607.

28. Ajayan, P.M., et al., *OPENING CARBON NANOTUBES WITH OXYGEN AND IMPLICATIONS FOR FILLING.* Nature, 1993. **362**(6420): p. 522-525.
29. Tsang, S.C., et al., *A SIMPLE CHEMICAL METHOD OF OPENING AND FILLING CARBON NANOTUBES.* Nature, 1994. **372**(6502): p. 159-162.
30. Hiura, H., T.W. Ebbesen, and K. Tanigaki, *OPENING AND PURIFICATION OF CARBON NANOTUBES IN HIGH YIELDS.* Advanced Materials, 1995. **7**(3): p. 275-276.
31. Gao, B., et al., *Electrochemical intercalation of single-walled carbon nanotubes with lithium.* Chemical Physics Letters, 1999. **307**(3-4): p. 153-157.
32. Zhao, J., et al., *First-principles study of Li-intercalated carbon nanotube ropes.* Physical Review Letters, 2000. **85**(8): p. 1706-1709.
33. Liu, X.L., et al., *Carbon nanotube field-effect inverters.* Applied Physics Letters, 2001. **79**(20): p. 3329-3331.
34. Frackowiak, E., et al., *Electrochemical storage of lithium multiwalled carbon nanotubes.* Carbon, 1999. **37**(1): p. 61-69.
35. Britto, P.J., et al., *Improved charge transfer at carbon nanotube electrodes.* Advanced Materials, 1999. **11**(2): p. 154-157.
36. Nugent, J.M., et al., *Fast electron transfer kinetics on multiwalled carbon nanotube microbundle electrodes.* Nano Letters, 2001. **1**(2): p. 87-91.
37. Dai, H.J., *Carbon nanotubes: Synthesis, integration, and properties.* Accounts of Chemical Research, 2002. **35**(12): p. 1035-1044.
38. Kingston, C.T. and B. Simard, *Fabrication of carbon nanotubes.* Analytical Letters, 2003. **36**(15): p. 3119-3145.
39. Zhou, O., et al., *Materials science of carbon nanotubes: Fabrication, integration, and properties of macroscopic structures of carbon nanotubes.* Accounts of Chemical Research, 2002. **35**(12): p. 1045-1053.
40. Ebbesen, T.W. and P.M. Ajayan, *LARGE-SCALE SYNTHESIS OF CARBON NANOTUBES.* Nature, 1992. **358**(6383): p. 220-222.
41. Journet, C., et al., *Large-scale production of single-walled carbon nanotubes by the electric-arc technique.* Nature, 1997. **388**(6644): p. 756-758.
42. Bethune, D.S., et al., *COBALT-CATALYZED GROWTH OF CARBON NANOTUBES WITH SINGLE-ATOMIC-LAYERWALLS.* Nature, 1993. **363**(6430): p. 605-607.
43. Thess, A., et al., *Crystalline ropes of metallic carbon nanotubes.* Science, 1996. **273**(5274): p. 483-487.
44. Eklund, P.C., et al., *Large-scale production of single-walled carbon nanotubes using ultrafast pulses from a free electron laser.* Nano Letters, 2002. **2**(6): p. 561-566.
45. Wang, J., *Carbon-nanotube based electrochemical biosensors: A review.* Electroanalysis, 2005. **17**(1): p. 7-14.
46. Sotiropoulou, S. and N.A. Chaniotakis, *Carbon nanotube array-based biosensor.* Analytical and Bioanalytical Chemistry, 2003. **375**(1): p. 103-105.
47. Valentini, F., et al., *Carbon nanotube purification: Preparation and characterization of carbon nanotube paste electrodes.* Analytical Chemistry, 2003. **75**(20): p. 5413-5421.
48. Junhua Fan, M.W., Daoben Zhu, Baohe Chang, Zhenwei Pan, Sishen Xie, *Synthesis, Characterizations, and Physical Properties of Carbon Nanotubes Coated by Conducting Polypyrrole.* J Appl Pol Sci, 1999. **74**.
49. Mercedes Alvaro, C.A., Belen Ferrer, and Hermenegildo Garcia, *Functional Molecules from Single Wall Carbon Nanotubes. Photoinduced Solubility of Short Single Wall Carbon Nanotube Residues by Covalent Anchoring of 2,4,6-Triarylpyrylium Units.* JACS, 2007. **129**.
50. Wu, H.Q., et al., *Synthesis of copper oxide nanoparticles using carbon nanotubes as templates.* Chemical Physics Letters, 2002. **364**(1-2): p. 152-156.
51. Hu, C.G., et al., *Systematic investigation on the properties of carbon nanotube electrodes with different chemical treatments.* Journal of Physics and Chemistry of Solids, 2004. **65**(10): p. 1731-1736.
52. Rubianes, M.D. and G.A. Rivas, *Carbon nanotubes paste electrode.* Electrochemistry Communications, 2003. **5**(8): p. 689-694.
53. Chicharro, M., et al., *Adsorptive stripping voltammetric determination of amitrole at a multi-wall carbon nanotubes paste electdrode.* Electroanalysis, 2005. **17**(5-6): p. 476-482.

54. Wang, J., A.N. Kawde, and M. Musameh, *Carbon-nanotube-modified glassy carbon electrodes for amplified label-free electrochemical detection of DNA hybridization.* Analyst, 2003. **128**(7): p. 912-916.
55. Musameh, M., et al., *Low-potential stable NADH detection at carbon-nanotube-modified glassy carbon electrodes.* Electrochemistry Communications, 2002. **4**(10): p. 743-746.
56. Zhang, M.G., A. Smith, and W. Gorski, *Carbon nanotube-chitosan system for electrochemical sensing based on dehydrogenase enzymes.* Analytical Chemistry, 2004. **76**(17): p. 5045-5050.
57. Wang, J.X., et al., *Electrocatalytic oxidation of 3,4-dihydroxyphenylacetic acid at a glassy carbon electrode modified with single-wall carbon nanotubes.* Electrochimica Acta, 2001. **47**(4): p. 651-657.
58. Wang, J., M. Musameh, and Y.H. Lin, *Solubilization of carbon nanotubes by Nafion toward the preparation of amperometric biosensors.* Journal of the American Chemical Society, 2003. **125**(9): p. 2408-2409.
59. Wang, J. and M. Musameh, *Carbon nanotube/teflon composite electrochemical sensors and biosensors.* Analytical Chemistry, 2003. **75**(9): p. 2075-2079.
60. Pumera, M., A. Merkoci, and S. Alegret, *Carbon nanotube-epoxy composites for electrochemical sensing.* Sensors and Actuators B-Chemical, 2006. **113**(2): p. 617-622.
61. Wang, J. and M. Musameh, *Carbon nanotube screen-printed electrochemical sensors.* Analyst, 2004. **129**(1): p. 1-2.
62. Sciau, P., *The Delivery of Nanoparticles*. 2012, InTech.
63. Colomban, P., *The Use of Metal Nanoparticles to Produce Yellow, Red and Iridescent Colour, from Bronze Age to Present Times in Lustre Pottery and Glass: Solid State Chemistry, Spectroscopy and Nanostructure.* Journal of Nano Research, 2009. **8**: p. 109-132.
64. Sciau, P., et al., *Double Nanoparticle Layer in a 12(th) Century Lustreware Decoration: Accident or Technological Mastery?* Journal of Nano Research, 2009. **8**: p. 133-139.
65. Freestone, I., et al., *The Lycurgus Cup — A Roman nanotechnology.* Gold Bulletin, 2007. **40**(4): p. 270-277.
66. Leonhardt, U., *Optical metamaterials - Invisibility cup.* Nature Photonics, 2007. **1**(4): p. 207-208.
67. Faraday, M., *Experimenta Relations of Gold (and other Metals) to Light.* Philos. Trans. R Soc. London, 1857. **147**: p. 145.
68. Mino, L., et al., *Low-dimensional systems investigated by x-ray absorption spectroscopy: a selection of 2D, 1D and 0D cases.* Journal of Physics D-Applied Physics, 2013. **46**(42).
69. Groeneveld, E., *Synthesis and optical spectroscopy of (hetero)-nanocrystals: an exciting interplay between chemistry and physics*, Ph.D. Thesis, Utrecht University, Utrecht, 2012
70. Haruta, M., *Size- and support-dependency in the catalysis of gold.* Catalysis Today, 1997. **36**(1): p. 153-166.
71. Kelsall, R., I. Hamley, and M. Geoghegan, *Nanoscale science and technology*. 2005, Wiley, New Jersey.
72. Bhattacharya, P., S. Ghosh, and A.D. Stiff-Roberts, *Quantum dot opto-electronic devices.* Annual Review of Materials Research, 2004. **34**: p. 1-40.
73. Mocatta, D., et al., *Heavily Doped Semiconductor Nanocrystal Quantum Dots.* Science, 2011. **332**(6025): p. 77-81.
74. Norris, D.J., A.L. Efros, and S.C. Erwin, *Doped nanocrystals.* Science, 2008. **319**(5871): p. 1776-1779.
75. Holder, E., N. Tessler, and A.L. Rogach, *Hybrid nanocomposite materials with organic and inorganic components for opto-electronic devices.* Journal of Materials Chemistry, 2008. **18**(10): p. 1064-1078.
76. Wang, J., *Nanomaterial-based electrochemical biosensors.* Analyst, 2005. **130**(4): p. 421-426.
77. Shipway, A.N., E. Katz, and I. Willner, *Nanoparticle arrays on surfaces for electronic, optical, and sensor applications.* Chemphyschem, 2000. **1**(1): p. 18-52.
78. Zhu, M., et al., *Novel nitric oxide microsensor and its application to the study of smooth muscle cells.* Analytica Chimica Acta, 2002. **455**(2): p. 199-206.
79. Raj, C.R., T. Okajima, and T. Ohsaka, *Gold nanoparticle arrays for the voltammetric sensing of dopamine.* Journal of Electroanalytical Chemistry, 2003. **543**(2): p. 127-133.
80. You, T.Y., et al., *Characterization of platinum nanoparticle-embedded carbon film electrode and its detection of hydrogen peroxide.* Analytical Chemistry, 2003. **75**(9): p. 2080-2085.

81. You, T.Y., et al., *An amperometric detector formed of highly dispersed Ni nanoparticles embedded in a graphite-like carbon film electrode for sugar determination.* Analytical Chemistry, 2003. **75**(19): p. 5191-5196.
82. Xu, J.Z., et al., *Nano-sized copper oxide modified carbon paste electrodes as an amperometric sensor for amikacin.* Analytical Letters, 2003. **36**(13): p. 2723-2733.
83. Xiao, Y., et al., *"Plugging into enzymes": Nanowiring of redox enzymes by a gold nanoparticle.* Science, 2003. **299**(5614): p. 1877-1881.
84. Wang, L. and E.K. Wang, *Direct electron transfer between cytochrome c and a gold nanoparticles modified electrode.* Electrochemistry Communications, 2004. **6**(1): p. 49-54.
85. Liu, S.Q., et al., *Immobilization of hemoglobin on zirconium dioxide nanoparticles for preparation of a novel hydrogen peroxide biosensor.* Biosensors & Bioelectronics, 2004. **19**(9): p. 963-969.
86. Kongkanand, A., et al., *Highly dispersed Pt catalysts on single-walled carbon nanotubes and their role in methanol oxidation.* Journal of Physical Chemistry B, 2006. **110**(33): p. 16185-16188.
87. Mu, Y.Y., et al., *Controllable Pt nanoparticle deposition on carbon nanotubes as an anode catalyst for direct methanol fuel cells.* Journal of Physical Chemistry B, 2005. **109**(47): p. 22212-22216.
88. Anson, A., et al., *Hydrogen capacity of palladium-loaded carbon materials.* Journal of Physical Chemistry B, 2006. **110**(13): p. 6643-6648.
89. Yildirim, T. and S. Ciraci, *Titanium-decorated carbon nanotubes as a potential high-capacity hydrogen storage medium.* Physical Review Letters, 2005. **94**(17).
90. Guldi, D.M., et al., *CNT-CdTe versatile donor-acceptor nanohybrids.* Journal of the American Chemical Society, 2006. **128**(7): p. 2315-2323.
91. Lee, H., et al., *In-situ growth of copper sulfide nanocrystals on multiwalled carbon nanotubes and their application as novel solar cell and amperometric glucose sensor materials.* Nano Letters, 2007. **7**(3): p. 778-784.
92. Lu, G., L.E. Ocola, and J. Chen, *Room-Temperature Gas Sensing Based on Electron Transfer between Discrete Tin Oxide Nanocrystals and Multiwalled Carbon Nanotubes.* Advanced Materials, 2009. **21**(24): p. 2487-+.
93. Sun, Y. and H.H. Wang, *High-performance, flexible hydrogen sensors that use carbon nanotubes decorated with palladium nanoparticles.* Advanced Materials, 2007. **19**(19): p. 2818-+.
94. Kong, B.-S., et al., *Single-walled carbon nanotube gold nanohybrids: Application in highly effective transparent and conductive films.* Journal of Physical Chemistry C, 2007. **111**(23): p. 8377-8382.
95. Zhang, Y., et al., *Composite anode material of silicon/graphite/carbon nanotubes for Li-ion batteries.* Electrochimica Acta, 2006. **51**(23): p. 4994-5000.
96. Valden, M., X. Lai, and D.W. Goodman, *Onset of catalytic activity of gold clusters on titania with the appearance of nonmetallic properties.* Science, 1998. **281**(5383): p. 1647-1650.
97. Yu, M.F., et al., *Strength and breaking mechanism of multiwalled carbon nanotubes under tensile load.* Science, 2000. **287**(5453): p. 637-640.
98. Landi, B.J., et al., *CdSe quantum dot-single wall carbon nanotube complexes for polymeric solar cells.* Solar Energy Materials and Solar Cells, 2005. **87**(1-4): p. 733-746.
99. Conner, W.C. and J.L. Falconer, *Spillover in heterogeneous catalysis.* Chemical Reviews, 1995. **95**(3): p. 759-788.
100. Banerjee, S. and S.S. Wong, *Synthesis and characterization of carbon nanotube-nanocrystal heterostructures.* Nano Letters, 2002. **2**(3): p. 195-200.
101. Haremza, J.M., M.A. Hahn, and T.D. Krauss, *Attachment of single CdSe nanocrystals to individual single-walled carbon nanotubes.* Nano Letters, 2002. **2**(11): p. 1253-1258.
102. Zhang, J.P., et al., *Periodic square-like gold nanoparticle arrays templated by self-assembled 2D DNA nanogrids on a surface.* Nano Letters, 2006. **6**(2): p. 248-251.
103. Han, X., Y. Li, and Z. Deng, *DNA-wrapped single-walled carbon nanotubes as rigid templates for assembling linear gold nanoparticle arrays.* Advanced Materials, 2007. **19**(11): p. 1518-+.
104. Smorodin, T., U. Beierlein, and J.P. Kotthaus, *Contacting gold nanoparticles with carbon nanotubes by self-assembly.* Nanotechnology, 2005. **16**(8): p. 1123-1125.
105. Chaudhary, S., et al., *Fluorescence microscopy visualization of single-walled carbon nanotubes using semiconductor nanocrystals.* Nano Letters, 2004. **4**(12): p. 2415-2419.
106. Wang, L., et al., *Alternate assemblies of polyelectrolyte functionalized carbon nanotubes and platinum nanoparticles as tunable electrocatalysts for dioxygen reduction.* Electrochemistry Communications, 2007. **9**(4): p. 827-832.

107. Jiang, K.Y., et al., *Selective attachment of gold nanoparticles to nitrogen-doped carbon nanotubes.* Nano Letters, 2003. **3**(3): p. 275-277.
108. Kim, B. and W.M. Sigmund, *Functionalized multiwall carbon nanotube/gold nanoparticle composites.* Langmuir, 2004. **20**(19): p. 8239-8242.
109. Han, L., et al., *A direct route toward assembly of nanoparticle-carbon nanotube composite materials.* Langmuir, 2004. **20**(14): p. 6019-6025.
110. Sainsbury, T., J. Stolarczyk, and D. Fitzmaurice, *An experimental and theoretical study of the self-assembly of gold nanoparticles at the surface of functionalizied multiwalled carbon nanotubes.* Journal of Physical Chemistry B, 2005. **109**(34): p. 16310-16325.
111. Lee, Y., et al., *Spontaneous formation of transition-metal nanoparticles on single-walled carbon nanotubes anchored with conjugated molecules.* Small, 2005. **1**(10): p. 975-979.
112. Xue, B., et al., *Growth of Pd, Pt, Ag and Au nanoparticles on carbon nanotubes.* Journal of Materials Chemistry, 2001. **11**(9): p. 2378-2381.
113. Yu, R.Q., et al., *Platinum deposition on carbon nanotubes via chemical modification.* Chemistry of Materials, 1998. **10**(3): p. 718-722.
114. Zanella, R., et al., *Deposition of gold nanoparticles onto thiol-functionalized multiwalled carbon nanotubes.* Journal of Physical Chemistry B, 2005. **109**(34): p. 16290-16295.
115. Shi, Y., R. Yang, and P.K. Yuet, *Easy decoration of carbon nanotubes with well dispersed gold nanoparticles and the use of the material as an electrocatalyst.* Carbon, 2009. **47**(4): p. 1146-1151.
116. Wu, H.-X., et al., *In situ growth of copper nanoparticles on multiwalled carbon nanotubes and their application as non-enzymatic glucose sensor materials.* Electrochimica Acta, 2010. **55**(11): p. 3734-3740.
117. Ling Meng, J.J., Gaixiu Yang, Tianhong Lu, Hui Zhang, and Chenxin Cai, *Nonenzymatic Electrochemical Detection of Glucose Based on Palladium-Single-Walled Carbon Nanotube Hybrid Nanostructures.* Anal Chem, 2009. **81**(17).
118. Zhang, M.N., L. Su, and L.Q. Mao, *Surfactant functionalization of carbon nanotubes (CNTs) for layer-by-layer assembling of CNT multi-layer films and fabrication of gold nanoparticle/CNT nanohybrid.* Carbon, 2006. **44**(2): p. 276-283.
119. Hu, J.P., et al., *Efficient method to functionalize carbon nanotubes with thiol groups and fabricate gold nanocomposites.* Chemical Physics Letters, 2005. **401**(4-6): p. 352-356.
120. Choi, H.C., et al., *Spontaneous reduction of metal ions on the sidewalls of carbon nanotubes.* Journal of the American Chemical Society, 2002. **124**(31): p. 9058-9059.
121. Qu, L.T. and L.M. Dai, *Substrate-enhanced electroless deposition of metal nanoparticles on carbon nanotubes.* Journal of the American Chemical Society, 2005. **127**(31): p. 10806-10807.
122. Wildgoose, G.G., C.E. Banks, and R.G. Compton, *Metal nanoparticles and related materials supported on carbon nanotubes: Methods and applications.* Small, 2006. **2**(2): p. 182-193.
123. Guo, D.J. and H.L. Li, *High dispersion and electrocatalytic properties of Pt nanoparticles on SWNT bundles.* Journal of Electroanalytical Chemistry, 2004. **573**(1): p. 197-202.
124. Day, T.M., et al., *Electrochemical templating of metal nanoparticles and nanowires on single-walled carbon nanotube networks.* Journal of the American Chemical Society, 2005. **127**(30): p. 10639-10647.
125. Quinn, B.M., C. Dekker, and S.G. Lemay, *Electrodeposition of noble metal nanoparticles on carbon nanotubes.* Journal of the American Chemical Society, 2005. **127**(17): p. 6146-6147.
126. Salimi, A., et al., *Electrochemical detection of trace amount of arsenic(III) at glassy carbon electrode modified with cobalt oxide nanoparticles.* Sensors and Actuators B-Chemical, 2008. **129**(1): p. 246-254.
127. Tessonnier, J.P., et al., *Pd nanoparticles introduced inside multi-walled carbon nanotubes for selective hydrogenation of cinnamaldehyde into hydrocinnamaldehyde.* Applied Catalysis a-General, 2005. **288**(1-2): p. 203-210.
128. Kim, H.S., et al., *Hydrogen storage in Ni nanoparticle-dispersed multiwalled carbon nanotubes.* Journal of Physical Chemistry B, 2005. **109**(18): p. 8983-8986.
129. Mu, S.C., et al., *Synthesis and evaluation on performance of hydrogen storage of multi-walled carbon nanotubes decorated with platinum.* Journal of Wuhan University of Technology-Materials Science Edition, 2003. **18**(3): p. 33-35.

130. Qu, J.Y., et al., *Preparation of hybrid thin film modified carbon nanotubes on glassy carbon electrode and its electrocatalysis for oxygen reduction.* Chemical Communications, 2004(1): p. 34-35.
131. Sheeney-Haj-Khia, L., B. Basnar, and I. Willner, *Efficient generation of photocurrents by using CdS/Carbon nanotube assemblies on electrodes.* Angewandte Chemie-International Edition, 2005. **44**(1): p. 78-83.
132. Bottini, M., et al., *Full-length single-walled carbon nanotubes decorated with streptavidin-conjugated quantum dots as multivalent intracellular fluorescent nanoprobes.* Biomacromolecules, 2006. **7**(8): p. 2259-2263.
133. Jia, N., et al., *Intracellular delivery of quantum dots tagged antisense oligodeoxynucleotides by functionalized multiwalled carbon nanotubes.* Nano Letters, 2007. **7**(10): p. 2976-2980.
134. Lu, Y.J., et al., *Room temperature methane detection using palladium loaded single-walled carbon nanotube sensors.* Chemical Physics Letters, 2004. **391**(4-6): p. 344-348.
135. Sun, Y. and H.H. Wang, *Electrodeposition of Pd nanoparticles on single-walled carbon nanotubes for flexible hydrogen sensors.* Applied Physics Letters, 2007. **90**(21).
136. Huang, J., et al., *Simultaneous electrochemical determination of dopamine, uric acid and ascorbic acid using palladium nanoparticle-loaded carbon nanofibers modified electrode.* Biosens Bioelectron, 2008. **24**(4): p. 632-7.
137. Rong, L.-Q., et al., *Study of the nonenzymatic glucose sensor based on highly dispersed Pt nanoparticles supported on carbon nanotubes.* Talanta, 2007. **72**(2): p. 819-824.
138. Shen, Y., et al., *Dendrimer-encapsulated Pd nanoparticles anchored on carbon nanotubes for electro-catalytic hydrazine oxidation.* Electrochemistry Communications, 2009. **11**(6): p. 1329-1332.
139. Zhao, W., et al., *A novel nonenzymatic hydrogen peroxide sensor based on multi-wall carbon nanotube/silver nanoparticle nanohybrids modified gold electrode.* Talanta, 2009. **80**(2): p. 1029-1033.
140. Chen, S., et al., *Amperometric third-generation hydrogen peroxide biosensor based on the immobilization of hemoglobin on multiwall carbon nanotubes and gold colloidal nanoparticles.* Biosensors & Bioelectronics, 2007. **22**(7): p. 1268-1274.
141. Vlasov, Y., et al., *Nonspecific sensor arrays ("electronic tongue") for chemical analysis of liquids (IUPAC Technical Report).* Pure and Applied Chemistry, 2005. **77**(11): p. 1965-1983.
142. McCulloch, W.S. and W. Pitts, *A logical calculus of the ideas immanent in nervous activity.* Bull Math Biophys, 1943. **5**((4)): p. 115-133.
143. Persaud, K. and G. Dodd, *ANALYSIS OF DISCRIMINATION MECHANISMS IN THE MAMMALIAN OLFACTORY SYSTEM USING A MODEL NOSE.* Nature, 1982. **299**(5881): p. 352-355.
144. Di Natale, C., et al. in *Proc. Intern. Conf. EUROSENSORS IX*. 1995, p. 512. Stockholm, Sweden.
145. Menche, N., *Biologie Anatomie Physiologie*. 2012, Elsevier GmbH, Munich.
146. Schmidt, R.F., F. Lang, and M. Heckmann, *Physiologie des Menschen - mit Pathophysiologie*. 31 ed. 2011, Springer, Heidelberg.
147. Cetó, X., et al., *Voltammetric Electronic Tongue in the Analysis of Cava Wines.* Electroanalysis, 2011. **23**(1): p. 72-78.
148. Huajin Tang, Kay Chen Tan, and Z. Yi, *Neural Networks: Computational, Models and Apllications*. 2007, Springer-Verlag, Berlin Heidelberg. 300.

CHAPTER 2 – OBJECTIVES

2. Objectives

The objectives of this work were:

1. To synthesise with an easy and quick protocol Nano-hybrid materials composed by CNTs and metal NPs;
2. To demonstrate the applicability of the CNTs/NPs Nano-hybrid materials as electrode platform for sensors and biosensors;
3. To gain a basic knowledge of ET systems and their data processing methods, like ANNs used in our lab;
4. To integrate the sensors modified with CNTs/NPs Nano-hybrid material, containing different metal NPs, into an ET system.

CHAPTER 3 – EXPERIMENTAL

3. Experimental

All the materials, instrument and procedure listed in this chapter are related to the works in the following list:

Article 1 – A. Cipri and M. del Valle, *Palladium nanoparticles/multiwalled carbon nanotubes electrode system for voltammetric sensing of Tyrosine*, Journal of Nanoscience and Nanotechnology, 2014, 14, 6692 – 6698;

Article 2 – A. C. d. Sá, A. Cipri, A. González-Calabuig et al., *Resolution of galactose, glucose, xylose and mannose in sugarcane bagasse employing a voltammetric electronic tongue formed by metals oxy-hydroxide/MWCNT modified electrodes*, Sensors and Actuators B: Chemical, 2015, 222, 645-653;

Article 3 – A. Cipri, C. Schulz et al., *A novel Bio-Electronic Tongue using cellobiose dehydrogenases to resolve mixtures of various sugars and interfering analytes*, (Manuscript submitted to Biosensors and Bioelectronics).

3.1 Materials

Purified multiwalled carbon nanotubes (MWCNTs) with an outer diameter of 30 nm were purchased from SES Research (Houston, Texas, USA). Palladium chloride ($PdCl_2$), Gold(III) chloride trihydrate ($HAuCl_4 \cdot 3H_2O$), Cobalt(II) chloride hexahydrate ($Cl_2Co \cdot 6H2O$), Nickel(II) sulfate hexahydrate ($NiSO_4 \cdot 6H_2O$), ammonium fluoride (NH_4F), boric acid (H_3BO_3), sodium borohydride ($NaBH_4$), N-N-Dimethylformamide 99.8% (C_3H_7NO), sodium chloride (NaCl), 3-(N-morpholino)propanesulfonic acid (MOPS), lactose, D-Glucose, D-Galactose, D-Mannose, D-Xylose, ethanol (EtOH), trisodium citrate dihydrate, sodium dodecyl sulfate (SDS), sodium hydroxide (NaOH), hydrogen peroxide (H_2O_2), 6-mercapto-1-hexanol 97%, and polystyrene were purchased from Sigma-Aldrich (St. Louis, MO, USA). Copper(II) sulfate pentahydrate ($CuSO_4 \cdot 5H_2O$), calcium chloride ($CaCl_2$), sulphuric acid 96% (H_2SO_4), nitric acid 69% (HNO_3), ammonia 32% (NH_3), mesitylene and L-Tyrosine were purchased from Merck (Darmstad, Germany). Dialysis membranes (Spectrapor, MWCO 12-14 kDA) were purchased from Spectrum Medical Industries (CA, USA).

Cellobiose dehydrogenase (CDH) from *Myriococcum thermophilum* (*Mt*CDH) [1] and a mutant of CDH from *Corynascus thermophilus* with enhanced activity for glucose (*Ct*CDHC291Y) [2, 3] were recombinantly expressed in *Pichia pastoris*. CDH from *Neurospora crassa* (*Nc*CDH) was harvested and purified from the fungus culture [4]. The CDH preparations were used directly without further dilution and had concentrations of 7 mg/ml for *Mt*CDH, 18.8 mg/ml for *Ct*CDHC291Y and 8.4 mg/ml for *Nc*CDH. The concentrations of the enzymes were determined photometrically converting the absorption measured at 280 nm to a protein concentration by using the calculated absorption coefficients based on the amino acid sequences.

All solutions were made using MilliQ water from MilliQ System (Millipore, Billerica, MA, USA), and the buffers used in the different papers are described in Table 3.1.

Table 3.1 – Buffer compositions

	Buffer composition	**pH value**
Article 1 – PBS buffer	187 mM NaCl, 2.7 mM KCl, 8.1 mM di-hydrated Na_2HPO_4 , 1.76 mM KH_2PO_4	7.0
Article 2 – PBS buffer	100 mM Na_2HPO_4 and 100 mM mono-hydrated NaH_2PO_4	7.0
Article 3 – MOPS buffer*	50 mM MOPS	6.7

* The buffer was adjusted to an ionic strength of 63mM with NaCl, the pH of 6.7 and an ionic strength of 63 mM were chosen to potentially mimic the conditions present in cow's milk [5].

3.2 Instruments

Transmission electron microscopy (TEM) images and microanalysis patterns were recorded with a JEOL JEM-2011 microscope equipped with an energy dispersive spectroscopy (EDS) detector. Scanning electron microscopy (SEM) images were performed on a Zeiss Merlin (FE-SEM) microscope. The voltammetric characterizations, mainly cyclic voltammetry and linear sweep voltammetry, were made with a DROPSENS μStat 8000 multi potentiostat/galvanostat (Dropsens, Oviedo, Spain), a 6-channel AUTOLAB PGSTAT20 potentiostat (Ecochemie, Utrecht, Netherlands) and an EmStat2 PalmSens potentiostat (PalmSens, Utrecht, Netherland). In *Paper 1* the electrode configuration used has been a DROPSENS carbon screen-printed electrode (DS110, working electrode = carbon, pseudo-reference = Ag, auxiliary electrode = carbon); in *Paper 2* the electrode configuration used has been a set of five glassy carbon (GC) electrode as working electrodes, a double junction Ag/AgCl electrode as reference electrode and a Platinum electrode as auxiliary electrode; in *Paper 3* the electrode configuration used has been a set of three gold electrodes as working electrodes (WE), a saturated calomel electrode (SCE) as a reference electrode and a platinum flag as an auxiliary electrode.

3.3 Electrode preparation

In this thesis work three different kind of electrodes were used, graphite-epoxy composite electrode (GEC), screen-printed electrode (SPE) and conventional Au and GC electrodes. The GEC electrodes have been used to test the goodness of the materials synthesised since this kind of electrodes have been used in our lab for a long time and are highly re-usable and with a high surface

area, they have been fabricated following a known procedure in our lab mixing 50 μM particle size graphite powder (BDH Laboratory Supplies, Poole, UK) and Epotek H77 resin and hardener (Epoxy Technologies, Billerica, MA).

The fabrication procedure of the GEC electrodes is as follow:

A small copper disk is soldered to an electrical connector and then fitted into a PVC tube (internal diameter 6 mm), the conductive paste (epoxy resin, hardener and graphite powder thoroughly mixed together) was deposited filling the cavity in the plastic body (Figure 3.1, right side). A comparison of the three styles of working electrode used is shown in Figure 3.1..

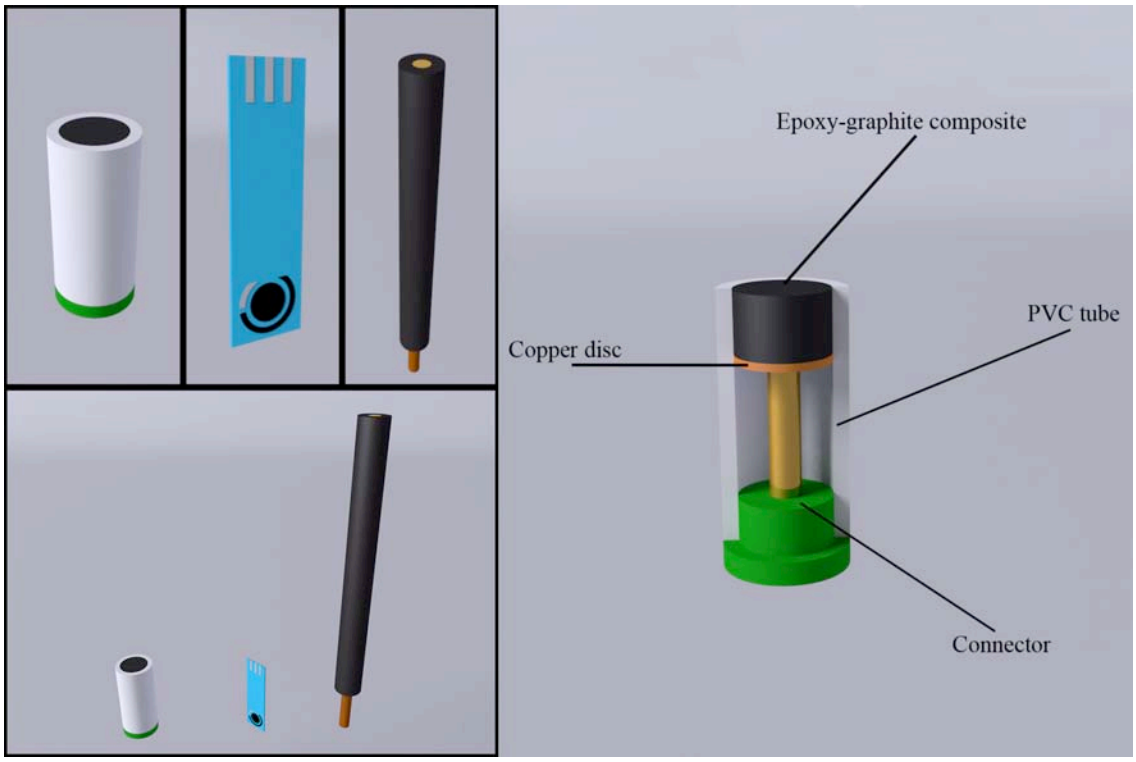

Figure 3.1 – Left side – Graphic representation of the working electrode used; Top left to right: GEC electrode, SPE and conventional rod electrode (as an example is shown a Au electrode); Bottom: comparison between the electrodes to have an idea of the difference in size. Right side – Epoxy-graphite composite electrode section view.

All the working electrodes were then modified with a layer of nano-hybrid material, CNTs/NPs (metal NPs of Pd, Au, CuO, Co, Ni) or enzymes.

Article 1: A GEC electrode was previously polished with a high precision wet/dry sandpaper, then an ink-like solution, made mixing CNTs/Pd NPs, graphite, polystyrene (respectively 20%, 48% and 32% w/w) and mesitylene as solvent[6], was casted on the GECs electrode surface to firstly test the goodness of the material and on the SPEs surface. After the right amount of solvent to have the right thickness of the ink was found, a SPE was modified with the same ink and used for the test and results reported in the *Article 1*.

Article 2: The GC electrodes were previously polished on a polishing cloth with 0.3 μm alumina powder (Merck, Darmstad, Germany), then a solution of CNTs/NPs (Pd, Au, CuO) in DMF was dropped on the GC electrode surface on 3 of 5 sensors and let them drying at 50 °C for 3 h, for the other 2 sensors a solution of purified CNTs in DMF was dropped on the GC electrode surface and immediately after the CNTs modification Co and Ni metal NPs were electrodeposited. To obtain the requested CNTs/metals oxy-hydroxide a further step was requested, all the sensors were passivated in a NaOH solution in a specific potential range for each metal, as reported in Table 3.2

Table 3.2 – Potential range for passivation of the different CNTs/NPs

CNT/NPs material	Potential range (V)	Scan rate (mV/s)	Cyclic Voltammetry scan number
CNTs/Pd	-0.8 – 0.8	50 mV/s	20 cycles
CNTs/Au	-0.4 – 0.5	50 mV/s	20 cycles
CNTs/CuO	-0.5 – 0.3	50 mV/s	20 cycles
CNTs/Co	-0.3 – 0.7	50 mV/s	45 cycles
CNTs/Ni	-0.5 – 1.0	100 mV/s	30 cycles

Article 3: The Au electrodes were cleaned by incubation in Piranha solution for 2 min (1:3 mixture conc. H_2O_2 with H_2SO_4. **Careful, the compounds react violently and highly exothermic with each other**), polished on polishing cloths with deagglomerated alumina slurry of a diameter of 1 μm (Struers, Ballerup, Danmark), sonicated in ultrapure water for 5 min and electrochemically cleaned in 0.5 M H_2SO_4 by cycling 30 times between 0.1 V and 1.7 V vs. SCE at a scan rate of 300 mV/s. The sensors were modified with a self-assembled monolayer (SAM) by immediately after rinsing with water, immersing the electrodes in a 10 mM ethanolic solution of 6-mercapto-1-hexanol overnight at room temperature. The electrodes were gently rinsed with ultrapure water and excess liquid was shaken off. On each of the three electrodes forming the ET 5 μL of a CDH solution, either *Mt*CDH, *Nc*CDH or *Ct*CDHC291Y was dropped on the SAM modified gold electrode surface and entrapped by covering it with a pre-soaked dialysis membrane, which was fixed with a rubber O-ring and Parafilm (Bemis, Neenah, WI, USA) as described by Haladjian and coworkers [7] and as shown in Figure 3.2.

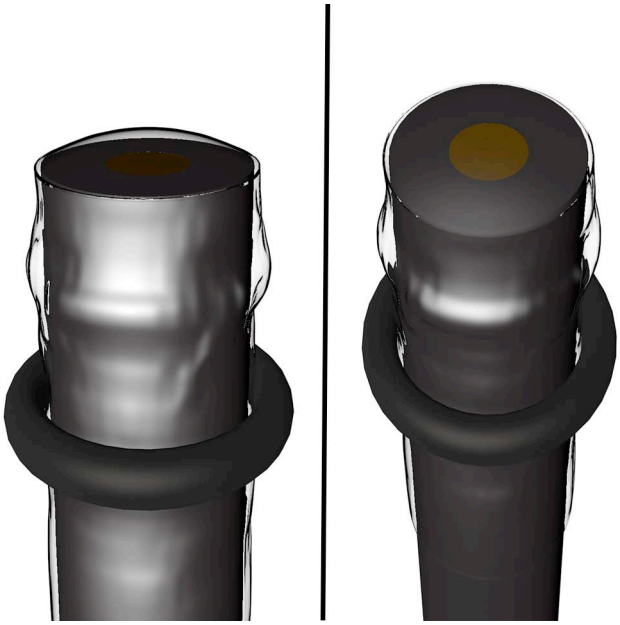

Figure 3.2 – Working electrode configuration for *Article 3*.

3.4 Data processing – ANN building

In order to prove the capabilities of the ET systems assembled in *Article 2* and *Article 3*, to be able to perform a simultaneous quantification of different analytes, a multivariate calibration process based on an ANN response model was prepared. The ANN building has been a bit different between the two papers mainly due to the number of targets involved.

Article 2: In this paper a total set of 46 samples, containing a mixture of glucose, galactose, mannose and xylose, was prepared with a concentration range of 0.5 to 2.5 mM for each target (Figure 3.3). The samples set was divided in two data subsets, training and test subset. The training subset was made of 36 samples distributed along a L36 Taguchi design [8], with 4 factors and 3 levels; the test subset was made of 10 samples randomly distributed inside the experimental domain. This approach was taken due to the number of targets involved in the experiment (4 sugars) not manageable with a simple 3-level factorial design. The amount of data generated from the sensors was really high (5 sensors x 336 current values x 46 samples, for a total of 77 280 values), so a pre-processing step was used to compress the original data. The aim of this step was to reduce the complexity of the input data, while preserving the relevant information, and reduce the training time needed from the ANN software, beside this advantages the pre-processing step allowed also to avoid redundancy in input data and to generate a model with better generalization ability. The compression of the data was performed using a Discrete Wavelet Transform (DWT) [9] with a Daubechies 4 (db4) wavelet mother function and a 4^{th} decomposition level. This pre-processing step allowed to reduce the original amount of data from 77 280 to 135 coefficients without any loss of relevant information; an additional refining step was added, using a Causal Index pruning strategy [10] to remove the inputs with a relatively small contribution to the model. With this additional step the 135 coefficients went down to 36, achieving a total compression ratio of 97.9%.

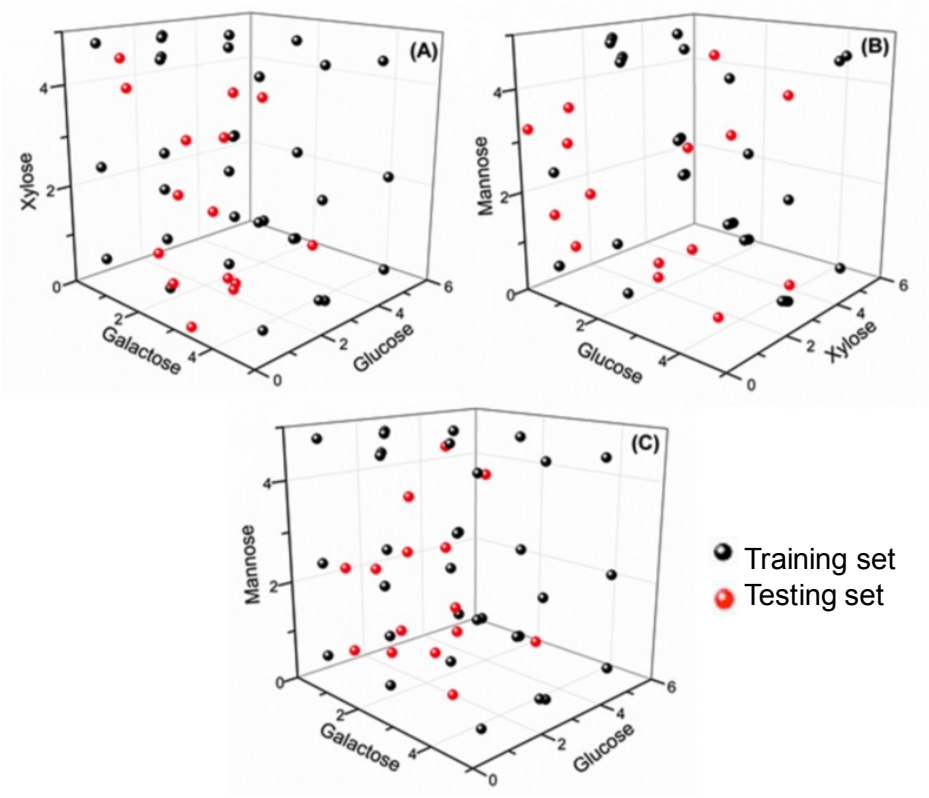

Figure 3.3 – Samples distribution along the concentration domain; Training sets (black dots) and testing sets (red dots) for the following mixtures of samples: (A) Galactose, Glucose and Xylose, (B) Glucose, Xylose and Mannose and (C) Galactose, Glucose and Mannose.

Article 3: In this paper the ANN approach was much easier than in *Article 2*, mainly regarding the sample preparation and design used then to generate the ANN model. For this work a set of 36 samples, containing a mixture of lactose, glucose and $CaCl_2$, was prepared with a concentration range of 0 to 250 µM for lactose and glucose and 0 to 10 mM for $CaCl_2$, and then divided in two subsets of 27 and 9 samples, training and test respectively. The 27 samples for the training were distributed along a simple 3-level factor design (a cubic shape), while the 9 test samples were randomly distributed inside the experimental domain (Figure 3.4). Also in this work has been used a pre-processing/compression step due to the amount of data generated from the sensors (3 sensors x 450 current values x 36 samples, for a total of 48 600 values). The pre-processing/compression step was performed using a DWT with a Daubechies 4 (db4) wavelet mother function and a 3rd decomposition level. The final amount of coefficients used from the ANN was so reduced to 186 from the initial 48 600. The architecture definition of the ANN was configured and optimised based on our group's previous experience with ET systems based on amperometric sensors. The parameters considered for the optimization were the number of neurons used in the ANN hidden layer (1-12 for *Paper 2* and 4-12 for *Paper 3*) and the transform functions

used in the ANN hidden and output layer (*logsig*: log-sigmoidal, *tansig*: hyperbolic tangent sigmoid, *purelin*: linear and *satlins*: saturated-linear)

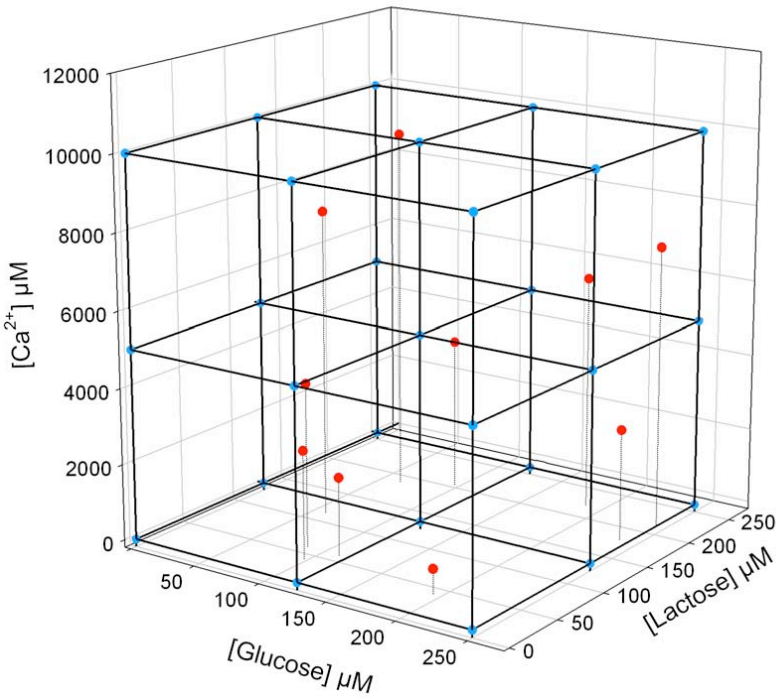

Figure 3.4 - Distribution of the training (blue) and test (red) concentrations of lactose, glucose, and Ca^{2+} used to train and test the Artificial Neural Network (ANN).

3.5 References

1. Zamocky, M., et al., *Cloning, sequence analysis and heterologous expression in Pichia pastoris of a gene encoding a thermostable cellobiose dehydrogenase from Myriococcum thermophilum.* Protein Expression and Purification, 2008. **59**(2): p. 258-265.
2. Ludwig, R., et al., *Mutated cellobiose dehydrogenase with increased substrate specificity*. 2013, Google Patents.
3. Harreither, W., et al., *Recombinantly produced cellobiose dehydrogenase from Corynascus thermophilus for glucose biosensors and biofuel cells.* Biotechnology Journal, 2012. **7**(11): p. 1359-1366.
4. Harreither, W., et al., *Catalytic Properties and Classification of Cellobiose Dehydrogenases from Ascomycetes.* Applied and Environmental Microbiology, 2011. **77**(5): p. 1804-1815.
5. Walstra, P., J.T. Wouters, and T.J. Geurts, *Dairy science and technology*. 2014, CRC press, Boca Raton (FL).
6. Authier, L., B. Schollhorn, and B. Limoges, *Detection of cationic phenolic derivatives at a surfactant-doped screen-printed electrode for the sensitive indirect determination of alkaline phosphatase.* Electroanalysis, 1998. **10**(18): p. 1255-1259.
7. Haladjian, J., et al., *A permselective-membrane electrode for the electrochemical study of redox proteins. Application to cytochrome c552 from Thiobacillus ferrooxidans.* Anal. Chim. Acta, 1994. **289**(1): p. 15-20.
8. Taguchi, G.Y.W., *Introduction to off-line quality control.* Central Japan Quality Control Assoc., 1979: p. 33-43.
9. M. del Valle, R.M. Guerrero, and J.M.G. Salgado, *Wavelets: Classification, Theory and Applications*. 2011, Nova Science Pub Inc, New York.
10. R.A. Johnson and D.W.Wichestein, *Applied multivariate statistical analysis*. 2007, Pearson Education, Harlow, GB.

CHAPTER 4 – RESULTS AND DISCUSSION

4. Results and discussion

The aim of this work has been firstly to find an easy and facile way to synthesise a nano-hybrid material based on CNTs and metal NPs exploitable as electrode platform for sensors and biosensors, and then use the material to modify the electrode surface acting as better sensing material compared to the unmodified electrode. To achieve this last step the nano-hybrid material has been applied in the beginning to a single electrode to verify how good it was, then to a system largely used in our lab, the Electronic Tongue system. The ET system, as explained before in Chapter 1 (Section 1.3.3), in few words is an array of sensors that shows cross-response, i.e. low selectivity, and therefore, with a specific data treatment, allows the resolution of multiple analytes. The CNTs/NPs material has been used to modify surfaces of different electrodes, each one with a different load of metal NPs on the CNTs. These steps have brought to two publications and an unexpected outcome from the secondment carried out in the Lo Gorton's group at Lund University (Sweden), that is in a manuscript version for now and being submitted. The first publication revealed the improvement brought from the integration of CNTs and metal NPs compared to the bare electrode. The second publication has been a natural consequence of the results showed from the nano-hybrid material and our lab main research line, ETs systems, so different nano-hybrid materials were applied to different electrodes to then compose an electrodes array that is the sensing

module of the ET system. For every electrode the nano-hybrid material was different, always using CNTs but changing the metal NPs loaded onto it, Pd, CuO, Au, Ni and Co NPs. The secondment in Lo Gorton's group at Lund University happened before the second publication, and it was meant to get my hands on the data treatment step of the ETs systems without having to worry about sensors fabrication having so the time to practice with the software and understand how it works, then the unexpected result came out. Our attempt was to build a fully Bio-Electronic tongue with cross-responsive enzymes as sensing elements, and the result was achieved with a proof-of-concept of the system using CDH enzymes never used for this purpose in literature, making so our proof-of-concept the first CDH Bio-ET system.

This chapter will be organised in Article sections, each one explaining the results obtained in each work. The first two of these sections will be related to the published articles as follow (full articles in Chapter X – Publications):

Article 1 – A. Cipri and M. del Valle, *Palladium nanoparticles/multiwalled carbon nanotubes electrode system for voltammetric sensing of Tyrosine*, Journal of Nanoscience and Nanotechnology, 2014, 14, 6692 – 6698;

Article 2 – A. C. d. Sá, A. Cipri, A. González-Calabuig et al., *Resolution of galactose, glucose, xylose and mannose in sugarcane bagasse employing a voltammetric electronic tongue formed by metals oxy-hydroxide/MWCNT modified electrodes*, Sensors and Actuators B: Chemical, 2015, 222, 645-653;

The third section will be related to the manuscript, that for easiness would be named as *Article 3*, as follow (full manuscript in the Annex):

Article 3 – A. Cipri, C. Schulz et al., *A novel Bio-Electronic Tongue using cellobiose dehydrogenase to resolve mixtures of various sugars and interfering analytes*, (Manuscript, submitted to Biosensors and Bioelectronics).

4.1 Article 1

Palladium nanoparticles/multiwalled carbon nanotubes electrode system for voltammetric sensing of Tyrosine

In this work a facile and quick synthesis of palladium decorated multi-walled carbon nanotubes is presented. The developed protocol allows a quasi-homogeneous distribution of the metal nanoparticles on the surface of the nanotubes, and a controlled size of the nanoparticles in a range between 3.5 and 4.5 nm. After the characterization of the hybrid nanocomposite a first attempt on a possible application has been made. A preliminary test, an ink-like nanocomposite as a modifier on the surface of a carbon screen-printed electrode, was performed in order to detect L-Tyrosine. Preliminary results are promising. A catalytic effect on the oxidation peak of the L-Tyrosine was shown and furthermore a low limit of detection, $1.46x10^{-10}$ M, was reached. The characterization of the nano-hybrid material and its application as Tyrosine sensor would be described in the following sections.

4.1.1 – Nano-hybrid material characterization

Meng L. et al. [1] showed how the acid treatment of the CNTs is an important step toward the synthesis of decorated CNTs. Without surface treatment the degree of the NPs is insignificant because of the hydrophobicity of the nanotubes. The acid treatment can functionalize the CNTs with carboxyl, carbonyl and hydroxyl groups. Halder et al. [2] showed that besides the attachment of metal NPs, the surface functionalization is also important for the catalytic activity, due to its connection with the active sites (oxygen-containing groups) on the surface of the CNTs. There are several different methods of oxidative treatment that can be used, with only one acid, with a mixture of concentrated acids and with or without heating [3, 4]. In this work, three different acidic treatments were tested, with a common acidic mixture of concentrated H_2SO_4 and HNO_3 (3:1), without heating and with differing durations, 90 min and according to literature 2 h, 24 h. Between 2 hours and 90 minutes, the difference was insignificant therefore the 90 min duration was chosen. The 24 h treatment was eliminated due to the defects generated on the surface of the CNTs that resulted in the breakage of the sidewalls as shown in the TEM comparison in Fig. 2 between the 90 min treatment (a) and the 24 h treatment (b). In Figure 4.1a, it can be seen how the surface even presenting some defect is still intact and the length of the nanotubes has not been affected from the treatment. Resulting from the second treatment, Figure 4.1b, it was seen that the extended duration caused an increase in surface defects, which compromised the integrity of the side-wall and thus cancelled out the benefits of the treatment.

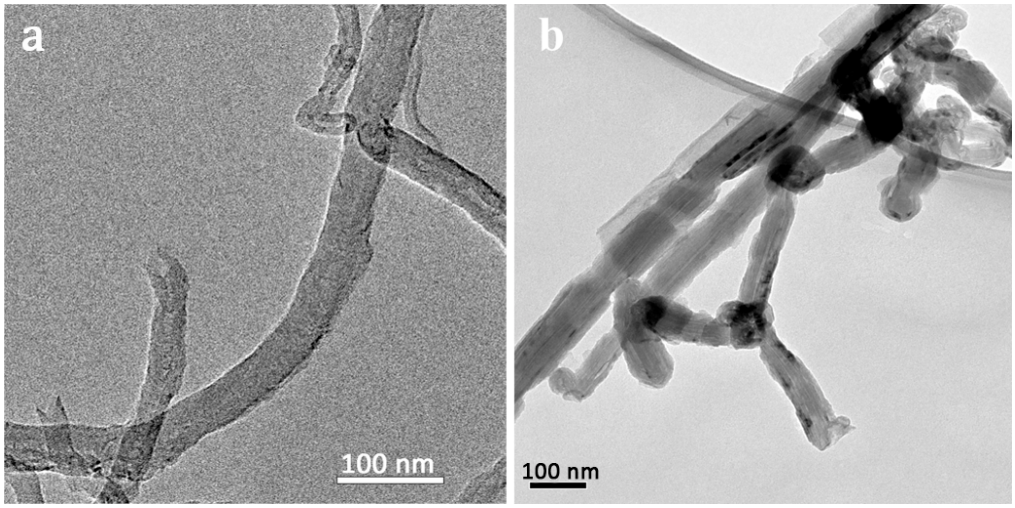

Figure 4.1 – TEM characterization of the only functionalised MWCNTs (a) 90 min treatment and (b) 24 h treatment

The TEM characterization of the MWCNT/Pd is displayed in Figure 4.2. The MWCNTs shown in the image have a declared outer diameter of 30 nm. A quasi-homogeneous distribution along the nanotube has been obtained and as can be observed the size of the nanoparticles is under 10 nm. The quasi-homogeneous distribution may be due to the small longitudinal size in comparison to the diameter of the nanotubes and to the in-situ growth of the palladium nanoparticles. This quasi-homogeneous distribution is expected to give better catalytic properties to the nanocomposite compared to its native properties.

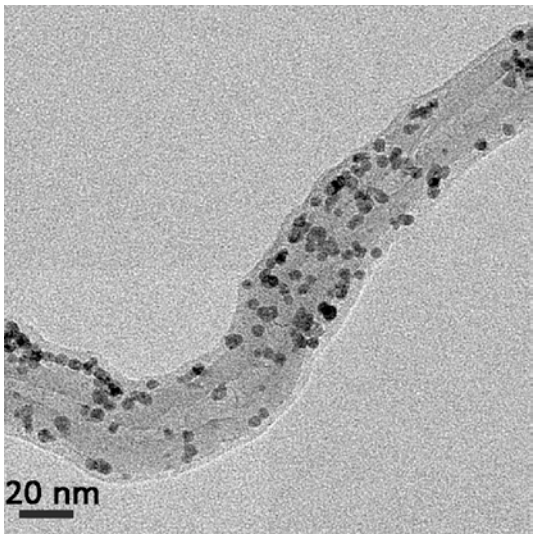

Figure 4.2 – TEM image of Pd-NPs decorated MWCNTs

It was seen that the nanoparticles were crystalline nanoparticles through their characterization by high-resolution TEM (Figure 4.3a). In the highlighted sections from Figure 4.3, the crystalline planes of the nanoparticle can be observed for every particle, all the planes have one direction and

this confirms the crystallinity of the species. To evaluate the composition of the MWCNTs/Pd, an energy dispersion spectroscopy (EDS) was recorded (Fig. 4.3b). The EDS is a built-in detector in the TEM instrument used for all the analysis and can be used to determine the elemental composition of the site under scrutiny. The presence of palladium in MWCNTs/Pd was confirmed from the peak at 3 keV; the carbon peak is due to the CNTs and the oxygen peak points to the carboxyl and carbonyl groups grafted on the surface with the functionalization step. The presence of copper in the EDS spectra, instead, was attributed to the copper grid used as TEM sample holder.

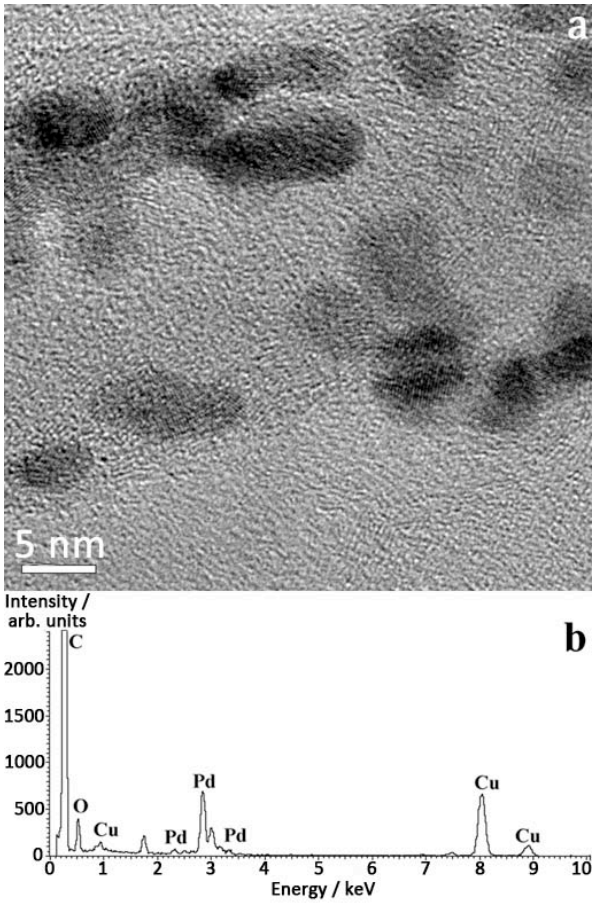

Figure 4.3 – (a) High resolution TEM image of a section of MWCNTs/Pd NPs; (b) EDS analysis of the area showed in (a).

A study of size distribution (Figure 4.4) was performed to verify the mean size and distribution of nanoparticles the protocol was able to generate. More than 300 nanoparticles were measured and the result was 4.78 (±1.07) nm. This size of the NPs compared to the outer diameter of the nanotubes (30 nm) is quite small, allowing for a good distribution at the external surface and thus allowing an increase in the efficacy of catalytic behaviour. Also remarkable is the standard deviation obtained (22.4% when relatively expressed), claiming for the reproducibility of the reduction procedure.

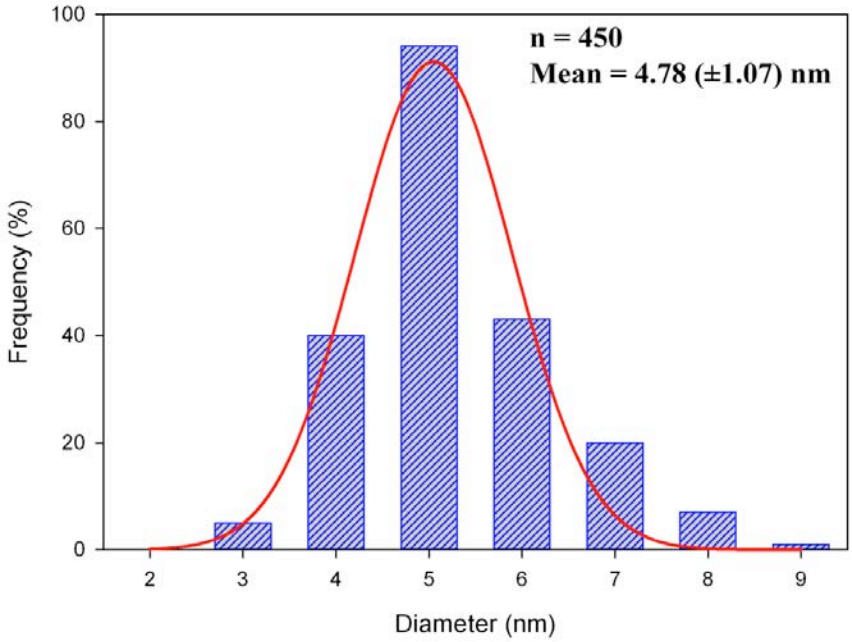

Figure 4.4 – Size distribution of the palladium NPs.

A SEM characterization was also performed in order to investigate the spatial distribution of the palladium nanoparticles and to verify the particles were all on the external surface or even in the inner layers. As an example a SEM image is displayed in Figure 4.5; it shows MWCNTs/Pd although unfortunately it is not possible to distinguish the nanoparticles well; only in the highlighted section can some nanoparticles be identified. This *vanishing* effect may be due to the small diameter of the nanoparticles having such a high possibility to be crossed from the electron beam of the SEM and hence not being displayed during the recording of the image.

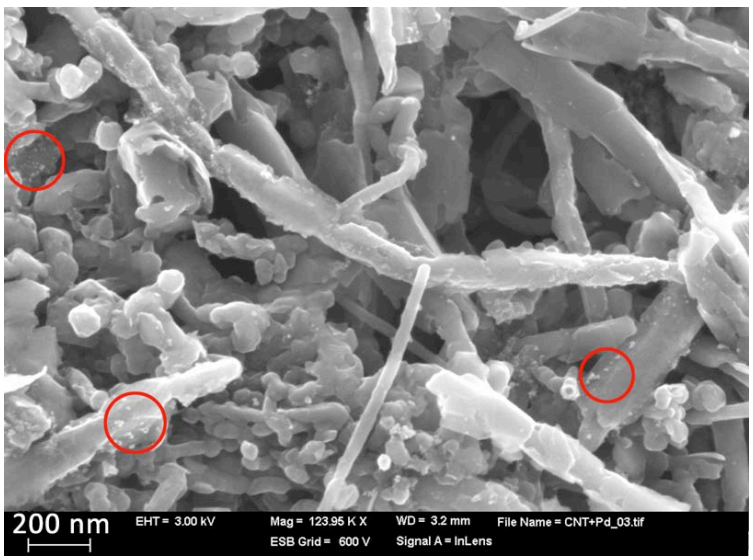

Figure 4.5 – SEM characterization of MWCNTs/Pd NPs.

4.1.2 – Application as a tyrosine voltammetric sensor

After the characterization of the nano-hybrid material MWCNTs/Pd NPs, a possible application as sensor was investigated. Considering the electrical properties of the CNTs and the catalytic properties of both CNTs and palladium NPs, a preliminary test as an electrode modifier in voltammetric analysis was attempted. To achieve this preliminary test, an ink-like nanocomposite was prepared as explained in Chapter 3 – Section 3.3.

The analyte chosen for this preliminary test was L-Tyrosine for its redox behaviour and for its important role as neurotransmitter precursors in mammalian animals. The characterisations were performed by linear sweep voltammetry and chronoamperometry.

Not only was the MWCNTs/Pd electrode characterised, by way of a control for the experiment, an electrode modified with an ink-like nanocomposite made only with MWCNTs and a bare carbon screen-printed electrode in a 2 mM PBS solution of L-Tyrosine were also tested. In Figure 4.6a a linear sweep voltammetry graph is displayed so as to compare the performance of the three electrodes. As can be noted, the MWCNTs electrode (B) already has a catalytic effect on the oxidation peak of the L-Tyrosine when compared to the bare electrode (C) and this can be associated with the properties of the CNTs given as high conductivity, catalytic effect, and fast electron transfer. From the comparison between the MWCNTs/Pd NPs electrode (A) and the MWCNTs electrode (B) a further increase in the catalytic effect of the modification on the electrode can be seen. The only difference between the two electrodes is the presence of palladium nanoparticles on the first; this confirms the catalytic behaviour of the Pd NPs. The shift to a less anodic potential of the oxidation peak using the MWCNTs/Pd NPs electrode demonstrates that the palladium NPs are acting as a catalytic enhancer on the surface of the nanotubes. Besides the reduction of the anodic potential, a higher current response using the same sample concentration (2 mM for all the electrodes) for the MWCNTs/Pd NPs electrode can be also considered. Therefore a preliminary test of calibration was performed with the new nano-hybrid material as electrode modifier to investigate the detection limit of the electrode and to compare it with what is reported in literature. The calibration curve shown in Figure 4.6b is from the preliminary test and, as can be seen, the detection limit is extraordinarily low, 1.46×10^{-10} M, the range of concentrations was from 1×10^{-10} to 5×10^{-8} mol L^{-1} with the corresponding linear regression equation as following:

$$y = 7.03 \times 10^{-7} + 1.45 \times 10^{-3} \ (R^2 = 0.999)$$

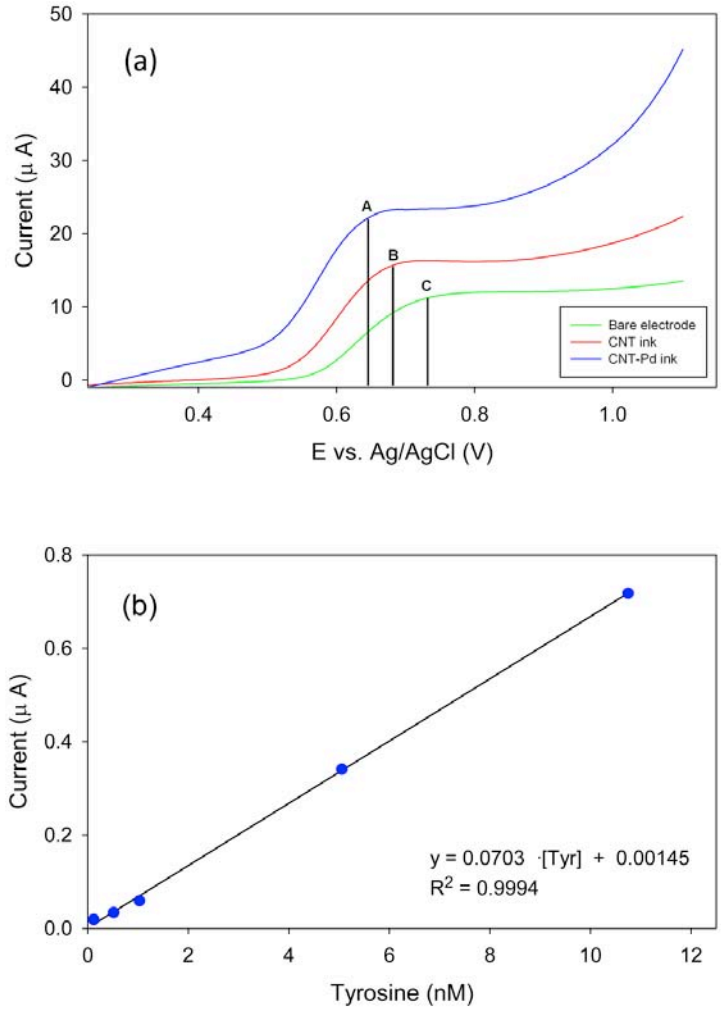

Figure 4.6 – (a) Comparison of the voltammetric responses between MWCNTs/Pd NPs/carbon SPE, MWCNTs/carbon SPE and the bare carbon SPE. The voltammetric technique used was a Linear Sweep Voltammetry with a range potential 0.2 – 1.1 V, E_{step} 2 mV, scan rate 50 mV/s; (b) Calibration curve for the determination of L-Tyrosine. The linear range is from $1.0x10^{-10}$ to $1.0x10^{-8}$ mol L^{-1}.

The detection limit (LOD), S/N = 3, was calculated considering the Standard Error of Estimate (SEE) as an estimation of the blank standard deviation, that is the standard deviation of the residual from the regression calculation.

In Table 1 is listed a comparison between MWCNTs/Pd modified screen-printed electrode and similar works in the literature. The results, when compared, show that the sensitivity of our system is more attractive and promising than previous reports.

Table 4.1 – Comparison of the MWCNTs/Pd performance with those previously reported

Modified electrodes	Technique	Linear working range (M)	Detection limit (M)	Ref.
MWCNT/GCE	SWSV	$2.0x10^{-6} – 5.0x10^{-4}$	$4.0x10^{-7}$	[5]
SWCNT/GCE	CV	$5.0x10^{-6} – 2.0x10^{-5}$	$9.3x10^{-8}$	[6]
MWCNT/IL/Cu^{2+}/GCE	DPV	$1.0x10^{-8} – 5.0x10^{-6}$	$8x10^{-9}$	[7]
CNF/CPE	I-T	$2.0x10^{-7} – 1.09x10^{-4}$	$1.0x10^{-7}$	[8]
Co_3O_4/GR/GCE	I-T	$1.0x10^{-8} – 4.0x10^{-5}$	$1.0x10^{-9}$	[9]
MWCNT/Pd/SPE	I-T	$1.0x10^{-10} – 1.0x10^{-8}$	$1.46x10^{-10}$	This work

MWCNT/GCE: multi-wall carbon nanotubes modified GC electrode. SWCNT/GCE: single-wall carbon nanotubes modified GC electrode. MWCNT/IL/Cu2+/GCE: multi-wall carbon nanotubes–ionic liquid composite coated GC electrodes in the presence of cupric ion. CNF/CPE: electrospun carbon nanofibers modified GC electrode. Co_3O_4/GR/GCE: tricobalt tetroxide nanoparticles-graphene nanocomposite modified GC electrode. SWSV: square wave stripping voltammetry. CV: cyclic voltammetry. DPV: differential pulse voltammetry. I-T: Chronoamperometry.

4.2 Article 2

Resolution of galactose, glucose, xylose and mannose in sugarcane bagasse employing a voltammetric electronic tongue formed by metals oxy-hydroxide/MWCNT modified electrodes

After the experience with the nano-hybrid material (CNTs/Pd NPs) as electrode modifier and the efficiency of the synthesis, the same protocol as one-pot synthesis was applied to the synthesis of two additional nano-hybrid materials with Au and CuO as metal NPs, and two other metals (Ni and Co) loaded onto the CNTs by an electrochemical deposition. The aim of this work is the characterization of a voltammetric ET using an array of glassy carbon electrodes modified with CNTs/metal oxy-hydroxide NPs (GCE/CNTs/Metals-OOH) and application towards a simpler analysis of carbohydrates (glucose, xylose, galactose and mannose) present in sugarcane bagasse. In the ET system the final architecture of the back-propagation ANN model had 36 input neurons and a hidden layer with 5 neurons. The ANN based prediction model has provided satisfactory concentrations for all carbohydrates; the obtained response had a maximum NRMSE of 12.4% with a maximum deviation of slopes in the obtained vs. expected comparison graph of 15%. For all species, the comparison correlation coefficient was of $r \geq 0.99$ for the training subset and of $r \geq 0.96$ for the test subset. In the following sections would be presented a description of the characterization and ET system results.

4.2.1 – Characterization of the nano-hybrid composites

In Figure 4.7 (A) a TEM image of the CNTs/Pd NPs is displayed, the characteristics and aspect are the same as the nano-hybrid material CNTs/Pd NPs discussed in the Article 1 section. The CNTs modified with Au and CuO NPs were obtained from joining and slightly modifying protocols already present in literature and the one-pot synthesis structure developed in our first article with CNTs/Pd NPs material. The morphology of the CNTs/Au NPs was characterized with TEM (Figure 4.7 (B)) and confirmed that the Au-NPs were attached on the walls and ends of CNT, showing a diameter of about 4-7 nm. The TEM Figure 4.7 (C) shows that each leaf-like CuO polycrystalline is composed of several single-crystalline pieces, which suggest the coexistence of CuO and CNTs. Therefore, CNTs and CuO nanoleaves do indeed form a nano-hybrid material, and are not simply mixed together. For Ni and Co electrochemically modified CNTs, which are mainly synthesised through electrochemical reduction as described in literature [10, 11], the characterization has been carried out by SEM analysis. In Figure 4.7 (D) it can be observed regular and spherical particles with size about 32 nm and their homogeneous distribution over the CNTs for the CNTs/Ni NPs nano-hybrid material. This better distribution and uniform sizes may be responsible for lower limits of detection in the analysis of sugars for this kind of material [12, 13]. In Figure 4.7 (E) is shown a SEM image of CNTs/Co NPs and can be observed that the particles are

in a wire shape. Some of the particles are in vertical position taking a representative wire the average particle size is around 20 nm for particles in an upright position as in the case of wire and 185 nm for the particles in horizontal position.

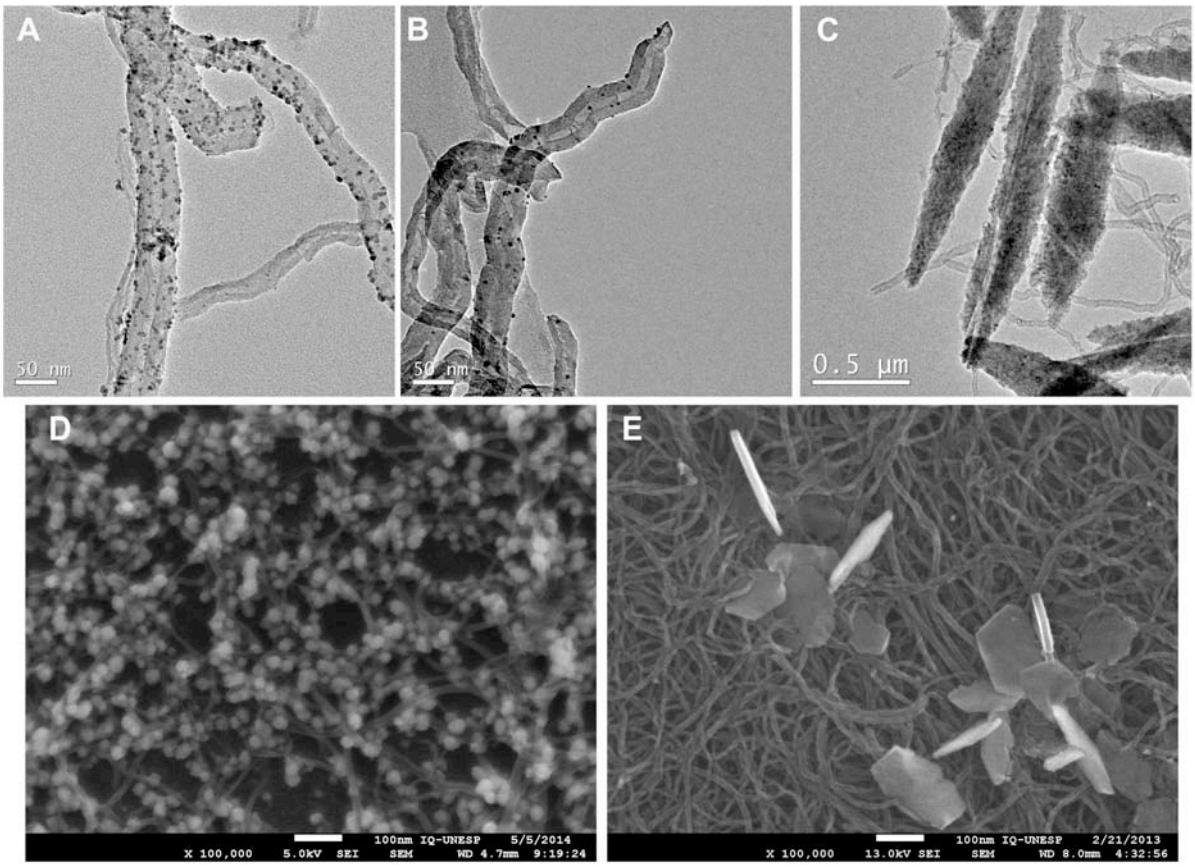

Figure 4.7 – TEM characterization of CNTs/Pd NPs (A), CNTs/Au NPs (B) and CNTs/CuO NPs (C). SEM characterization of CNTs/Ni NPs (D) and CNTs/Co NPs (E)

4.2.2 – Modified sensors response

The voltammetric response for each electrode towards individual compounds was the first response feature checked. In this way was tested the cross-response of the sensors that is requested from a multivariate calibration model. To this aim individual standard solutions of galactose, glucose, xylose and mannose were analysed and their voltammograms inspected, in Figure 4.8 is shown the voltammetric behaviour of the different GCE/CNTs/Metals-OOH modified electrodes.

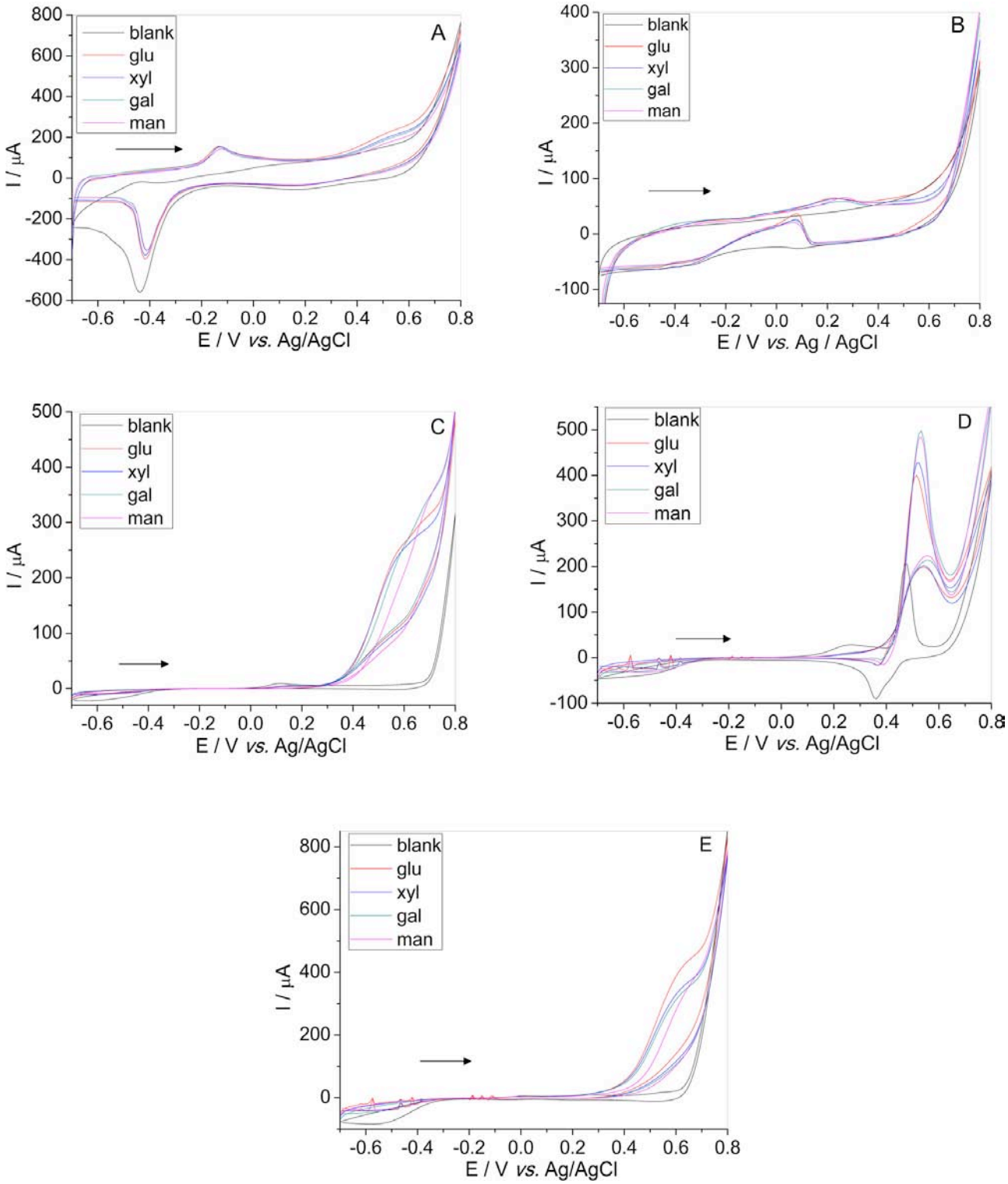

Figure 4.8 – Example of different Cyclic Voltammetry responses of (A) GCE/CNTs/Pd-OOH, (B) GCE/CNTs/AuO, (C) GCE/CNTs/Cu-OOH, (D) GCE/CNTs/Ni-OOH and (E) GCE/CNTs/Co-OOH in a 0.1 mol L-1 NaOH solution and 5.0 x 10-3 mol L-1 stock solution of each carbohydrate; (blank) Absence, (glu) Glucose, (xyl) Xylose, (gal) Galactose and (man) Mannose.

In Figure 4.8 (A) are shown the overlaid voltammograms of GCE/MWCNT/Pd-OOH electrode during oxidation of the four carbohydrates that occurs at potentials around −0.1 V vs. Ag/AgCl associated with an anodic peak current and also the decrease in cathodic peak current, the results

suggest that Pd (I)/Pd (II) redox couple in form of Pd-OOH [14] can catalyse the oxidation of the carbohydrates.

Figure 4.8 (B) shows the voltammogram of GCE/CNTs/AuO electrode during oxidation of the four carbohydrates that occurs with an oxidation peak at an anodic potential around 0.25 V vs. Ag/AgCl, and a re-oxidation peak at –0.07 V vs Ag/AgCl in cathodic direction. This can be state as typical behaviour of gold electrodes, which electro-catalytic activity can be rationalized by the incipient hydrous oxide/adatom model for the oxidation catalysis of carbohydrates [15-17].

The voltammogram of GCE/CNTs/Cu-OOH is shown in Figure 4.8 (C), for which the oxidation of carbohydrates occurs at a potential around 0.60 V vs. Ag/AgCl, with the presence of an anodic wave. During the positive scan, the Cu nanoparticles can be oxidized to Cu-OOH. The Cu(II)/Cu(III) redox couple can catalyse the carbohydrates oxidation [18-20].

The carbohydrates oxidation on the GC/CNTs/Ni-OOH electrode, as shown in the Figure 4.8 (D), occurred at a potential around 0.52 V vs. Ag/AgCl associated with an increase in the anodic peak current and a decrease in the cathodic peak current. The results suggest that the redox couple Ni(II)/Ni(III) can catalyse the oxidation of carbohydrates [21].

The voltammograms of GCE/CNTs/Co-OOH shown in Figure 4.8 (E) demonstrated the oxidation of carbohydrates occurring at a potential around 0.65 V vs. Ag/AgCl, with the presence of an anodic wave. This fact suggests that carbohydrates are oxidised by Co-OOH species through Co(III)/Co(IV) redox couple moiety and through a cyclic mediation redox process [22, 23].

The observed results indicate that the different GCE/CNTs/Metals-OOH modified electrodes can catalyse the oxidation of Galactose, Glucose, Xylose and Mannose to ketones, forming galactonolactone, gluconolactone, xylonolactone and mannonalactone, respectively [21]. Besides, clearly differentiated curves are obtained for each modified electrode and each considered sugar giving the desirable condition for an Electronic Tongue (ET) study. This cross-response nature of the voltammograms can be summarized when plotting max currents (sensitivities) and oxidation peak potential observed for the 5 CNTs/Metal NPs modified electrodes. This representation is shown in Figure 4.9, where it can be observed that carbohydrates anodic peak current (Ipa) is different according to each metal in the nano-hybrid composite of the ET and was also observed that the oxidation potentials (Epa) shows different behaviours according to each metal, this is a desirable condition for any ET study.

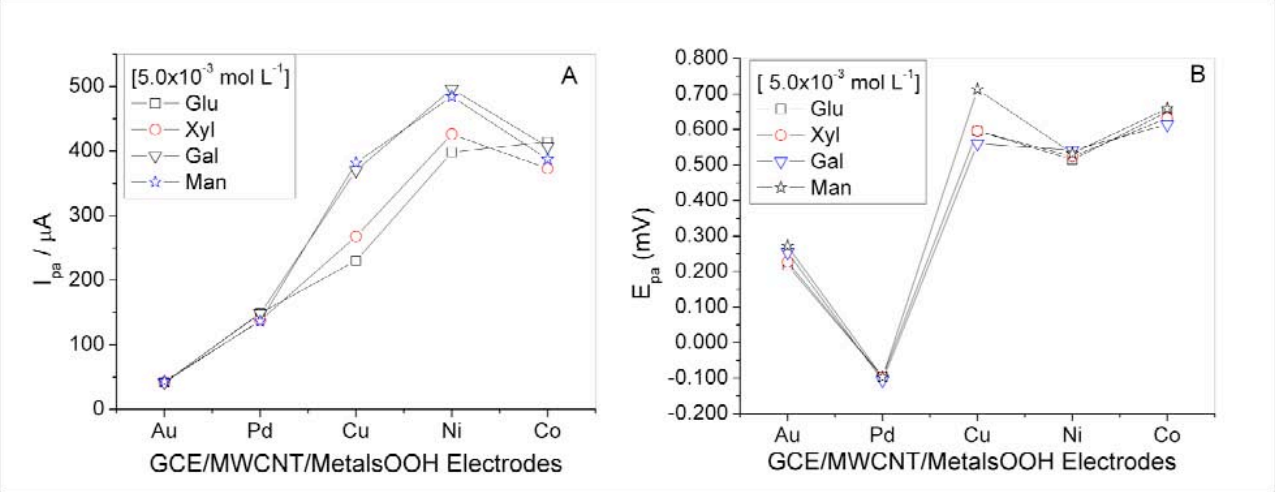

Figure 4.9 – (A) anodic peak current (Ipa) and (B) oxidation potential (Epa) response for each of the four carbohydrates (glucose, xylose, galactose and mannose) with a concentration of 5.0 x 10^{-3} mol L^{-1} considering the ET formed by GCE/CNTs/Metals-OOH NPs (metals = Au, Pd, Cu, Ni and Co)

The analytical reproducibility (%RSD) for the sensors was estimated using standard solutions of 2 × 10^{-3} mol L^{-1} glucose measured along 3 different days, obtaining values for GCE/CNTs/AuO of 3.28%, for GCE/CNTs/PdO 6.89%, for GCE/CNTs/Cu-OOH 3.85%, for GCE/CNTs/Ni-OOH 1.73% and for GCE/CNTs/Co-OOH 6.35%. The analytical reproducibility shown seems reasonable, because the electrodes are subjected to analysis of many samples thus requiring maintaining its reproducibility and stability. Complete calibrations of considered sugars were conducted in 0.1 mol L^{-1} NaOH solution with scan rate of 50 mV s^{-1} in order to fully characterize the used sensors. It was observed in all cases an increase of anodic peak current which was linear with the increase of concentration of sugars; Table 4.2 shows the electrochemical parameters for all carbohydrates studied. It has been observed that the electronic tongue formed by GCE/MWCNT/Metals-OOH modified electrodes has good amperometric sensitivity. The values of limit of detection (LOD) and quantification (LOQ) are very close, meaning that the behaviour of the different sugars on the electrode is comparable. Therefore the ET may be applied in the same concentration range for all sugars considered.

Table 4.2. Analytical parameters for various carbohydrates at electronic tongue formed by GCE/MWCNT/Metals oxy-hydroxide nanoparticle modified electrodes in 0.1 mol L^{-1} NaOH by Cyclic Voltammetry (v = 50 mV s^{-1}; n = 3).

Palladium

Carbohydrate	LOD (mM)	LOQ (mM)	Sensitivity (μA mM^{-1})	Concentration range (mM)
Glucose	0.32	1.05	25.5	0.4 - 5.0
Xylose	0.38	1.25	11.9	0.4 - 5.0
Galactose	0.87	2.97	14.1	0.9 - 5.0
Mannose	0.08	0.27	14.3	0.2 - 5.0

Gold

Glucose	0.64	2.11	7.3	0.8- 5.0
Xylose	0.62	2.04	5.8	0.8- 5.0
Galactose	0.57	1.88	5.5	0.6- 5.0
Mannose	1.00	3.33	6.0	1.0 - 5.0

Copper

Glucose	0.10	0.33	51.1	0.2 - 5.0
Xylose	0.06	0.19	49.5	0.2 - 5.0
Galactose	0.38	1.26	41.5	0.4 - 5.0
Mannose	0.36	1.19	7.18	0.4 - 5.0

Nickel

Glucose	0.23	0.76	32.0	0.4 - 5.0
Xylose	0.38	1.26	39.2	0.4 - 5.0
Galactose	0.41	1.36	46.7	0.5 - 5.0
Mannose	0.47	1.56	42.0	0.5 - 5.0

Cobalt

Glucose	0.31	1.03	83.6	0.4 - 5.0
Xylose	0.10	0.33	67.9	0.2 - 5.0
Galactose	0.25	0.83	75.7	0.4 - 5.0
Mannose	0.38	1.26	69.2	0.4 - 5.0

4.2.3 – Building of the ANN Model

For the ET study, a total set of 46 carbohydrates standard mixtures were manually prepared as described in Chapter 3 – Section 3.4. These standards were first analysed and used to build and validate the ANN model according to the conditions mentioned in Chapter 3, the training and testing sets of samples were measured employing the GCE/CNTs/Metals-OOH modified electrodes array, obtaining a complete voltammogram for each of the electrodes, and each sample. Because of the dimensionality and complexity of the information generated (5 voltammograms per each sample), a double compression strategy with wavelet transform and causal index pruning was used. Once the optimal set of coefficients was selected through the two compressing steps, the ANN final architecture was optimized. The parameters that were optimized were the 4 transfer functions employed in the hidden and output layers, the functions evaluated were *tansig*, *logsig*, *satlins* and *purelin*, and the number of neurons in the hidden layer was varied from 1 to 12. In this manner 192 architectures were evaluated. The final architecture of the back-propagation ANN model had 36 input neurons, a hidden layer with 5 neurons and the *tansig* transfer function, and an output layer with 4 neurons and the *purelin* transfer function. The representation of the modelling performance of the system is illustrated in Figure 4.10. This figure shows the comparison graphs of predicted vs. expected concentrations for the four carbohydrates and for training and testing subsets, which were built to check the prediction ability of the ANN model. It is possible to see that a satisfactory trend was obtained, with the regression line almost indistinguishable from the theoretical one for the training subset. From these data it appears that all species show a very good correlation coefficients with an R value ≥ 0.99 on the training subset. The model prediction is satisfactory for all carbohydrates and the accuracy of the obtained response is adequate. The results obtained for external test subset with much more significance than the latter, are close to the ideal values, with 0 intercepts, 1 slopes and good correlation coefficients R values ≥ 0.96.

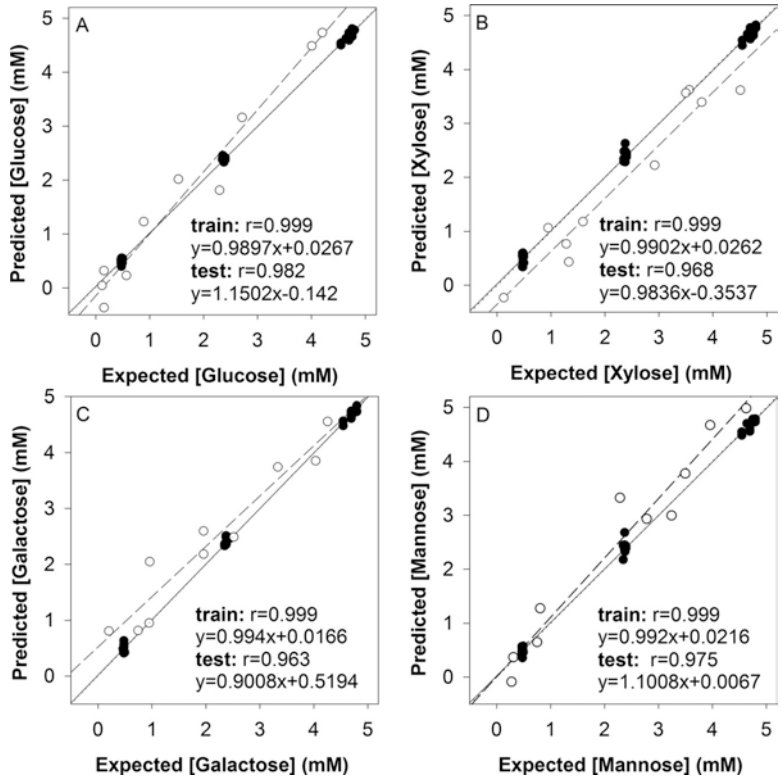

Figure 4.10 – Modelling ability of the optimized ET formed by GCE/CNTs/Metals-OOH modified electrodes. Comparison graphs of predicted vs. expected concentrations for (A) Glucose, (B) Xylose, (C) Galactose and (D) Mannose, both for training (−, solid line) and testing subsets (---, dashed line). Dotted line corresponds to theoretical Y=X.

After optimizing its performance, the electronic tongue was assessed through studies on synthetic samples of sugars shown in Table 4.3, with three different sugar mixtures. As it can be seen found results are in good agreement with those expected.

Table 4.3: Results in synthetic samples obtained from the electronic tongue formed by GCE/MWCNT/MetalsOOH modified electrodes in the analysis of Glucose, Xylose, Galactose and Mannose

Samples	Glucose / mmol L^{-1}	Glucose found / mmol L^{-1}
1	4.0	4.5
2	2.7	3.2
3	4.2	4.7
	Xylose / mmol L^{-1}	Xylose found / mmol L^{-1}
1	3.6	3.6
2	2.9	2.2
3	3.5	3.6
	Galactose / mmol L^{-1}	Galactose found / mmol L^{-1}
1	2.0	2.6
2	2.0	2.2
3	1.0	1.0
	Mannose / mmol L^{-1}	Mannose found / mmol L^{-1}
1	4.0	4.7
2	4.6	4.9
3	0.3	0.4

4.3 Article 3

A novel Bio-Electronic Tongue using cellobiose dehydrogenase from different origins to resolve mixtures of various sugars and interfering analytes. (*Manuscript, submitted to Biosensors and Bioelectronics*)

In this section is explained a novel application of cellobiose dehydrogenase (CDH) as sensing element for an electronic tongue (ET) system. CDH from different origins and substrate specificities has been used to discriminate between various sugars (lactose and glucose) plus an interfering analyte (Ca^{2+}) in mixtures working in a direct electron transfer mode at low potentials. The work exploits the advantage of an ET system with practically zero pre-treatment of samples and operation at low voltages in a direct electron transfer mode, characteristic of CDH. The Artificial Neural Network (ANN) used in the ET system to treat the voltammetric data was able to give a good prediction of the concentrations of the analytes considered, showing high correlation coefficients especially for lactose and Ca^{2+}, R^2 of respectively 0.975 and 0.945. This application has a high potential especially in the food and dairy industries and also, in a future miniaturized system, for in situ food analysis. The research and lab work behind these results have been carried out before the *Article 2*, they have been useful to improve my understanding of the ETs systems and ANN data treatment by practicing on those tasks without having to prepare and characterise the sensors from zero, being so a kind of connection between *Article 1* and *Article 2*. Since this work is still under editorial consideration, for this reason it has been moved after the published articles and results are discussed below.

4.3.1 Characterisation of each CDH biosensor

The sensor array used for the ET consisted of three different CDH modified gold/SAM electrodes – one was modified with *Mt*CDH, one with *Nc*CDH, and one with *Ct*CDHC291Y[1], expecting different substrate specificities depending on the enzyme origin. Before developing the ET application, the integrity and linear ranges for each of the biosensors versus each of the three analytes of interest, lactose, glucose and Ca^{2+} were determined. In Figure 4.11 the cyclic voltammograms of the gold/SAM electrodes modified with either *Mt*CDH, *Nc*CDH or *Ct*CDHC291Y are shown. In the absence of substrate, clear redox waves originating from the oxidation and reduction of the heme *b* cofactor located in the CYT_{CDH} is visible. The midpoint potentials range between –153 mV vs. SCE for *Mt*CDH, –144 mV vs. SCE for *Nc*CDH and –148 mV vs. SCE for *Ct*CDHC291Y, which are close to literature values [24-26]. The additional oxidative redox wave present for *Nc*CDH at –210 mV vs. SCE might originate from the oxidation of the FAD cofactor located in the DH_{CDH} as found out to be possible recently [Schulz et al., in manuscript]. The peak separations between the anodic and cathodic peak potentials vary between 42 mV and 52 mV and thus lay between a solution and a surface confined redox process typical for

[1] The full description and origin of the CDH enzymes can be found in Chapter 3 – Section 3.1

thin layer protein electrochemistry [27, 28]. When lactose as the standard substrate is added clear catalytic waves can be seen for all CDH modified electrodes proving they are catalytically active. For *Mt*CDH and *Ct*CDHC291Y, the catalytic waves start at potentials around the oxidation peak potential the CYT_{CDH} peak indicating DET from the CYT_{CDH} domain. For *Nc*CDH it seems that there are traces of catalysis at potentials already below the oxidation potential of the CYT_{CDH} peak indicating a potential DET from the DH_{CDH} as found out to be possible recently [Schulz et al., in manuscript].

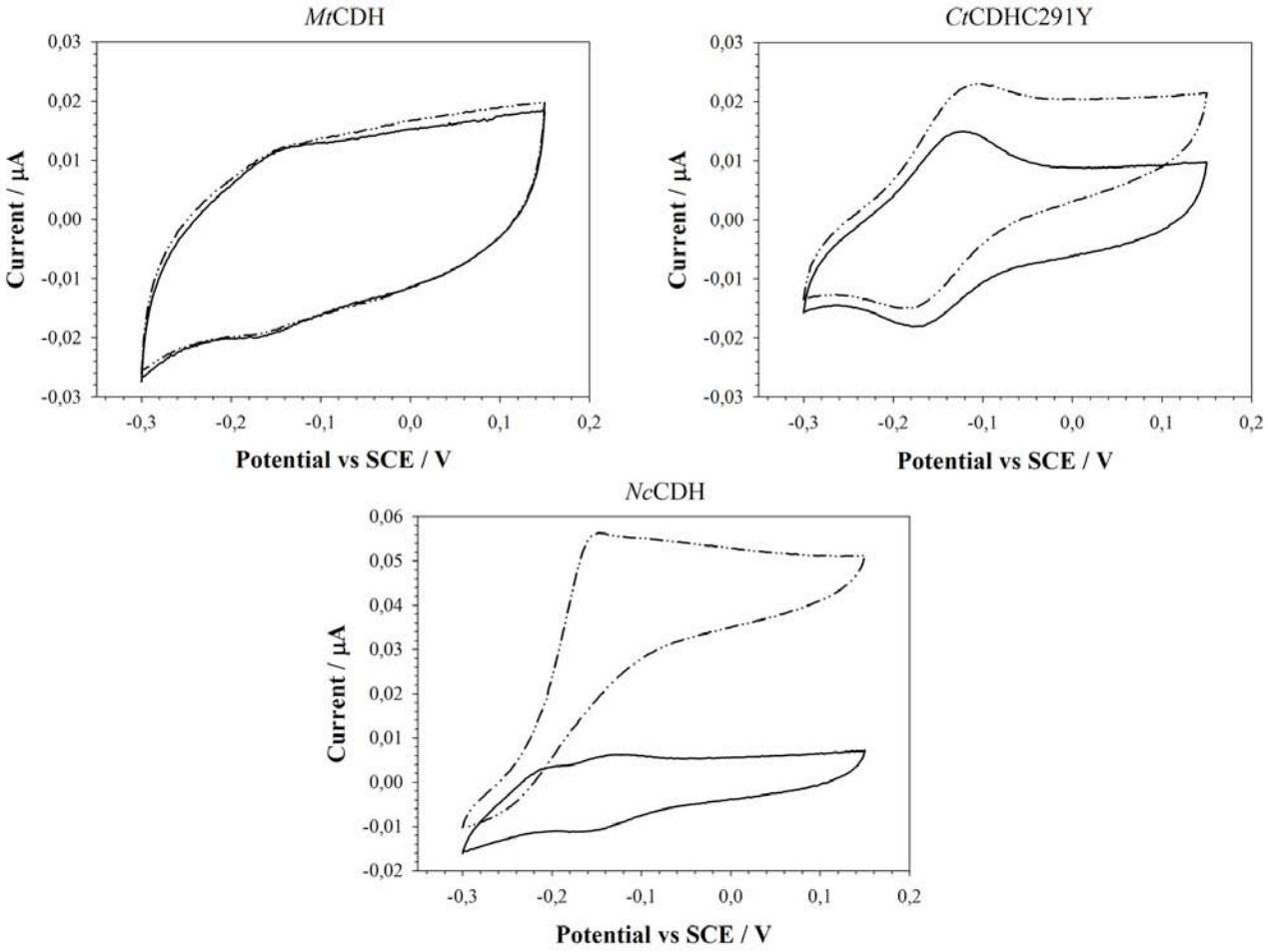

Figure 4.11 - Cyclic voltammetric characterisation of the enzyme modified electrodes used for the construction of the electronic tongue. CDH was entrapped under a dialysis membrane on mercaptohexanol modified gold electrodes. From top to bottom it is possible to see the behaviour of *Mt*CDH, *Ct*CDHC291Y and *Nc*CDH in a 50 mM MOPS buffer solution at pH 6.7 in the absence (solid line) and in the presence of 250 µM lactose (dashed line). All experiments were performed at a scan rate of 20 mV/s with a SCE reference electrode and a Pt flag as counter electrode.

To determine the linear measuring ranges, the response of each CDH biosensor to varying analyte concentrations of lactose, glucose and Ca^{2+} was determined, as shown in Figure 4.12. The investigation with Ca^{2+} as analyte was performed in the presence of 7 mM lactose, since Ca^{2+} is not a substrate for CDH but only potentially increases the existing catalytic currents as described in the full article Introduction. As shown in Figure 4.12 all CDH biosensors tested respond to lactose. The

best responding biosensors are the ones modified with *Nc*CDH and *Ct*CDHC291Y, possibly because their pH optima for DET of 5.5 [29] and 7.5 [25] respectively are close to the investigated pH of 6.7. The pH optimum for DET of *Mt*CDH is also at pH 5.5 [30] but its decline of activity with increasing pH is steeper compared to that of *Nc*CDH [29, 30] possibly explaining the comparable low response of the *Mt*CDH biosensor to lactose. The linear measuring range for lactose can be estimated to reach up to around 500 µM.

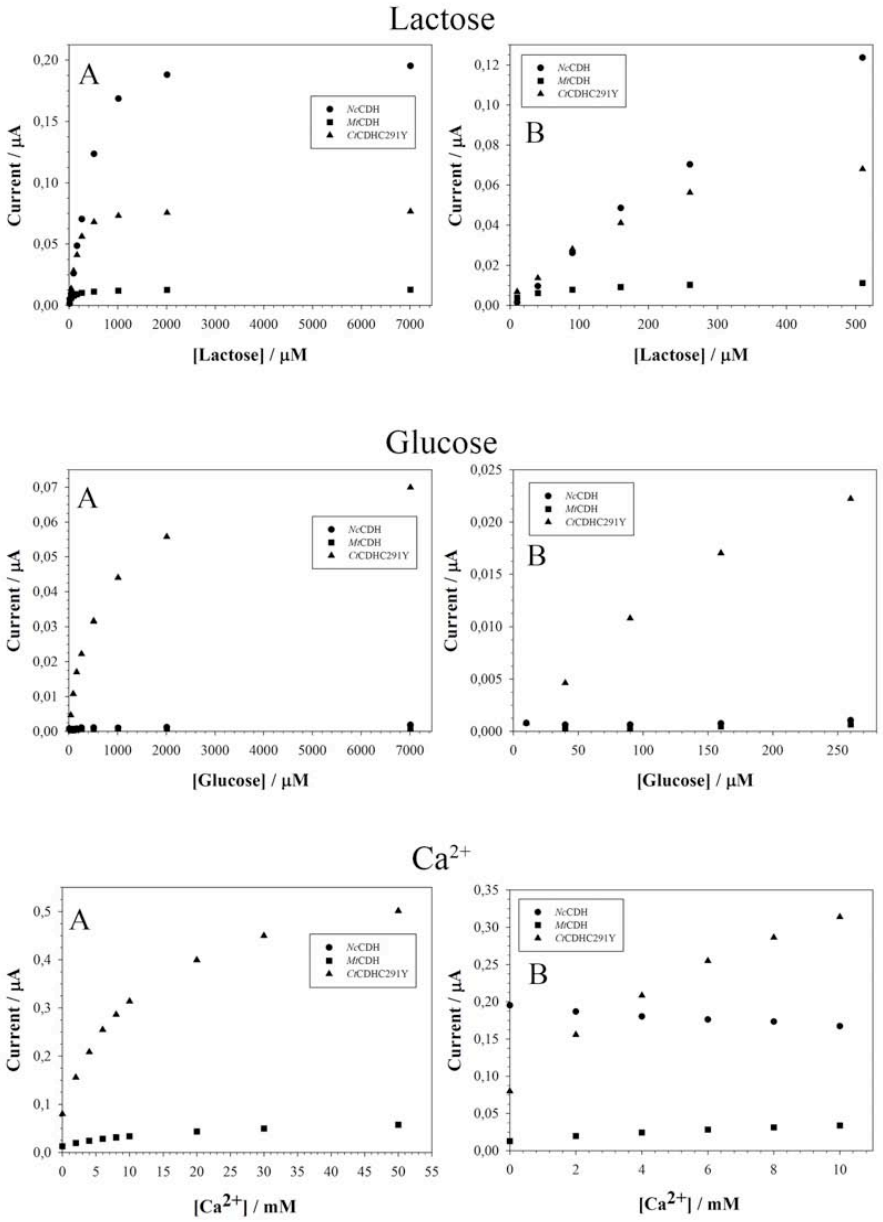

Figure 4.12 - Calibration graphs of the *Mt*CDH, *Ct*CDHC291Y and *Nc*CDH based biosensors obtained for the three analytes lactose (top), glucose (middle) and Ca^{2+} (bottom). In the left column the fully investigated concentration ranges are shown, in the right column only the linear concentration ranges are shown.

When looking into glucose as substrate (Figure 4.12, middle row) clearly the *Ct*CDHC291Y mutant designed for high activity with glucose responds best to glucose with a linear measuring range to up

to 260 μM. When looking into Ca^{2+} as analyte the *Ct*CDHC291Y and *Mt*CDH modified biosensors are sensitive to additional Ca^{2+}. The absolute currents are higher for *Ct*CDHC291Y, since its activity in the absence of Ca^{2+} is already higher than that for *Mt*CDH. However, looking into the relative increases of the catalytic currents in the presence of 50 mM Ca^{2+} increases of around 6.3 times for *Ct*CDHC291Y and 4.5 times for *Mt*CDH show similar dependencies for both enzymes on additional concentrations of Ca^{2+}. The dependency of the activity of *Mt*CDH on additional [Ca^{2+}] is comparable to what has been found in other studies done at pH 5.5 and 7.5 [31, 32]. The activity of the glucose mutant, *Ct*CDHC291Y, has not been studied before in the presence of Ca^{2+} but when comparing its activity with that of the wild type *Ct*CDH in solution with cytochrome *c* as electron acceptor, the Ca^{2+} induced activity increase found here is around twice as high [31]. The nearly independence of the activity of *Nc*CDH on additional [Ca^{2+}] compares well with the literature, where no increase for *Nc*CDH was found when investigated in solution with cytochrome *c* as electron acceptor [31]. The linear ranges found here for the detection of Ca^{2+} range up to around 10 mM.

Summarising, each investigated biosensor responds differently to the investigated analytes, a desired departure point for any ET design. This cross-response pattern has been used then to create a BioET with the help of an artificial neural network to resolve mixtures of all three analytes containing varying concentrations of lactose and glucose between 0 and 250 μM and between 0 and 10 mM for Ca^{2+}. The Bio-ET contained the three biosensors modified with *Mt*CDH, *Nc*CDH, or *Ct*CDHC291Y and an auxiliary and a reference electrode. The response of the Bio-ET was tested preparing a set of 27 training samples and 9 test samples containing all three analytes as described in Chapter 3 – Section 3.4. Than the data collected from the analysis were used as input data for building the response model.

4.3.2 ANN response model

The training method used in the Artificial Neural Network has been described in Chapter 3 – Section 3.4. To define the best architecture 144 different configurations were evaluated (product of the number of neurons in the hidden layer, the tested transfer functions in the hidden layer and the transfer functions in the output layer). The best result was as follows: 9 neurons in the hidden layer with the transform function *"logsig"* and 3 neurons in the output layer with a *"purelin"* as transform function. With this configuration the responses of the 9 test samples with known concentrations of lactose, glucose, and Ca^{2+} were then used to compare their calculated concentrations according to the ANN with their real concentrations. The correlations between

predicted (by the ANN) and expected concentrations for all analytes are shown in Figure 4.13, in this case for the external test set, the samples not intervening for the training process. Considering that the samples are mixtures of similar and/or interfering compounds and the typology of the sensors used, satisfactory R^2 values were calculated especially for lactose (0.975) and Ca^{2+} (0.945).

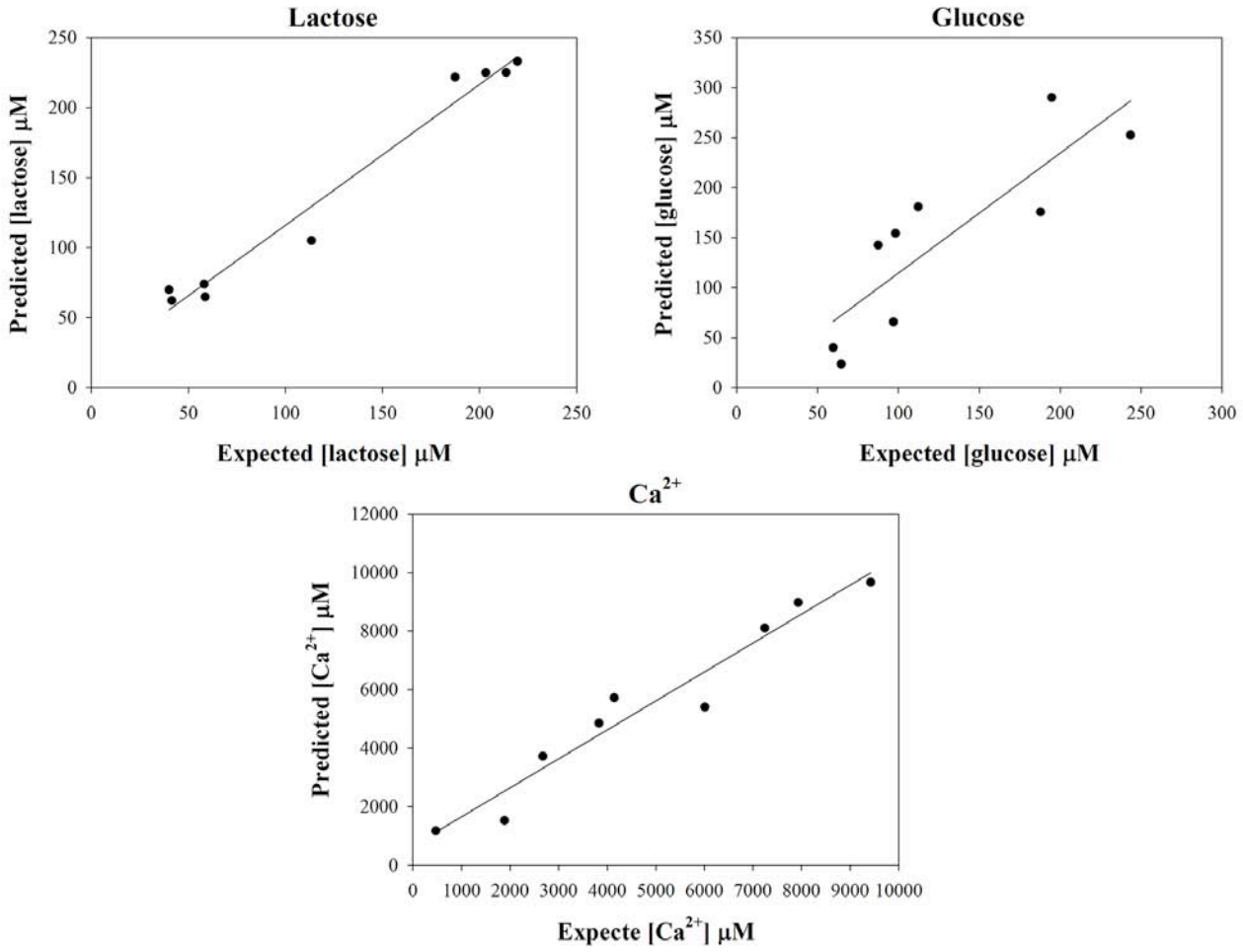

Figure 4.13 - Comparison graphics of the "expected vs. predicted" concentrations for the target analytes; lactose, glucose, and Ca^{2+} calculated by the ANN using the external test set samples with known (expected) concentrations.

For glucose a rather low R^2 of 0.726 was obtained. Despite the R^2 value for glucose being rather low, the presence of the data related to glucose in the model supports the prediction of the other two targets, lactose and Ca^{2+}. This behaviour could be explained considering that in the array there is only one biosensor to detect glucose, which can lead to a little less accurate detection; moreover for the *Ct*CDH291Y modified electrode, the enzyme is involved also in the conversion of lactose resulting in that the active site of the enzyme is partly occupied by the preferred substrate, giving a little lower sensitivity for glucose. To demonstrate how keeping the data related to glucose supported the prediction of lactose and Ca^{2+}, a few tests were run using 2 neurons for the output layer, to predict only lactose and Ca^{2+} while keeping the rest of the configuration as it was for the

original ANN. This resulted in significantly lower regression values showing that the ANN was less able to make a good prediction for lactose and Ca^{2+} when excluding the glucose related data. Also the prediction was completely random, being different every time the software was run. This behaviour of the ANN led to the conclusion that even if the glucose concentration predictions were poor, those data were essential for the complete prediction of the three analytes. As an example of the goodness of the prediction model the samples, used as external test to verify the ANN, are grouped in Table 4.4 showing the expected and predicted concentrations. The deviations between predicted and expected concentrations are on average +6.9% for lactose, +4.8% for Ca^{2+} and +12.3% for glucose, a highly valuable result, derived in this case from the different specificities shown by the different CDH enzymes used. It is not the first time where glucose quantification has shown added difficulties even with more specific enzymes [33], it is not sure but these difficulties could be originated by sample degradation or by glucose chemical equilibrium.

Table 4.4. Comparison of expected and predicted concentrations of the external test samples for the three analytes.

Lactose (µM)		**Glucose (µM)**		**Ca^{2+} (mM)**	
Expected	*Predicted*	*Expected*	*Predicted*	*Expected*	*Predicted*
2.03E+02	2.25E+02	9.69E+01	6.57E+01	3.83E+03	4.85E+03
5.81E+01	7.40E+01	1.12E+02	1.81E+02	1.89E+03	1.53E+03
2.14E+02	2.25E+02	2.43E+02	2.53E+02	7.24E+03	8.11E+03
1.13E+02	1.05E+02	5.97E+01	4.01E+01	7.93E+03	8.98E+03
5.86E+01	6.49E+01	8.75E+01	1.43E+02	4.14E+03	5.73E+03
4.14E+01	6.22E+01	9.82E+01	1.54E+02	2.67E+03	3.72E+03
4.00E+01	7.00E+01	1.95E+02	2.90E+02	4.70E+02	1.18E+03
1.87E+02	2.22E+02	6.47E+01	2.35E+01	9.42E+03	9.68E+03
2.19E+02	2.33E+02	1.88E+02	1.76E+02	6.01E+03	5.41E+03

4.4 – References

1. Ling Meng, J.J., Gaixiu Yang, Tianhong Lu, Hui Zhang, and Chenxin Cai, *Nonenzymatic Electrochemical Detection of Glucose Based on Palladium-Single-Walled Carbon Nanotube Hybrid Nanostructures.* Anal Chem, 2009. **81**(17).
2. Halder, A., et al., *Controlled Attachment of Ultrafine Platinum Nanoparticles on Functionalized Carbon Nanotubes with High Electrocatalytic Activity for Methanol Oxidation.* Journal of Physical Chemistry C, 2009. **113**(4): p. 1466-1473.
3. Guha, A., et al., *Surface-modified carbons as platinum catalyst support for PEM fuel cells.* Carbon, 2007. **45**(7): p. 1506-1517.
4. Raghuveer, M.S., et al., *Microwave-assisted single-step functionalization and in situ derivatization of carbon nanotubes with gold nanoparticles.* Chemistry of Materials, 2006. **18**(6): p. 1390-1393.
5. Xu, Q. and S.F. Wang, *Electrocatalytic oxidation and direct determination of L-tyrosine by square wave voltammetry at multi-wall carbon nanotubes modified glassy carbon electrodes.* Microchimica Acta, 2005. **151**(1-2): p. 47-52.
6. Yu, X.Z., et al., *Electrochemical behavior and determination of L-tyrosine at single-walled carbon nanotubes modified glassy carbon electrode.* Electroanalysis, 2008. **20**(11): p. 1246-1251.
7. Liu, L.Q., et al., *Improved Voltammetric Response L-Tyrosine on Multiwalled Carbon Nanotubes-Ionic Liquid Composite Coated Glassy Electrodes in the Presence of Cupric Ion.* Electroanalysis, 2008. **20**(19): p. 2148-2152.
8. Tang, X.F., et al., *Electrochemical determination of L-Tryptophan, L-Tyrosine and L-Cysteine using electrospun carbon nanofibers modified electrode.* Talanta, 2010. **80**(5): p. 2182-2186.
9. Jiang, L., et al., *Amperometric sensor based on tricobalt tetroxide nanoparticles-graphene nanocomposite film modified glassy carbon electrode for determination of tyrosine.* Colloids Surf B Biointerfaces, 2013. **107**: p. 146-51.
10. Salimi, A., et al., *Electrochemical detection of trace amount of arsenic(III) at glassy carbon electrode modified with cobalt oxide nanoparticles.* Sensors and Actuators B-Chemical, 2008. **129**(1): p. 246-254.
11. Cheng, Q., et al., *Electrochemical Tuning the Activity of Nickel Nanoparticle and Application in Sensitive Detection of Chemical Oxygen Demand.* Journal of Physical Chemistry C, 2011. **115**(46): p. 22845-22850.
12. Wittenberg, N.J. and C.L. Haynes, *Using nanoparticles to push the limits of detection.* Wiley Interdisciplinary Reviews-Nanomedicine and Nanobiotechnology, 2009. **1**(2): p. 237-254.
13. Welch, C.M. and R.G. Compton, *The use of nanoparticles in electroanalysis: a review.* Analytical and Bioanalytical Chemistry, 2006. **384**(3): p. 601-619.
14. Hu, C.C. and T.C. Wen, *Voltammetric investigation of Palladium oxides-II. Their formationreduction behavior during Glucose-oxidation in NaOH.* Electrochimica Acta, 1994. **39**(18): p. 2763-2771.
15. Zhou, Y.-G., et al., *Gold nanoparticles integrated in a nanotube array for electrochemical detection of glucose.* Electrochemistry Communications, 2009. **11**(1): p. 216-219.
16. Jena, B.K. and C.R. Raj, *Enzyme-free amperometric sensing of glucose by using gold nanoparticles.* Chemistry-a European Journal, 2006. **12**(10): p. 2702-2708.
17. Pasta, M., F. La Mantia, and Y. Cui, *Mechanism of glucose electrochemical oxidation on gold surface.* Electrochimica Acta, 2010. **55**(20): p. 5561-5568.
18. Zhou, S., et al., *Direct growth of vertically aligned arrays of Cu(OH)(2) nanotubes for the electrochemical sensing of glucose.* Sensors and Actuators B-Chemical, 2013. **177**: p. 445-452.
19. Yang, J., W.-D. Zhang, and S. Gunasekaran, *An amperometric non-enzymatic glucose sensor by electrodepositing copper nanocubes onto vertically well-aligned multi-walled carbon nanotube arrays.* Biosensors & Bioelectronics, 2010. **26**(1): p. 279-284.
20. Ensafi, A.A., M.M. Abarghoui, and B. Rezaei, *A new non-enzymatic glucose sensor based on copper/porous silicon nanocomposite.* Electrochimica Acta, 2014. **123**: p. 219-226.
21. de Sa, A.C., L.L. Paim, and N.R. Stradiotto, *Sugars electro-oxidation at glassy carbon electrode decorate with multi-walled carbon nanotubes with Nickel oxy-hydroxide.* International Journal of Electrochemical Science, 2014. **9**(12): p. 7746-7762.

22. Cataldi, T.R.I., et al., *Cobalt-based glassy-carbon chemically modified electrode for constant-potential amperometric detection of carbohydrates in flow-injection analysis and liquid chromatography.* Analytica Chimica Acta, 1992. **270**(1): p. 161-171.
23. Karim-Nezhad, G., et al., *Kinetic Study of Electrocatalytic Oxidation of Carbohydrates on Cobalt Hydroxide Modified Glassy Carbon Electrode.* Journal of the Brazilian Chemical Society, 2009. **20**(1): p. 141-151.
24. Sygmund, C., et al., *Characterization of the two Neurospora crassa cellobiose dehydrogenases and their connection to oxidative cellulose degradation.* Applied and Environmental Microbiology, 2012. **78**(17): p. 6161-6171.
25. Harreither, W., et al., *Recombinantly produced cellobiose dehydrogenase from Corynascus thermophilus for glucose biosensors and biofuel cells.* Biotechnology Journal, 2012. **7**(11): p. 1359-1366.
26. Coman, V., et al., *Investigation of electron transfer between cellobiose dehydrogenase from Myriococcum Thermophilum and gold electrodes.* Chemia Analityczna, 2007. **52**(6): p. 945-960.
27. Haladjian, J., et al., *A permselective-membrane electrode for the electrochemical study of redox proteins. Application to cytochrome c552 from Thiobacillus ferrooxidans.* Anal. Chim. Acta, 1994. **289**(1): p. 15-20.
28. Laviron, E., *General expression of the Linear Potential Sweep voltammogram in the case of diffusionless electrochemical system.* Journal of Electroanalytical Chemistry, 1979. **101**(1): p. 19-28.
29. Kovacs, G., et al., *Graphite electrodes modified with Neurospora crassa cellobiose dehydrogenase: Comparative electrochemical characterization under direct and mediated electron transfer.* Bioelectrochemistry, 2012. **88**(0): p. 84-91.
30. Harreither, W., et al., *Investigation of graphite electrodes modified with cellobiose dehydrogenase from the ascomycete Myriococcum thermophilum.* Electroanalysis, 2007. **19**(2-3): p. 172-180.
31. Kracher, D., et al., *Interdomain Electron Transfer in Cellobiose Dehydrogenase: Modulation by pH and Divalent Cations.* Febs Journal, 2015: p. in press; DOI: 10.1111/febs.13310.
32. Schulz, C., et al., *Enhancement of enzymatic activity and catalytic current of cellobiose dehydrogenase by calcium ions.* Electrochemistry Communications, 2012. **17**(0): p. 71-74.
33. A.Gutés, A.B.I., M. del Valle, F. Céspedes, *Automated SIA e-Tongue Employing a Voltammetric Biosensor Array for the Simultaneous Determination of Glucose and Ascorbic Acid.* Electroanalysis, 2006. **18**: p. 82-88.

CHAPTER 5 – CONCLUSIONS

5. Conclusions

1. An easy and quick protocol for the CNTs/NPs Nano-hybrid material has been achieved setting a quick one-pot synthesis able to give the final material in 24-36h with different metal NPs (Pd, Au and CuO) involved in the CNTs modification;
2. A first attempt to verify the applicability of the CNTs/NPs material has been done with the Nano-hybrid material CNTs/Pd-NPs used as platform for a Tyrosine sensor (Article 1). It showed a high increase in sensitivity compared to use only CNTs or the bare sensor itself;
3. A better understanding of how ANNs works was achieved during the secondment spent at Lund University (Sweden), where the sensors for a probable ET system were mostly optimized leaving more time for having the hands-on on the ANN software part. This experience was actually more fruitful then initially thought, resulting in a proof of concept of the first fully enzymatic Bio-ET system made using CDH enzymes used for the resolution of a mixture of lactose, glucose and Ca^{2+} as interfering species;

4. After testing the improvement given from the CNTs/NPs material compared to other configurations and having had some more understanding of how ET systems and ANNs works, other Nano-hybrid materials were synthesised, changing the loaded metal NPs on the CNTs (Au and CuO). These materials were then applied to a sensor array system largely used in our lab (ET system) to further test their properties. To achieve this result and go a bit further other two sensors with a different modification protocol of the CNTs (Ni and Co NPs, using and electrodeposition process instead of a reduction reaction process), and all the sensors together showed an incredible result with an ET system for sugars resolution (glucose, galactose, xylose and mannose) in sugarcane bagasse (Article 2).

5.1 Future perspectives

After having achieved all the proposed objectives, the next logical step would be to miniaturize the ET system taking advantage of the screen-printing technology. In our lab everything is technically ready to be tested, but it has not been tried yet. The concept would be to modify the electrode surface of a custom SPE (Figure 5.1) that has been designed from DropSens Company, following our requests. This kind of system would be tested and optimized in the near future.

Figure 5.1 – Custom screen-printed multi electrode, the black outer circles are eight working electrodes, the quasi-complete black circle in the middle is the auxiliary electrode and the small silver circle in the middle is the pseudo-reference electrode; a normal key is showed to size comparison.

CHAPTER 6 – PUBLICATIONS

Article 1:

Pd Nanoparticles/Multiwalled Carbon Nanotubes Electrode System for Voltammetric Sensing of Tyrosine

A. Cipri, M. del Valle, *Journal of Nanoscience and Nanotechnology*, **14** (2014), 6692 – 6698

Article

Journal of
Nanoscience and Nanotechnology
Vol. 14, 6692–6698, 2014
www.aspbs.com/jnn

Pd Nanoparticles/Multiwalled Carbon Nanotubes Electrode System for Voltammetric Sensing of Tyrosine

Andrea Cipri and Manel del Valle*

Sensors and Biosensors Group, Department of Chemistry, Universitat Autònoma de Barcelona, Edifici Cn, 08193 Bellaterra, Barcelona, Spain

A facile and quick synthesis of palladium decorated multi-walled carbon nanotubes is presented in this work. The developed protocol allowed a quasi-homogeneous distribution of the metal nanoparticles on the surface of the nanotubes, and a controlled size of the nanoparticles in a range between 3.5 and 4.5 nm. After the characterization of the hybrid nanocomposite a first attempt on a possible application was made. The preliminary test, an ink-like nanocomposite as a modifier on the surface of a carbon screen-printed electrode, was performed in order to detect L-Tyrosine. Preliminary results are promising. A catalytic effect on the oxidation peak of the L-Tyrosine was shown and furthermore a low limit of detection, 1.46×10^{-10} M, was reached.

Keywords: Multi-Walled Carbon Nanotubes, Palladium Nanoparticles, Nanocomposite, Screen-Printed Electrode.

1. INTRODUCTION

Carbon nanotubes (CNTs), which are fundamentally mere 'rolled-up' sheets of carbon atoms, are one of a family of carbon nanostructures and have been at the forefront of nanotechnological research and development for the last decade. Though initially discovered as unique entities in 1991 by Iijima,[1] CNTs have been readily produced in naturally occurring and man-made combustion reactions[2] and thus are in the atmosphere and throughout city air; Indeed, the 'contiguous hollow tubes' at the core of carbon fibres first reported over 40 years ago were later redefined as CNTs when the landmark paper was published less than 2 decades later.[3] The degree to which one encounters CNTs is surprising: a casual walk along a city promenade—albeit a smoggy city—could be taken as a prime opportunity to perform a passive collection of CNTs solely via respiration.[4] With such an abundance of this nanostructure in the atmosphere, it might be surprising to note how costly these 'carbon-roll-ups' were to be synthesised or isolated at the beginning. This, with the aide of modern and innovative synthesis techniques,[5] is changing for the better with prices plummeting two orders of magnitude in the past 20 years.

CNTs are highly versatile and are being used in many applications from tennis rackets[6] to intra-cellular surgery (nanotweezers),[7] to name just two applications. Hydrogen storage, solar cells, electrical cables and circuits, textiles and low grade heat converters are a few of the applications.[8–15] Indeed, the published literature discussing CNT applications is voluminous to say the least.

Nowadays, besides the increasing in strength of materials, the role played by the CNTs in food and pharmacological analysis is also relevant, thus the exploitation of their highly unique properties in the field of sensing, in which they are playing an increasingly significant part.[16–18] These properties include good electrical conductivity, strength, excellent bioconsistency, tube structure, fast electron transfer rate and a good electrocatalytic effect.[19]

Presently, the field of CNT research has diversified greatly to an umbrella of variants to include each and all of the various types of CNT structures defined as single-walled, multi-walled, bamboo-like, graphenated CNTs and nitrogen-doped nanotubes.[20–23]

CNTs do have a secondary exploitable function which is their ability to accept surface functionalizations so as to modify the aforementioned characteristics. One possible structure used for such surface modifications of CNTs is nanoparticles (NPs). The wide attention garnered to NPs has been awarded due to their unique and unusual physical properties which differentiate them from their bulk form. Sometimes referred to as the 'size-effect,' the characteristic physical aspects of nanoparticles encompass their

*Author to whom correspondence should be addressed.

 1533-4880/2014/14/6692/007 doi:10.1166/jnn.2014.9370

structural, electronic, magnetic and optical features. This is in addition to the changes in the chemical (catalytic) behaviour exhibited by these nanoscopic versions of the current bulk materials.

The allure of NPs lies within their controllability in preparation and diversity in function. The control of size, shape and surface chemistry of inorganic NPs allows for innovations in optical, electronic and catalytic properties which allows of the 'tailoring' of nanomaterials for specific objectives.[23–26]

Nowadays, inorganic nanoparticles can be fabricated with the use of several different techniques, including vapour deposition, lithographic techniques and electrochemical deposition.[27–29] However, the synthesis of inorganic nanoparticles via soft-chemical colloidal techniques has been shown to be the more effective and versatile mode of production.[30]

To exploit the advantageous properties of both the CNTs and the NPs in various applications, the nanoparticles need to be properly integrated and immobilized on the surface of the CNTs.[19] One example of this is the so-called metal nanoparticle decoration of the CNT exterior.[31] This can be achieved via two different synthesis routes: *in-situ* growth of the NPs or assembly of pre-formed NPs on the CNT surface. In both cases, surface modification is required which can involve the chemical development of defect-sites and subsequent covalent functionalization[32–34] or the non-covalent adsorption of macromolecules on the side walls.[35–37] Non-covalent adsorption is receiving major interest due to its enablement of the functionalization of the CNTs while simultaneously preserving their electronic structure, since the sp^2-hybridized carbon structure and the conjugation remains unaltered (which conversely provides the CNT surface with some inert and hydrophobic character, thus putting difficulties in the adsorption of any hydrophilic compound). Therefore, the recent challenge has been facilitating the fabrication of these nanocomposites and investigating on their possible applications. Among all the possibilities, some attention should be directed towards one-dimensional hybrid materials using CNT/nanoparticles as templates for applications like photoelectrochemical cells, electrocatalyst supports, and sensor or biosensor devices.[38–41] This is usually achieved by loading metal nanoparticles onto the CNTs surface, and obliging the maximum uniformity achievable in the layer. In order to do this, it is necessary to pre-treat the CNTs and thereby functionalise their surface. Normally, the nanotubes are acid-treated to create carboxylic, carbonyl, and hydroxyl groups that act as the anchoring functionalizations for metal nanoparticles.[42, 43] A direct result of this is the significant increase in active surface area which has afforded such functionalised CNTs much attention within the field of electrochemical sensors and biosensors.

In this work it is shown a facile and quick procedure to enhance the surface of multiwalled CNTs (MWCNTs) with palladium nanoparticles and thus generating a quasi-homogeneous dispersion which in turn exhibits a reduced size distribution. In this way, it is possible to increase the catalytic properties of the nanotubes by combining and exploiting the electrical characteristics of the nanotubes and the catalytic behaviour of the nanoparticles. Moreover, by way of a first attempt, a preliminary test has been made to show one of the possible applications of the MWCNTs/Pd hybrids. In this preliminary test, an ink-like composite is synthesised and used to modify the surface of a screen-printed electrode (SPE); the new material properties are screened and the possible use of this modified electrode as a sensor to detect electro-active molecules is investigated, in this case Tyrosine (Tyr).

Tyr is an amino acid made from another amino acid called phenylalanine. It is building block for several brain chemicals as epinephrine, noepinephrine and dopamine. These molecules help nerve cells communication and can influence the mood. Also the production of melanin involves Tyr as a precursor. The organs responsible for making and regulating hormones (adrenal, thyroid and pituitary glands) are helped in their functions by Tyr. This means that Tyr is involved in the structure of almost every protein in the body. One of the reasons to choose Tyr as target in this work is the presence of a genetic disorder called Phenylketonuria (PKU). This disease is due to the impossibility of the body to transform Phenylalanine into Tyr, generating a subsequent lack of Tyr leaving a high concentration of Phenylalanine in blood. If PKU is not treated can lead to serious problems as intellectual disability and other serious health problems.[44] PKU can be treated if early diagnosed, with food containing Tyr, following a specific diet, and medicals. Even depression can be treated with medicals containing Tyr, as it is a precursor of dopamine. Therefore, determination of Tyr is relevant due to its role in the food processing industry, pharmaceutical field and as a precursor of neurotransmitters.[45]

2. EXPERIMENTAL DETAILS

2.1. Reagent and Instruments

Purified multiwalled carbon nanotubes (MWCNTs) with an outer diameter of 30 nm were purchased from SES Research (Houston, Texas, USA). Palladium chloride ($PdCl_2$), ammonium fluoride (NH_4F), boric acid (H_3BO_3), sodium borohydride ($NaBH_4$) and polystyrene were purchased from Sigma-Aldrich (St. Louis, MO, USA). Sulphuric acid 96% (H_2SO_4), nitric acid 69% (HNO_3), ammonia 32% (NH_3), mesitylene and L-Tyrosine were purchased from Merck (Darmstad, Germany). All solutions were made using MilliQ water from MilliQ System (Millipore, Billerica, MA, USA). The buffer used for the preliminary test of the nanocomposite was PBS (187 mM NaCl, 2.7 mM KCl, 8.1 mM di-hydrated Na_2HPO_4, 1.76 mM KH_2PO_4, pH 7.0).

Transmission electron microscopy (TEM) images and microanalysis patterns were recorded with a JEOL

JEM-2011 microscope equipped with an energy dispersive spectroscopy (EDS) detector. Scanning electron microscopy (SEM) images were performed on a Zeiss Merlin (FE-SEM) microscope. The voltammetric characterizations were made with a DROPSENS multi potentiostat/galvanostat (μStat 8000) and using a DROPSENS carbon screen printed electrode (DS110), WE = carbon, pseudo-RE = Ag, CE = carbon.

2.2. Preparation of Palladium Decorated MWCNTs (MWCNT/Pd)

As shown in Figure 1(a), before the modification with palladium, an acidic pre-treatment was carried out to modify the protocol as reported by Alvaro et al.[46] Briefly, the MWCNTs were dispersed in a 3:1 mixture of concentrated H_2SO_4/HNO_3 acids using an ultrasonic bath for 90 min. The suspension was then filtered using a membrane of 0.2 μm and washed with a large amount of water until the pH value between 6 and 7 was reached at which point it was then dried under vacuum at 60 °C for 12 h. The decoration with palladium was then performed following the procedure reported by Meng et al.[31] Briefly, an Erlenmeyer flask was charged with a solution consisting of $PdCl_2$ (42 mg), H_3BO_3 (208 mg), NH_4F (42 mg) and 17 mL of double distilled water. Then, acid-treated MWCNTs (100 mg) were dispersed in the above solution via ultrasonication for approximately 1 h. The pH of the solution was then adjusted to 8–9 using concentrated ammonia. A solution of $NaBH_4$ (17 mL) was added dropwise under vigorous stirring and followed by another 8 h of stirring to complete the reaction. The MWCNT/Pd were isolated by filtering, using a membrane of 0.2 μm, then washed with a large amount of water and dried under vacuum at 60 °C.

2.3. Preparation of MWCNT/Pd Ink

The nanomaterial made by MWCNT/Pd is an ink-like composite. MWCNT/Pd, graphite and polystyrene (10%, 58% and 32% w/w respectively) were thoroughly mixed with mesitylene for 15–20 min with some sporadic 30 s sonication in order to obtain a medium thick solution.[47] The ink-like composite was dropped onto the surface of a carbon screen-printed electrode and dried at room temperature for at least 4 h, in order to perform a preliminary test. The carbon screen-printed electrodes used as support are provided by DROPSENS (DS110) with a carbon working and auxiliary electrode and a Ag pseudo-reference electrode on a ceramic support.

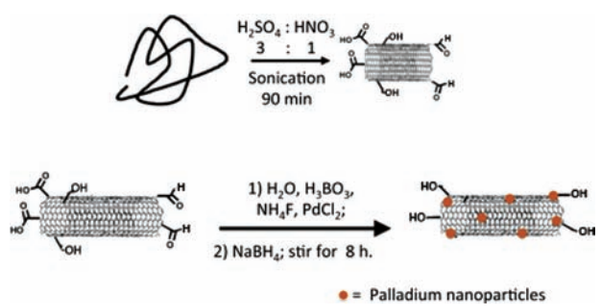

Figure 1. Scheme of the decoration of the multi-walled carbon nanotubes. (a) Surface functionalization of the MWCNTs; (b) *In-situ* synthesis of the palladium nanoparticles on the surface of the functionalized MWCNTs.

3. RESULTS AND DISCUSSION

3.1. Characterization

Meng et al.[31] showed how the acid treatment of the CNTs is an important step toward the synthesis of decorated CNTs. Without surface treatment, the degree of the NPs is insignificant because of the hydrophobicity of the nanotubes. The acid treatment can functionalize the CNTs with carboxyl, carbonyl and hydroxyl groups. Halder et al.[48] showed that besides the attachment of metal NPs, the surface functionalization is also important for the catalytic activity, due to its connection with the active sites (oxygen-containing groups) on the surface of the CNTs. There are several different methods of oxidative treatment that can be used, with only one acid, with a mixture of concentrated acids and with or without heating.[49, 50] In this work, three different acidic treatments were tested, with a common acidic mixture of concentrated H_2SO_4 and HNO_3 (3:1), without heating and with differing durations, 90 min, 2 h, 24 h. Between 2 hours and 90 minutes, the difference was insignificant therefore the 90 min duration was chosen. The 24 h treatment was discarded due to the defects generated on the surface of the CNTs that resulted in the breakage of the side-walls; this is shown in the TEM comparison in Figure 2 between the 90 min treatment (a) and the 24 h treatment (b). In Figure 2(a), it can be seen how the surface, even presenting some defects, is still intact and the length of the nanotubes has not been affected from the treatment. Resulting from the second treatment, Figure 2(b), it was seen that the extended duration caused an increase in surface defects which compromised the integrity of the side-wall and thus cancelled out the benefits of the treatment.

TEM characterization of the MWCNT/Pd is displayed in Figure 3. The MWCNTs shown in the image have a declared outer diameter of 30 nm. A quasi-homogeneous

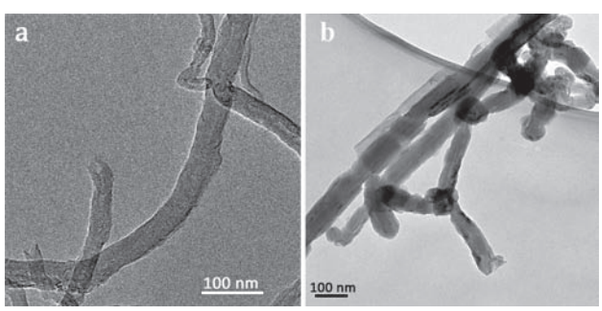

Figure 2. TEM characterization of only functionalized MWCNTs (a) 90 min treatment; (b) 24 h treatment.

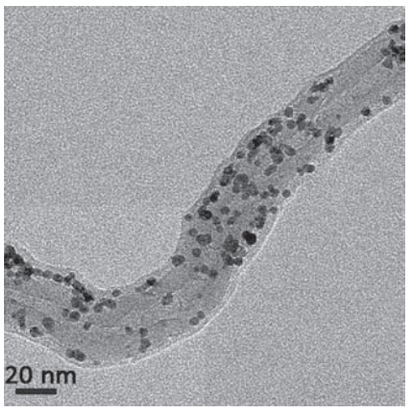

Figure 3. TEM image of Pd-NPs decorated MWCNTs.

distribution along the nanotube has been obtained and as can be observed the size of the nanoparticles is below 10 nm. The quasi-homogeneous distribution may be due to the small longitudinal size in comparison to the diameter of the nanotubes and to the in-situ growth of the palladium nanoparticles. This quasi-homogeneous distribution is expected to give better catalytic properties to the nanocomposite compared to its native properties. It was seen that the nanoparticles were crystalline nanoparticles through their characterization by high-resolution TEM (Fig. 4(a)). In the highlighted sections of Figure 4, the crystalline planes of the nanoparticle can be discerned. For every particle, all the planes have one direction and

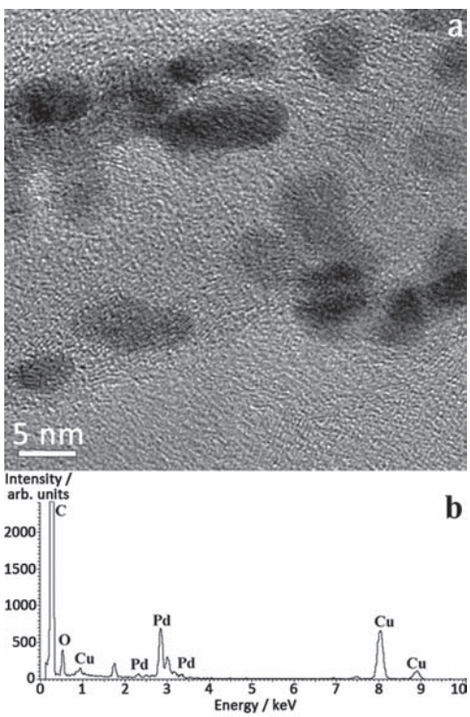

Figure 4. (a) High resolution TEM image of a section of MWCNTs/Pd-NPs; (b) EDS analysis of area showed in (a).

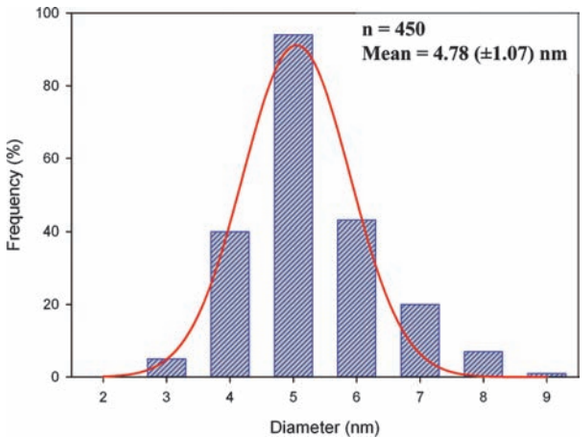

Figure 5. Partition distribution of the palladium nanoparticles.

this confirms the crystallinity of the species. To evaluate the composition of the MWCNTs/Pd, an energy dispersion spectra (EDS) was recorded (Fig. 4(b)). The EDS is a built-in detector in the TEM instrument used and can be employed to determine the elemental composition of the site under scrutiny. The presence of palladium in MWCNTs/Pd was confirmed from the peak at 3 keV; the carbon peak is due to the CNTs and the oxygen peak points to the carboxyl and carbonyl groups grafted on the surface during the functionalization stage. The presence of copper in the EDS spectra, instead, was attributed to the copper grid used as TEM sample holder.

A study of size distribution (Fig. 5) was performed to verify the mean size and distribution of nanoparticles the protocol was able to generate. More than 300 nanoparticles were measured and the diameter resulted 4.78 ($\pm$ 1.07) nm. This size of the NPs compared to the outer diameter of the nanotubes (30 nm) is quite small, allowing for a good distribution at the external surface and thus allowing an increase in the efficacy of catalytic behaviour. Also remarkable is the standard deviation obtained (22.4% when relatively expressed), claiming for the reproducibility of the reduction procedure.

A SEM characterization was also performed in order to investigate the spatial distribution of the palladium nanoparticles and to verify if the particles were all on the external surface or in the inner layers. As an example a SEM image is displayed in Figure 6; it shows MWCNTs/Pd although unfortunately it is not possible to distinguish the nanoparticles well; only in the highlighted section can some nanoparticles be identified. This *vanishing* effect may be due to the small diameter of the nanoparticles having such a high possibility to be crossed from the electron beam of the SEM and hence not being displayed during the recording of the image.

3.2. Application as a Sensor

After the characterization of the MWCNTs/Pd, its possible application as sensor material was investigated.

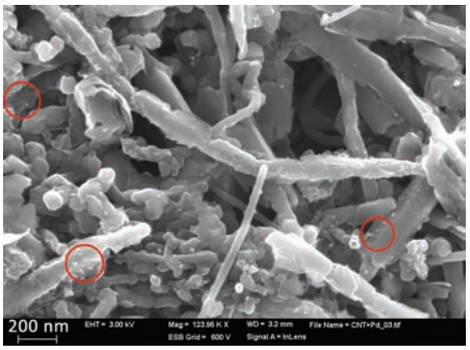

Figure 6. SEM characterization of MWCNTs/Pd-NPs.

Considering the electrical properties of the CNTs and the catalytic properties of both CNTs and palladium NPs, a preliminary test as an electrode modifier in voltammetric analysis was attempted.

To achieve this preliminary test, an ink-like nanocomposite was prepared. Starting with a modification protocol for screen-printed electrodes shown from Authier et al.[47] a predetermined amount of graphite, MWCNTs/Pd, polystyrene and mesitylene was thoroughly mixed until a correct thickness was achieved so as to avoid an overly rapid dispersion on the electrode upon deposition. Using a micropipette a volume of 25 μL of the ink-like nanocomposite was then dropped onto the surface of the working electrode to modify it.

The analyte chosen for this preliminary test was L-Tyrosine for its redox behaviour and for its important role as neurotransmitter precursor in mammalian animals. The characterisations were performed by linear sweep voltammetry and chronoamperometry.

Not only was the MWCNTs/Pd electrode characterised, by way of a control for the experiment, an electrode modified with an ink-like nanocomposite made only with MWCNTs and a bare carbon screen-printed electrode in a 2 mM L-Tyr solution in PBS were also tested. In Figure 7(a) a linear sweep voltammetry graph is displayed so as to compare the performance of the three electrodes. As can be noted, the MWCNTs electrode (B) already has a catalytic effect on the oxidation peak of the L-Tyrosine when compared to the bare electrode (C) and this can be associated with the properties of the CNTs given as high conductivity, catalytic effect, and fast electron transfer. From the comparison between the MWCNTs/Pd electrode (A) and the MWCNTs electrode (B) a further increase in the catalytic effect of the modification on the electrode can be seen. The only difference between the two electrodes is the presence of palladium nanoparticles on the first, this confirms the catalytic behaviour of the Pd NPs. The shift to a less anodic potential of the oxidation peak using the MWCNTs/Pd electrode demonstrates that the palladium nanoparticles are acting as a catalytic enhancer on the surface of the nanotubes. Besides the reduction of the anodic potential, a higher current response using the same sample concentration (2 mM

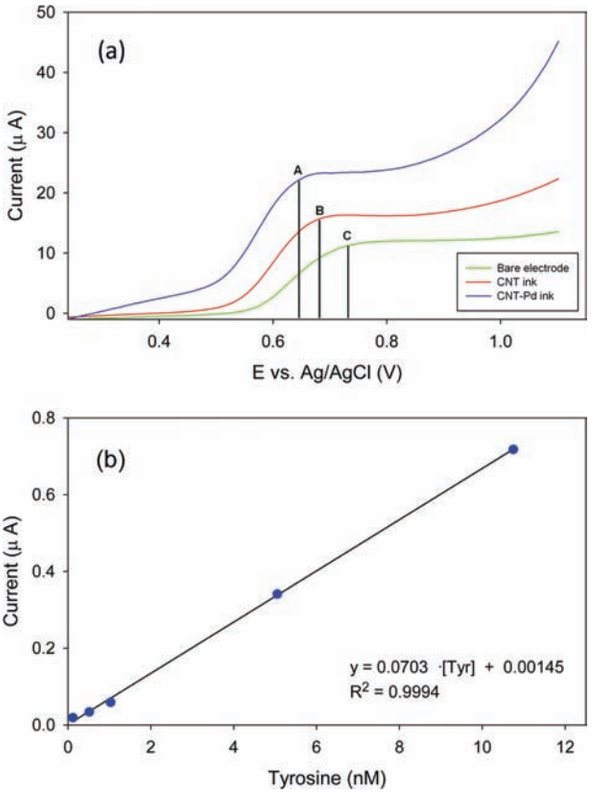

Figure 7. (a) Comparison of the voltammetric responses between MWCNTs/Pd-NP/Carbon screen-printed electrode, MWCNTs/Carbon screen-printed electrode and the bare carbon screen-printed electrode. The voltammetric technique used was a Linear Sweep Voltammetry with a range potential 0.2–1.1 V, E_{step} 2 mV, scan rate 50 mV/s; (b) Calibration curve for the determination of L-Tyrosine. The linear range is from 1.0×10^{-10} to 1.0×10^{-8} mol L^{-1}.

for all the electrodes) for the MWCNTs/Pd electrode can be also considered. Therefore a preliminary test of calibration was performed with the new nanocomposite electrode to investigate the detection limit of the electrode and to compare it with what is reported in literature. The calibration curve shown in Figure 7(b) is from the preliminary test and, as can be seen, the detection limit is extraordinarily low, 1.46×10^{-10} M, the range of concentrations was from 1×10^{-10} to 5×10^{-8} mol L^{-1} with the corresponding linear regression equation as following: $y = 7.03 \times 10^{-7} + 1.45 \times 10^{-3}$ Miss the X or Tyrosine concentration [Tyr] after 7.03×10^{-7} ($R^2 = 0.999$).

The detection limit (LOD), $S/N = 3$, was calculated considering the Standard Error of Estimate (SEE) as an estimation of the blank standard deviation, that is the standard deviation of the residual from the regression calculation.

In Table I is listed a comparison between MWCNTs/Pd modified screen-printed electrode and similar works in the literature. The results, when compared, show that the sensitivity of our system is more attractive and promising than previous reports.

Table I. Comparison of the MWCNTs/Pd performance with those previously reported.

Modified electrodes	Technique	Linear working range (M)	Detection limit (M)	Ref.
MWCNT/GCE	SWSV	2.0×10^{-6}–5.0×10^{-4}	4.0×10^{-7}	[51]
SWCNT/GCE	CV	5.0×10^{-6}–2.0×10^{-5}	9.3×10^{-8}	[52]
MWCNT/IL/Cu^{2+}/GCE	DPV	1.0×10^{-8}–5.0×10^{-6}	8×10^{-9}	[53]
CNF/CPE	I–T	2.0×10^{-7}–1.09×10^{-4}	1.0×10^{-7}	[54]
Co_3O_4/GR/GCE	I–T	1.0×10^{-8}–4.0×10^{-5}	1.0×10^{-9}	[45]
MWCNT/Pd/SPE	I–T	1.0×10^{-10}–1.0×10^{-8}	1.46×10^{-10}	This work

Notes: MWCNT/GCE: Multi-wall carbon nanotubes modified GC electrode. SWCNT/GCE: Single-wall carbon nanotubes modified GC electrode. MWCNT/IL/Cu2+/GCE: multi-wall carbon nanotubes–ionic liquid composite coated GC electrodes in the presence of cupric ion. CNF/CPE: electrospun carbon nanofibers modified carbon paste electrode. Co_3O_4/GR/GCE: tricobalt tetroxide nanoparticles-graphene nanocomposite modified GC electrode.

4. CONCLUSIONS

In summary, a facile and rapid route to synthetize palladium decorated MWCNTs has been developed. The efficiency of the protocol can be confirmed considering the quasi-homogeneous distribution and the small size of the palladium nanoparticles. The first attempt using this hybrid nanocomposite as a modifier for a carbon screen-printed electrode confirmed the good catalytic properties yielded from the combination of the two original materials, MWCNTs and palladium NPs. This catalytic behaviour is reflected in the very low detection limit seen while using the MWCNTs/Pd for the detection of the L-Tyrosine. Regarding this advantage in lowering the detection limit, future effort will aim to optimize the fabrication process of the electrode by screen-printing technologies.

Acknowledgment: This research was supported by the Research Executive Agency (REA) of the European Union under Grant Agreement number PITN-GA-2010-264772 (ITN CHEBANA), by the Ministry of Science and Innovation (MCINN, Madrid, Spain) through the project CTQ2010-17099 and by the Catalonia program ICREA Academia.

References and Notes

1. S. Iijima, *Nature* 354, 56 (**1991**).
2. L. E. Murr, K. F. Soto, P. A. Guerrero, D. A. Lopez, and D. A. Ramirez, *Microsc. Microanal.* 10, 410 (**2004**).
3. A. Oberlin, M. Endo, and T. Koyama, *J. Cryst. Growth* 32, 335 (**1976**).
4. C. W. Lam, J. T. James, R. McCluskey, S. Arepalli, and R. L. Hunter, *Crit. Rev. Toxicol.* 36, 189 (**2006**).
5. J. Prasek, J. Drbohlavova, J. Chomoucka, J. Hubalek, O. Jasek, V. Adam and R. Kizek, *J. Mater. Chem.* 21, 15872 (**2011**).
6. P. M. Ajayan and J. M. Tour, *Nature* 447, 1066 (**2007**).
7. P. Kim and C. M. Lieber, *Science* 286, 2148 (**1999**).
8. R. Hu, B. A. Cola, N. Haram, J. N. Barisci, S. Lee, S. Stoughton, G. Wallace, C. Too, M. Thomas, A. Gestos, M. E. d. Cruz, J. P. Ferraris, A. A. Zakhidov, and R. H. Baughman, *Nano Lett.* 10, 838 (**2010**).
9. A. C. Dillon, K. M. Jones, T. A. Bekkedahl, C. H. Kiang, D. S. Bethune and M. J. Heben, *Nature* 386, 377 (**1997**).
10. D. M. Guldi, G. M. A. Rahman, M. Prato, N. Jux, S. H. Qin, and W. Ford, *Angew. Chem. Int. Edit.* 44, 2015 (**2005**).
11. Y. Zhao, J. Q. Wei, R. Vajtai, P. M. Ajayan, and E. V. Barrera, *Sci. Rep-Uk* 1 (**2011**).
12. E. Artukovic, M. Kaempgen, D. S. Hecht, S. Roth, and G. GrUner, *Nano Lett.* 5, 757 (**2005**).
13. L. B. Hu, M. Pasta, F. La Mantia, L. F. Cui, S. Jeong, H. D. Deshazer, J. W. Choi, S. M. Han, and Y. Cui, *Nano Lett.* 10, 708 (**2010**).
14. B. Vidhya and A. Ford, *Nanosci. Nanotech. Lett.* 5, 980 (**2013**).
15. B. A. Gonfa, M. E. A. Khakani, and D. Ma, *Rev. Nanosci. Nanotech.* 1, 22 (**2012**).
16. N. Sinha, J. Z. Ma, and J. T. W. Yeow, *J. Nanosci. Nanotechno.* 6, 573 (**2006**).
17. S. Ghosh, A. K. Sood, and N. Kumar, *Science* 299, 1042 (**2003**).
18. Z. L. Li, P. Dharap, S. Nagarajaiah, E. V. Barrera, and J. D. Kim, *Adv. Mater.* 16, 640 (**2004**).
19. L. Y. Jiang, R. X. Wang, X. M. Li, L. P. Jiang, and G. H. Lu, *Electrochem. Commun.* 7, 597 (**2005**).
20. J. W. Mintmire, B. I. Dunlap, and C. T. White, *Phys. Rev. Lett.* 68, 631 (**1992**).
21. E. Flahaut, R. Bacsa, A. Peigney, and C. Laurent, *Chem. Commun.* 1442 (**2003**).
22. B. R. Stoner, A. S. Raut, B. Brown, C. B. Parker, and J. T. Glass, *Appl. Phys. Lett.* 99, (**2011**).
23. L. W. Yin, Y. Bando, M. S. Li, Y. X. Liu, and Y. X. Qi, *Adv. Mater.* 15, 1840 (**2003**).
24. L. M. Liz-Marzan, *Langmuir* 22, 32 (**2006**).
25. R. Mout, D. F. Moyano, S. Rana, and V. M. Rotello, *Chem. Soc. Rev.* 41, 2539 (**2012**).
26. G. He, Y. Song, B. Phebus, K. Liu, C. P. Deming, P. Hu, and S. Chen, *Sci. Adv. Mater.* 5, 1727 (**2013**).
27. B. M. I. van der Zande, L. Pages, R. A. M. Hikmet, and A. van Blaaderen, *J. Phys. Chem. B* 103, 5761 (**1999**).
28. X. D. Wang, J. H. Song, and Z. L. Wang, *J. Mater. Chem.* 17, 711 (**2007**).
29. Y. N. Xia and N. J. Halas, *Mrs. Bull.* 30, 338 (**2005**).
30. W. Stöber, A. Fink, and E. Bohn, *Journal of Colloid, and Interface Science* 26, 62 (**1968**).
31. L. Meng, J. Jin, G. Yang, T. Lu, H. Zhang, and C. Cai, *Anal. Chem.* 81, 7271 (**2009**).
32. J. M. Haremza, M. A. Hahn, and T. D. Krauss, *Nano Lett.* 2, 1253 (**2002**).
33. S. Banerjee and S. S. Wong, *Nano Lett.* 2, 195 (**2002**).
34. B. R. Azamian, K. S. Coleman, J. J. Davis, N. Hanson, and M. L. Green, *Chem. Commun.* 4, 366 (**2002**).
35. J. Chen, H. Liu, W. A. Weimer, M. D. Halls, D. H. Waldeck, and G. C. Walker, *J. Am. Chem. Soc.* 124, 9034 (**2002**).
36. S. Fullam, D. Cottell, H. Rensmo, and D. Fitzmaurice, *Adv. Mater.* 12, 1430 (**2000**).
37. M. J. O'Connell, P. Boul, L. M. Ericson, C. Huffman, Y. H. Wang, E. Haroz, C. Kuper, J. Tour, K. D. Ausman, and R. E. Smalley, *Chem. Phys. Lett.* 342, 265 (**2001**).
38. X. Peng, J. Chen, J. A. Misewich, and S. S. Wong, *Chem. Soc. Rev.* 38, 1076 (**2009**).
39. M. A. Correa-Duarte and L. M. Liz-Marzan, *J. Mater. Chem.* 16, 22 (**2006**).
40. M. Scarselli, C. Scilletta, F. Tombolini, P. Castrucci, M. Diociaiuti, S. Casciardi, E. Gatto, A. Venanzi, and M. De Crescenzi, *J. Phys. Chem. C* 113, 5860 (**2009**).
41. X. Hu and S. Dong, *J. Mater. Chem.* 18, 1279 (**2008**).
42. C. Gao, W. W. Li, Y. Z. Jin, and H. Kong, *Nanotechnology* 17, 2882 (**2006**).
43. T. W. Ebbesen, H. Hiura, M. E. Bisher, M. M. J. Treacy, J. L. S. Keyer, and R. C. Haushalter, *Adv. Mater.* 8, 155 (**1996**).

44. X. M. Mo, Y. Li, A. G. Tang, and Y. P. Ren, *Clin. Biochem.* 46, 1074 **(2013)**.
45. L. Jiang, S. Gu, Y. Ding, D. Ye, Z. Zhang, and F. Zhang, *Colloids Surf., B Biointerfaces* 107, 146 **(2013)**.
46. M. Alvaro, C. Aprile, B. Ferrer, and H. Garcia, *J. Am. Chem. Soc.* 129, 5647 **(2007)**.
47. L. Authier, B. Schollhorn, J. Moiroux, and B. Limoges, *J. Electroanal. Chem.* 488, 48 **(2000)**.
48. A. Halder, S. Sharma, M. S. Hegde, and N. Ravishankar, *J. Phys. Chem. C* 113, 1466 **(2009)**.
49. A. Guha, W. J. Lu, T. A. Zawodzinski, and D. A. Schiraldi, *Carbon* 45, 1506 **(2007)**.
50. M. S. Raghuveer, S. Agrawal, N. Bishop, and G. Ramanath, *Chem. Mater.* 18, 1390 **(2006)**.
51. Q. Xu and S. F. Wang, *Microchim. Acta* 151, 47 **(2005)**.
52. X. Z. Yu, Z. B. Mai, Y. Xiao, and X. Y. Zou, *Electroanal* 20, 1246 **(2008)**.
53. L. Q. Liu, F. Q. Zhao, F. Xiao, and B. Z. Zeng, *Electroanal* 20, 2148 **(2008)**.
54. X. F. Tang, Y. Liu, H. Q. Hou, and T. Y. You, *Talanta* 80, 2182 **(2010)**.

Received: 30 June 2013. Accepted: 4 September 2013.

Article 2:

Resolution of galactose, glucose, xylose and mannose in sugarcane bagasse employing a voltammetric electronic tongue formed bymetals oxy-hydroxide/MWCNT modified electrodes

A. C. de Sá, A. Cipri, A. González-Calabuig, N. R. Stradiotto, M. del Valle, *Sensors and Actuators B*, **222** (2016), 645 – 653

Sensors and Actuators B 222 (2016) 645–653

Contents lists available at ScienceDirect

Sensors and Actuators B: Chemical

journal homepage: www.elsevier.com/locate/snb

Resolution of galactose, glucose, xylose and mannose in sugarcane bagasse employing a voltammetric electronic tongue formed by metals oxy-hydroxide/MWCNT modified electrodes

Acelino Cardoso de Sá[a,b,*], Andrea Cipri[b], Andreu González-Calabuig[b], Nelson Ramos Stradiotto[a], Manel del Valle[b,*]

[a] Department of Analytical Chemistry, Institute of Chemistry, Universidade Estadual Paulista (UNESP), 55 Rua Francisco Degni, Araraquara 14800-060, SP, Brazil

[b] Sensors and Biosensors Group, Department of Chemistry, Universitat Autònoma de Barcelona, Edifici Cn, 08193 Bellaterra, Barcelona, Spain

ARTICLE INFO

Article history:
Received 4 June 2015
Received in revised form 29 July 2015
Accepted 19 August 2015
Available online 21 August 2015

Keywords:
Electronic tongue
Carbohydrates
Artificial neural network
Multi-walled carbon nanotubes
Metal nanoparticles
Second generation ethanol

ABSTRACT

Second generation ethanol is produced from the carbohydrates released from the cell wall of bagasse and straw of sugarcane. The objective of this work is the characterization and application of a voltammetric electronic tongue using an array of glassy carbon electrodes modified with multi-walled carbon nanotubes containing metal (Paladium, Gold, Copper, Nickel and Cobalt) oxy-hydroxide nanoparticles (GCE/MWCNT/MetalsOOH) towards a simpler analysis of carbohydrates (glucose, xylose, galactose and mannose). The final architecture of the back-propagation Artificial Neural Network (ANN) model had 36 input neurons and a hidden layer with 5 neurons. The ANN based prediction model has provided satisfactory concentrations for all carbohydrates; the obtained response had a maximum NRMSE of 12.4% with a maximum deviation of slopes in the obtained vs. expected comparison graph of 15%. For all species, the comparison correlation coefficient was of $r \geq 0.99$ for the training subset and of $r \geq 0.96$ for the test subset.

1. Introduction

The biomass sugarcane bagasse is a by-product of the production process for sugar and ethanol from sugarcane. New applications for the bagasse have been developed and among them we can highlight the production of second generation biofuels (ethanol) [1,2]. Second generation ethanol is produced from the carbohydrates released from the cell walls of sugarcane bagasse and straw [3,4].

Biomass as sugarcane bagasse is formed in its majority by lignocellulosic materials, in other words composed of hardly soluble carbohydrate polymers with crystalline and amorphous structures, formed by three main fractions: cellulose, hemicellulose and lignin [3,4]. The most abundant fraction is cellulose (32–44%), a linear homopolysaccharide formed by glucose units strongly bound. Hemicellulose (27–32%), consists of different carbohydrates, mainly xylose, configured in an easily hydrolysable chain. Finally, there is a series of aromatic alcohols polymerized, called lignin fraction (19–24%), that linked to hemicellulose wrap up the cellulose and protects it from the chemical or enzymatic hydrolytic attack [3,4].

Hemicelluloses are a heterogeneous class of polymers configured in an easily hydrolysable chain formed by carbohydrates as, pentoses (β-D-xylose, α-L-arabinose), hexoses (β-D-mannose, β-D-glucose, α-D-galactose) and uronic acids (α-D-glucuronic, α-D-4-O-methylgalacturonic and α-D-galacturonic) [5,6]

Abundant applications of enzymatic sensors for carbohydrates are reported in literature, with the majority dedicated to glucose in contrast to non-enzymatic ones. In their description, there is a balance of advantages and disadvantages of which both are significant. Despite dominating the glucose sensor market, some enzymatic systems, as the oxidases, have one critical flaw such the oxygen dependency, and can be therefore questioned for maximum reliability; other, like the dehydrogenases are highly limited by the use of co-substrates, making more difficult their use. Apart, the biosensing features of enzymatic sugar biosensors can be highly impacted by the presence of other electroactive interferences that are always commonplace in real industrial samples; and still, they will always be constrained by usage of mild enzymatic conditions, being proteins that may suffer denaturalization [7,8].

* Corresponding author. Tel.: +34 935813235; fax: +34 935812477.
E-mail addresses: manel.delvalle@uab.es, manel.delvalle@uab.cat (M. del Valle).

http://dx.doi.org/10.1016/j.snb.2015.08.088
0925-4005/

Sensitive and selective carbohydrate sensors are relevant for use in blood sugar monitoring, food industry, bio-processing and in the development of renewable and sustainable fuel cells. Non-enzymatic carbohydrate electrodes used in direct oxidation may show considerably greater sensitivity, with high oxidation currents being reported over the past decade [8].

The development of non-enzymatic carbohydrates sensors has risen at a considerable rate, many efforts have been made to find new electrocatalytic materials for oxidation of glucose and carbohydrates such as: cobalt hydroxide nanoparticles electrodeposited on the surface of glassy carbon electrode [9], multi-wall carbon nanotubes containing copper oxide nanoparticles [10], copper hydroxide nanotubes [11], nickel hydroxide nanoparticles on boron-doped diamond electrodes [12], carbon nanotubes/copper composite electrodes [13], copper(II) oxide nanorod bundles [14], gold nanoparticle-constituted nanotube array electrode [15], palladium nanoparticles supported on functional carbon nanotubes[16], palladium nanoparticles distributed on surfactant-functionalized multi-wall carbon nanotubes [17], Nickel/cobalt alloys modified electrodes [18], nickel hydroxide deposited indium tin oxide electrodes [19], Au–CuO nanoparticles decorated reduced graphene oxide [20] and glassy carbon electrode decorated with multi-wall carbon nanotubes with nickel oxy-hydroxide [21].

Accurate measurement of the carbohydrate content in the samples of sugarcane bagasse is very important, because the quantification of these sugars is directly linked to what type of microorganism has to be used in fermentation and is also extremely important in the evaluation and optimization of different processes for the production of second generation ethanol [2].

The use of non-enzymatic chemically modified electrodes represents an attractive alternative to classical analytical methods for detection of carbohydrates; unfortunately, these sensors exhibit lower selectivity than those enzymatic ones, discriminating with difficulties individual carbohydrates. Although this can be as the possibility to predict total carbohydrates present, the only alternative to the lack of selectivity seen can be the use of chromatographic stages [22–25]. Besides that to such specific equipment are high cost, laboratory conditions and trained personnel.

A new methodology in the sensors field is the use of sensors in arrays coupled with complex data treatment, that is, the use of electronic tongues; these are versatile sensor systems capable to simultaneously monitor the level of different analytes, or analytes in presence of their interferents, or to resolve mixtures of similar analytes [26–31].

An electronic tongue is a multisensor system, which consists of a number of low-selective sensors and uses advanced mathematical procedures for signal processing based on Pattern Recognition and/or Multivariate data analysis – Artificial Neural Networks (ANNs), Principal Component Analysis (PCA), etc. [32]. Therefore, the electronic tongue is an analytical system applied to liquid analysis formed by a sensor array in order to generate multidimensional information, plus a chemometric processing tool to extract meaning from these complex data [27,33].

From the beginning of this technique, there are electronic tongues devised using potentiometric sensors, but also using of the voltammetric type. In these original works, originated at the laboratories of Prof. Winquist in Linkoping (Sweden), the sensor array was formed by an array of different metallic disc electrodes, and a scanning voltammetric technique was used to generate the analytical information [30]. The voltammetric principle has also been applied to develop electronic tongues since its early years, such as simultaneous identification and quantification of nitro-containing explosives by advanced chemometric data treatment of cyclic voltammetry at screen-printed electrodes [28], instrumental measurement of wine sensory descriptors using a voltammetric electronic tongue [33], evaluation of red wines polyphenolic content by means of a voltammetric e-tongue with an optimized sensor array [34], voltammetric electronic tongue for the qualitative analysis of beers [27] and cava wine authentication employing a voltammetric electronic tongue [35].

The present work reports the characterization and application of a voltammetric electronic tongue using glassy carbon electrode modified with multi-wall carbon nanotubes decorated with metal (Copper, Cobalt, Paladium, Gold and Nickel) oxy-hydroxide nanoparticles (GCE/MWCNT/MetalsOOH) towards the analysis of carbohydrates (galactose, glucose, xylose and mannose). As such, it combines the responses from voltammetric electronic tongue formed by GCE/MWCNT/MetalsOOH modified electrodes, plus an advanced response model employing a specifically trained Artificial Neural Network (ANNs), with pretreatment of the data employing standard compression methods (Wavelet transform) and pruning step. This preprocessing is needed given the high dimensionality of the considered data.

2. Materials and methods

2.1. Reagent and instruments

Purified multiwalled carbon nanotubes (MWCNTs) with an outer diameter of 30 nm were purchased from SES Research (Houston, Texas, USA). Cobalt (II) chloride hexahydrate ($CoCl_2{\cdot}6H_2O$), nickel(II) sulfate hexahydrate ($NiSO_4{\cdot}6H_2O$), palladium chloride ($PdCl_2$), ammonium fluoride (NH_4F), boric acid (H_3BO_3), sodium borohydride ($NaBH_4$), N-N-Dimethylformamide 99.8% (C_3H_7NO), D-Glucose, D-Galactose, D-Mannose, D-Xylose $HAuCl_4.3H_2O$, Trisodium Citrate, Sodium dodecyl sulfate (SDS) and sodium hydroxide (NaOH) were purchased from Sigma–Aldrich (St. Louis, MO, USA). Sulphuric acid 96% (H_2SO_4), nitric acid 69%(HNO_3) $CuSO_4.5H_2O$ and ammonia 32% (NH_3) were purchased from Merck (Darmstad, Germany). All solutions were made using MilliQ water from MilliQ System (Millipore, Billerica, MA, USA). The buffer used for formation of nickel and cobalt nanoparticles was phosphate buffer (0.1 mol L^{-1} Na_2HPO_4 and 0.1 mol L^{-1} mono-hydrated NaH_2PO_4 pH 7.0).

2.2. Characterization by scanning electron microscopy

Transmission electron microscopy (TEM) images and micro-analysis patterns were recorded with a JEOL JEM-2011 microscope equipped with an energy dispersive spectroscopy (EDS) detector. Scanning electron microscopy (SEM) images were performed on JSM 7500F model Brand Jeol FE-SEM microscope.

2.3. Measuring procedure

The amperometric measurement cell was formed by the 5 (five) GCE/MWCNT/MetalsOOH modified electrodes plus a reference double junction Ag/AgCl electrode (Thermo Orion 900200, Beverly, MA, USA) and a commercial platinum counter electrode (Model 52-67, Crison Instruments, Barcelona, Spain). Cyclic voltammetry measurements were taken using a 6-channel AUTOLAB PGSTAT20 potentiostat (Ecochemie, Netherlands), in multichannel configuration, using the GPES Multichannel 4.7 software package. For this, potentials were cycled between −0.7 V and +0.8 V vs. Ag/AgCl, with a scan rate of 50 mV s^{-1}. Electroanalytical experiments were carried out at room temperature (25 °C) under quiescent conditions. Briefly, samples were measured as described with the GCE/MWCNT/MetalsOOH sensor voltammetric array, and afterwards obtained responses were analysed by means of the different chemometric tools described below.

2.4. Experimental design for the quantification model

In order to prove the capabilities of the ET to achieve the simultaneous quantification of different carbohydrates mixtures, resolution of Galactose, Glucose, Xylose and Mannose a response model using ANNs was prepared. To this aim, a total set of 46 samples were manually prepared with a concentration range of 0.5 to 2.5 mM for each carbohydrate. The set of samples was divided into two data subsets: a training subset formed by 36 samples (78%) which were distributed based on a L36 Taguchi design [36], with 4 factors and 3 levels, and used to build the response model, plus 10 additional samples (22%) for the testing subset, distributed randomly along the experimental domain and used to evaluate the model predictive ability.

2.5. Data processing

In order to reduce the large dataset generated for each sample (5 sensors x 336 current values at different potential) a preprocessing stage was necessary to compress the original data. The objective of this step was to reduce the complexity of the input data while preserving the relevant information, the compression of the data allows also to reduce the training time, to avoid redundancy in input data and to obtain a model with better generalization ability.

The data was compressed using the Discrete Wavelet Transform (DWT) [37]: each voltammogram was compressed using Daubechies 4 wavelet mother function and a fourth decomposition level. In this manner, the original data was reduced to 135 coefficients without any loss of relevant information; additionally Causal Index pruning strategy [38] was employed to further refine the model by eliminating the inputs that make relatively small contributions to the model. With this, the 135 inputs per sample were further reduced down to 36 coefficients, achieving a total compression ratio up to 97.9%.

2.6. Preparation of electrodes for electronic tongue

2.6.1. Decoration of MWCNTs with Pd, CuO and Au nanoparticles

Before the modification with metal nanoparticles MWCNTs were purified with an acidic pre-treatment. Briefly, the MWCNTs were dispersed in a 3:1 mixture of concentrated H_2SO_4/HNO_3 acids using an ultrasonic bath for 90 min [39]. Purified MWCNTs were then used for further modification with different metal nanoparticles.

2.6.2. Palladium decorated multi-wall carbon nanotubes (MWCNT/Pd)

This modification was performed following the protocol reported by Cipri et al. [39]. Briefly, a flask was prepared with a solution consisting of $PdCl_2$ (14.0×10^{-3} mol L^{-1}), H_3BO_3 (1.57×10^{-1} mol L^{-1}) and NH_4F (6.67×10^{-2} mol L^{-1}). Then, purified MWCNTs (100 mg) were dispersed in the above solution via ultrasonication for approximately 1 h and the pH was adjusted to 8–9. A solution of $NaBH_4$ (17 mL) was added dropwise under vigorous stirring and followed by another 8 h of stirring to complete the reaction. The MWCNT/Pd were filtered, washed and then dried under vacuum at 50 °C.

2.6.3. Gold decorated multiwalled carbon nanotubes (MWCNT/Au)

The decoration with Gold was performed following and slightly modifying the procedure reported by Shi et al. [40]. Briefly, a flask was prepared with a solution of 0.5 mL of $HAuCl_4 \cdot 3H_2O$ (1.0×10^{-2} mol L^{-1}), 0.5 mL of an aqueous solution of trisodium citrate (1.0×10^{-2} mol L^{-1}) and 18.4 mL of double distilled water. Purified CNTs (20 mg for a Au loading ratio of 10% wt%) were added to the above solution and then 10–12 mL of ethanol were immediately introduced under vigorous stirring and the mixture was ultrasonicated for 10 min. Ice-cold freshly prepared $NaBH_4$ aqueous solution (0.6 mL, 0.1 mol L^{-1}) was then added to the above mixture while stirring and leaving it overnight. The MWCNT/Au were separated by centrifuging, washed with double distilled water for several cycles and then dried under vacuum overnight at 50 °C.

2.6.4. Carbon nanotubes integrated with copper oxide nanoleaves (MWCNT/CuO)

The modification with copper was performed by modifying the procedure reported by Yang et al. [41]. Briefly, in a flask sodium dodecyl sulfate (SDS) was dissolved (0.1 mol L^{-1}) in 300.0 mL of distilled water stirring at 60 °C; Then 50 mg of purified MWCNTs were ultrasonically dispersed in 25.0 mL of DMF and then added to the SDS solution and ultrasonicated for 10 min, then $CuSO_4 \cdot 5H_2O$ (2.5 g) was added to the above solution and ultrasonicated for 10 min. The solution of 100 mL of NaOH (0.5 mol L^{-1}) was slowly dropped into the above solution and then stirred for 10.0 min. The resulting solution was then centrifuged, washed with doubly distilled water for few cycles and then dried at 60 °C.

2.6.5. Glassy carbon surface modification GCE/MWCNT/PdOOH

All surfaces of the GC electrodes were polished with 0.3 μm alumina powder (Merck) and cleaned in ethanol and Milli-Q water.

2.0 mg MWCNT/Pd were dispersed in 1.0 mL N,N-dimethylformamide (DMF) with a ultrasonic bath to give a 2.0 mg mL^{-1} black solution. 3 steps of 10 μL of the black solution were dropped on the GC electrode surface to prepare the GCE/MWCNT/Pd electrode surface at the end of each step, the electrode was allowed to dry at 50 °C for 3.0 h. After modification, the glassy carbon electrode modified with carbon nanotubes containing palladium nanoparticles (GCE/MWCNT/Pd) was passivated to form palladium oxy-hydroxide using a solution of NaOH 0.1 mol L^{-1} in the potential range of −0.8 to 0.8 V at a scan rate of 50 mV s^{-1} for 20 cycles in cyclic voltammetry. Then, the GCE/MWCNT/PdOOH was washed thoroughly with deionized water and dried. The electrochemical behavior of the GCE/MWCNT/PdOOH electrode was evaluated in aqueous solutions with supporting electrolyte NaOH 0.1 mol L^{-1}.

2.6.6. GCE/MWCNT/AuO

2.0 mg MWCNT/Au were dispersed in 1.0 mL N,N-dimethylformamide (DMF) with a ultrasonic bath to give a 2.0 mg mL^{-1} black solution. 3 steps of 10 μL of the black solution were dropped on the GC electrode surface to prepare the GCE/MWCNT/Au electrode surface. At the end of each step the electrode was allowed to dry at 50 °C for 3.0 h. After each modification the glassy carbon electrode modified with carbon nanotubes containing gold nanoparticles (GCE/MWCNT/Au) was passivated to form gold oxide using a solution of NaOH 0.1 mol L^{-1} in the potential range of −0.4 to 0.5 V at a scan rate of 50 mV s^{-1} for 20 cycles in cyclic voltammetry. Then, the GCE/MWCNT/AuO was washed thoroughly with deionized water and dried. The electrochemical behavior of the GCE/MWCNT/AuO electrode was evaluated in aqueous solutions with supporting electrolyte NaOH 0.1 mol L^{-1}.

2.6.7. GCE/MWCNT/CuOOH

2.0 mg MWCNT/Cu was dispersed in 20.0 mL N,N-dimethylformamide (DMF) with a ultrasonic bath to give a 0.1 mg mL^{-1} black solution. 2 steps of 10 μL of the black solution were dropped at the GC electrode surface to prepare the

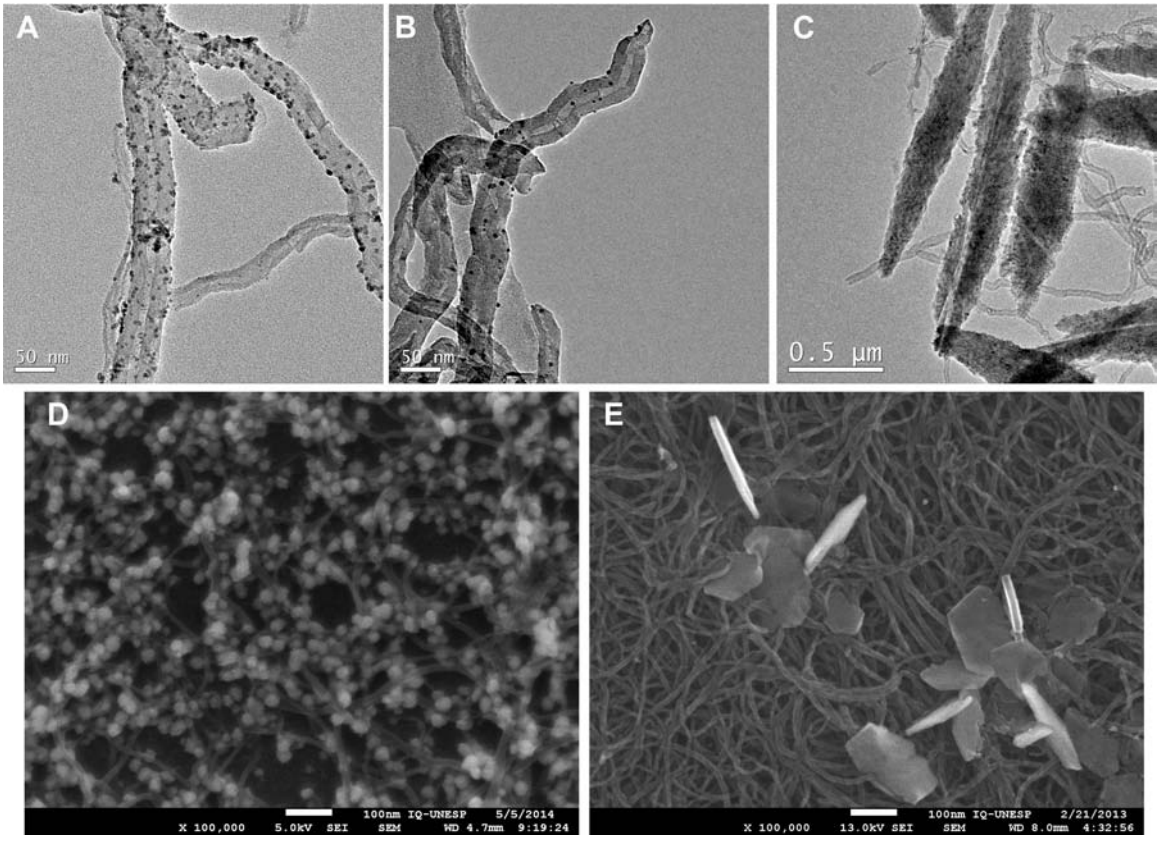

Fig. 1. TEM characterization of (A) MWCNT/PdO, (B) MWCNT/AuO and (C) MWCNT/CuO. SEM characterization of (D) MWCNT/NiOOH and (E) MWCNT/CoOOH composite materials.

GCE/MWCNT/Cu electrode surface at the end of each step, the electrode was dried at 50 °C for 3.0 h. After each modification the glassy carbon electrode modified with carbon nanotubes containing copper nanoparticles (GCE/MWCNT/Cu) was passivated to form copper oxy-hydroxide with a solution of NaOH 0.1 mol L^{-1} in the potential range of −0.5 to 0.3 V at a scan rate of 50 mV s^{-1} for 20 cycles in cyclic voltammetry. Then, the GCE/MWCNT/CuOOH was washed thoroughly with deionized water and dried. The electrochemical behavior of the GCE/MWCNT/CuOOH electrode was evaluated in aqueous solutions with supporting electrolyte NaOH 0.1 mol L^{-1}.

2.6.8. GCE/MWCNT/CoOOH

1.0 mg MWCNT was dispersed in 10.0 mL N,N-dimethylformamide (DMF) with a ultrasonic bath to give a 0.1 mg mL^{-1} black solution. 5.0 µL of the black solution was deposited at the GC electrode surface to prepare the GCE/MWCNT electrode surface. Immediately after the glassy carbon electrode was modified with carbon nanotubes (GCE/MWCNT) cobalt nanoparticles were electrodeposited using 1.0×10^{-3} mol L^{-1} of $CoCl_2$ in phosphate buffer 0.1 mol L^{-1} (pH 6.5). The electrodeposition was carried out by cyclic voltammetry in a potential range of −1.1 to 1.2 V at a rate of 100 mV s^{-1} for 30 cycles [42]. To complete the modification, the glassy carbon electrode modified with carbon nanotubes containing cobalt nanoparticles (GCE/MWCNT/Co) was passivated to form cobalt oxy-hydroxide at NaOH 0.1 mol L^{-1} in the potential range of −0.3 to 0.7 V at a scan rate of 50 mV s^{-1} for 45 cycles in cyclic voltammetry. Then, the GCE/MWCNT/CoOOH was washed thoroughly with deionized water and dried. The electrochemical behavior of the GC/MWCNT/CoOOH electrode was evaluated in aqueous solutions with supporting electrolyte NaOH 0.1 mol L^{-1}.

2.6.9. GCE/MWCNT/NiOOH

1.0 mg MWCNT was dispersed in 10.0 mL N,N-dimethylformamide (DMF) with a ultrasonic bath to give a 0.1 mg mL^{-1} black solution. 5.0 µL of the black solution was deposited at the GC electrode surface to prepare the GC/MWCNT electrode surface. Immediately after the glassy carbon electrode was modified with carbon nanotubes (GCE/MWCNT) a solution of $NiSO_4$ (5.0×10^{-3} mol L^{-1}), in phosphate buffer 0.1 mol L^{-1} (pH 6.5), was used for the electrodeposition of nickel nanoparticles. The electrodeposition was carried out by cronoamperometry at a potential of −1.3 V for 30 s. To complete the modification, the glassy carbon electrode modified with carbon nanotubes containing nickel nanoparticles (GCE/MWCNT/Ni) was passivated to form nickel oxy-hydroxide at NaOH 0.5 mol L^{-1} in the potential range of −0.5 to 1.0 V at a scan rate of 100 mV s^{-1} for 30 cycles in cyclic voltammetry [43]. Then, the GCE/MWCNT/NiOOH was washed thoroughly with deionized water and dried. The electrochemical behavior of the GCE/MWCNT/NiOOH electrode was evaluated in aqueous solutions with supporting electrolyte NaOH 0.1 mol L^{-1}.

3. Results and discussion

3.1. Characterization of GCE/MWCNT/Metals oxy-hydroxide modified electrodes

TEM characterization of the MWCNT/Pd is displayed in Fig. 1A, as can be observed the size of the nanoparticles is below 10 nm. The quasi-homogeneous distribution may be due to the small longitudinal size in comparison to the diameter of the nanotubes and to the in-situ growth of the palladium nanoparticles. This hybrid nanomaterial is expected to give better catalytic properties than the two materials by themselves. The morphology of

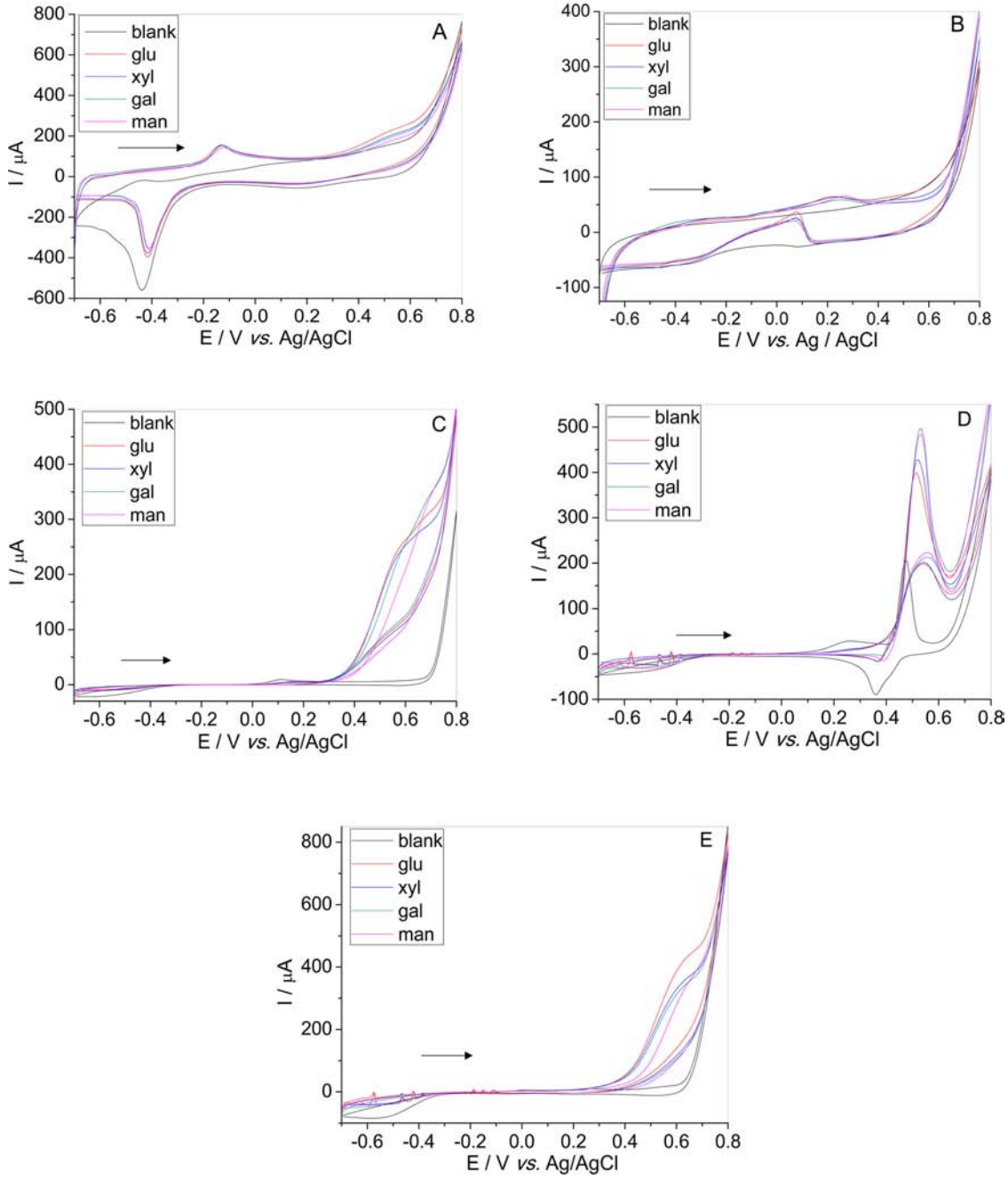

Fig. 2. Example of the different voltammograms obtained with (A) GCE/MWCNT/PdOOH, (B) GCE/MWCNT/AuO, (C) GCE/MWCNT/CuOOH, (D) GCE/MWCNT/NiOOH and (E) GCE/MWCNT/CoOOH for 0.1 mol L^{-1} NaOH and stock solutions 5.0×10^{-3} mol L^{-1} of each of the five carbohydrates (blank) Absence, (glu) Glucose,(xyl) Xylose, (gal) Galactose and (man) Mannose.

the MWCNT/Au composites was further characterized with TEM (Fig. 1B) and confirmed that the Au-NPs were attached on the MWCNT and ends, showing a diameter of about 4-7 nm. The TEM Fig. 1C shows that each leaf-like CuO polycrystalline is composed of several single-crystalline pieces, which suggest the coexistence of CuO and MWCNTs. Therefore, MWCNTs and CuO nanoleaves do indeed form a nanocomposite, and are not simply mixed together. In Fig. 1D it can be observed regular and spherical particles with size about 32 nm and their homogeneous distribution over the MWCNT. This better distribution and uniform sizes may be responsible for lower limits of detection in the analysis of sugars by the electrode modified with MWCNT/Ni [44,45]. In Fig. 1E it can be observed that the particles are in a wire shape. Some of the particles are in vertical position taking a representative wire; the average particle size is around 20 nm for particles in an upright position as in the case of wire and 185 nm for the particles in horizontal position.

3.2. GCE/MWCNT/Metals oxy-hydroxide modified electrodes response

The voltammetric responses for each of the electrodes towards individual compounds was the first response feature checked. That is, to ensure that enough differentiated signals were observed for the different electrodes, generating rich data that might be a useful departure point for the multivariate calibration model.

Table 1
Analytical parameters for various carbohydrates at electronic tongue formed by GCE/MWCNT/Metals oxy-hydroxide nanoparticle modified electrodes in 0.1 mol L^{-1} NaOH by Cyclic Voltammetry (ν = 50 mV s^{-1}; n = 3).

Palladium				
Carbohydrate	Limit of Detection (mM)	Limit of Quantification (mM)	Sensitivity (μA mM^{-1})	Concentration range (mM)
Glucose	0.32	1.05	25.5	0.4–5.0
Xylose	0.38	1.25	11.9	0.4–5.0
Galactose	0.87	2.97	14.1	0.9–5.0
Mannose	0.08	0.27	14.3	0.2–5.0
Gold				
Glucose	0.64	2.11	7.3	0.8–5.0
Xylose	0.62	2.04	5.8	0.8–5.0
Galactose	0.57	1.88	5.5	0.6–5.0
Mannose	1.00	3.33	6.0	1.0–5.0
Copper				
Glucose	0.10	0.33	51.1	0.2–5.0
Xylose	0.06	0.19	49.5	0.2–5.0
Galactose	0.38	1.26	41.5	0.4–5.0
Mannose	0.36	1.19	7.18	0.4–5.0
Nickel				
Glucose	0.23	0.76	32.0	0.4–5.0
Xylose	0.38	1.26	39.2	0.4–5.0
Galactose	0.41	1.36	46.7	0.5–5.0
Mannose	0.47	1.56	42.0	0.5–5.0
Cobalt				
Glucose	0.31	1.03	83.6	0.4–5.0
Xylose	0.10	0.33	67.9	0.2–5.0
Galactose	0.25	0.83	75.7	0.4–5.0
Mannose	0.38	1.26	69.2	0.4–5.0

To this aim, and under the described conditions in Section 2.5, individual standard solutions of galactose, glucose, xylose and mannose were analyzed and their voltammograms inspected, in Fig. 2 displays the voltammetric behavior from the different GCE/MWCNT/MetalsOOH modified electrodes in the electrooxidation study of carbohydrates.

In Fig. 2 (A) the selected is shown the voltammogram of GCE/MWCNT/PdOOH electrode during electro-oxidation of carbohydrates that occurs at potentials around −0.1 V vs. Ag/AgCl associated with an anodic peak current and also the decrease in cathodic peak current, the results suggest that $Pd^{(II)}/Pd^{(I)}$ redox couple in form of PdOOH [46] can catalyze the electro-oxidation of carbohydrates.

In Fig. 2 (B) is shown the voltammogram of GCE/MWCNT/AuO electrode during electro-oxidation of carbohydrates that occurs at potential around 0.25 V vs. Ag/AgCl, with the appearance of the anodic peak current and cathodic peak current of reoxidation at potentials −0.07 V vs. Ag/AgCl. This can be state as typical behavior of gold electrodes, which electrocatalytic activity of can be rationalized by the incipient hydrous oxide/adatom model can catalyze the oxidation of carbohydrates [15,47,48].

The voltammogram of GCE/MWCNT/CuOOH is shown in Fig. 2(C), for which in electro-oxidation of carbohydrates occurs at a potential of around 0.60 V vs. Ag/AgCl, with the appearance of the anodic wave. During the positive scan, the Cu nanoparticles can be oxidized to CuOOH. The $Cu^{(III)}/Cu^{(II)}$ redox couple can catalyze the oxidation of carbohydrates [11,49,50].

The electro-oxidation of carbohydrates on GC/MWCNT/NiOOH electrode, as shown in the Fig. 2 (D), occurred at a potential of around 0.52 V vs. Ag/AgCl associated with increased anodic peak current and decrease in cathodic peak current. The results suggest that $Ni^{(III)}/Ni^{(II)}$ redox couple can catalyze the electro-oxidation of carbohydrates [21].

The voltammogram of GCE/MWCNT/CoOOH shown in Fig. 2(E) demonstrated electro-oxidation of carbohydrates occurring at potential around 0.65 V vs. Ag/AgCl, with the appearance of the anodic wave. This fact suggests that carbohydrates are oxidized by CoOOH species through $Co^{(IV)}/Co^{(III)}$ redox couple moiety and through a cyclic mediation redox process [9,51].

The observed results as a whole, indicate the different GCE/MWCNT/MetalsOOH modified electrodes forming the electronic tongue can catalyze the electro-oxidation of carbohydrates (galactose, Glucose, Xylose and Mannose) to ketones, forming galactonolactone, gluconolactone, xylonolactone and mannonalactone, respectively [21]. Besides, clearly differentiated curves are obtained for each modified electrode and each considered sugar giving the desirable condition for an Electronic Tongue (ET) study.

This cross-response nature of the voltammograms can be summarized when plotting max currents (sensitivities) and oxidation peak potential observed for the 5 MWCNT/Metals NPs modified electrodes. This representation is shown in Fig. S3, where it can be observed that carbohydrates anodic peak current (Ipa) is different according to each metal nano-composite of the ET formed by GCE/MWCNT/Metals oxy-hydroxides modified electrodes and was also observed that the oxidation potentials (Epa) showed different behaviors according to each metal, this is a desirable condition for any ET study.

The Principal Component Analysis (PCA) is one of the most important methods used in chemometrics and it is the basis for many standards recognition, is a way of reducing a large multivariate data matrix into a matrix with a much smaller number of variables, without losing important information within the data. The principle behind PCA is that the multivariate data can be decomposed by linear projections onto a new co-ordinate system. The new axes, known as principal components (PCs), are orientated so that the first PC captures the largest amount of common variance

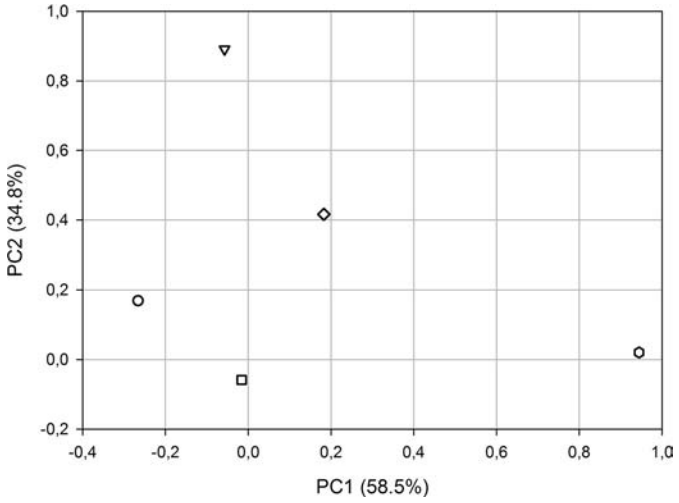

Fig. 3. PCA analysis loadings plot for five GCE/MWCNT/Metals oxy-hydroxide nanoparticle modified electrodes (metals = (□) gold, (▽) palladium, (⧉) copper, (◊) nickel and (◯) cobalt).

[52]. PCA can be one way to demonstrate the complementary of the generated information by each electrode, if electrodes are redundant they would appear superimposed, while different response will manifest in their separation. In Fig. 3 is shown the PCA for the five GCE/MWCNT/MetalsOOH modified electrodes (metals = gold, palladium, copper, nickel and cobalt); the PCA was prepared by treatment of the sensitivities of carbohydrates and was observed that each sensor showed performance in different regions this is very positive because that is a desirable condition for any ET study, justifying the inclusion of the five prepared electrodes in the sensor array.

The analytical reproducibility (%RSD) for the sensors was estimated using standard solutions of 2×10^{-3} mol L^{-1} glucose measured along 3 different days, obtaining values for GCE/MWCNT/AuO of 3.28%, for GCE/MWCNT/PdO 6.89%, for GCE/MWCNT/CuOOH 3.85%, for GCE/MWCNT/NiOOH 1.73% and for GCE/MWCNT/CoOOH 6.35%. The analytical reproducibilities shown seem reasonable values, because the electrodes are subjected to analysis of many samples thus requiring maintain its reproducibility and stability.

Complete calibrations of considered sugars were conducted in 0.1 mol L^{-1} NaOH solution with scan rate of 50 mV s^{-1} in order to fully characterize the used sensors. It was observed in all cases an increase of anodic peak current which was linear with the increase of concentration of sugars; Table 1 shows the electrochemical parameters for all carbohydrates studied. We observed that the electronic tongue formed by GCE/MWCNT/MetalsOOH modified electrodes has good amperometric sensitivity. The values of limit of detection and quantification are very close, meaning that the behavior of the different sugars on the electrode is comparable. Therefore we may apply the electronic tongue in the same concentration range for all sugars considered.

3.3. Building of the ANN Model

For the electronic tongue study, a total set of 46 carbohydrate standard mixtures were manually prepared (shown in Fig. S2 supplementary material), 36 corresponding to the train subset and

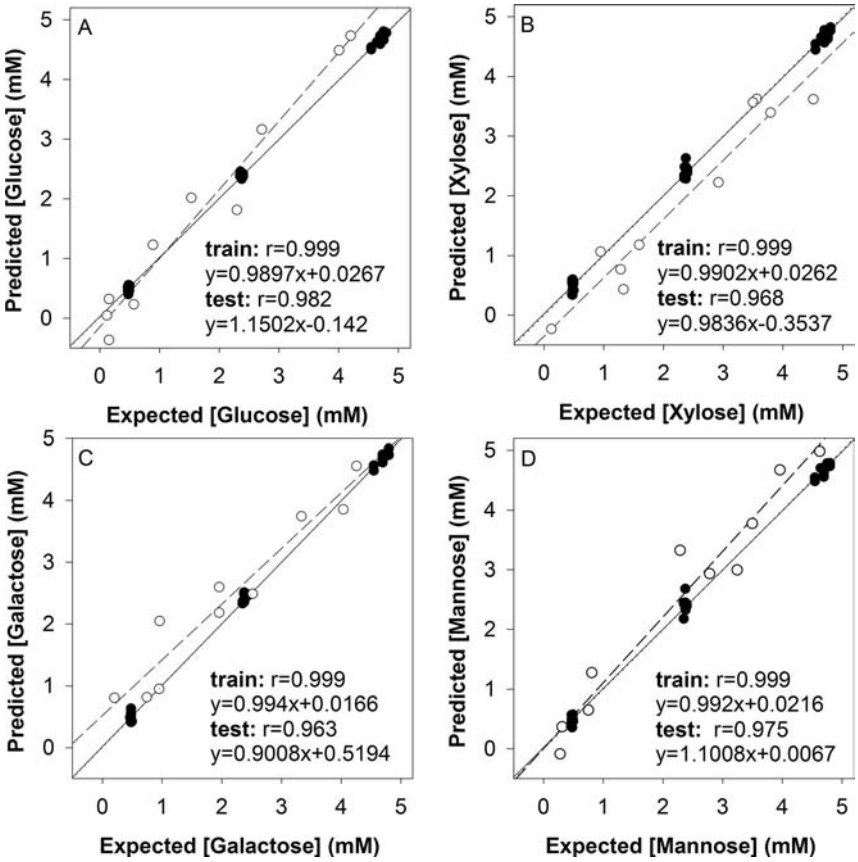

Fig. 4. Modelling ability of the optimized electronic tongue formed by GCE/MWCNT/MetalsOOH modified electrodes. Comparison graphs of predicted vs. expected concentrations for (A)Glucose, (B) Xylose, (C) Galactose and (D) Mannose, both for training (●, solid line) and testing subsets (◯, Dashed line). Dotted line corresponds to theoretical Y=X.

10 to the testing subset with concentrations ranged from 0.5 to 5.0 mM for each compound. These standards were first analyzed and used to build and validate the ANN model under the conditions previously described, the training and testing sets of samples were measured employing the GCE/MWCNT/MetalsOOH modified electrodes array, obtaining a complete voltammogram for each of the electrodes, and each sample. Because of the dimensionality and complexity of descriptive information generated (5 voltammograms per each sample), a double compression strategy with wavelet transform and causal index pruning was used.

Once the optimal set of coefficients was selected through Wavelet compressing and pruning the ANN final architecture was optimized. The parameters that were optimized were the 4 transfer functions employed in the hidden and output layers, the functions evaluated were *tansig*, *logsig*, *satlins* and *purelin*, and the number of neurons in the hidden layer, from 1 to 12 neurons.

In this manner 192 architectures were evaluated. The final architecture of the back-propagation ANN model had 36 input neurons, a hidden layer with 5 neurons and the *tansig* transfer function, an output layer with 4 neurons and the *purelin* transfer function.

The representation of the modeling performance of the system is illustrated in Fig. 4. This figure shows the comparison graphs of predicted vs. expected concentrations for the four carbohydrates and for training and testing subsets, that were built to check the prediction ability of the ANN model. It may be seen that a satisfactory trend was obtained, with the regression line almost indistinguishable from the theoretical one for the training subset. From these data it appears that all species demonstrate very good correlation coefficients with an R value ≥ 0.99 on the training subset. The model prediction is satisfactory for all carbohydrates and the accuracy of the obtained response is adequate. The results obtained for external test subset with much more significance than the latter, are close to the ideal values, with 0 intercepts, 1 slopes and good correlation coefficients R values ≥ 0.96.

With the aim of contrasting the goodness of these data, results were compared with those obtained from the most widely used in the chemometrics field data processing, PLS-1, with linear fittings from the comparison regression in Table S3 (supplementary material), and comparison plots, Fig. S3 (supplementary material). Both with the numeric data and with the represented plots, a slightly worst performance is evidenced from PLS treatment, from the comparison slopes more discrepant to 1.0, correlation coefficients different from 1.0, and more evidenced scatter of points in the comparison graphs. Probably the non-linear features present in the sensors result better modeled with use of the ANN than with PLS.

Table 2
Results in synthetic samples obtained from the electronic tongue formed by GCE/MWCNT/MetalsOOH modified electrodes in the analysis of Glucose, Xylose, Galactose and Mannose.

Samples	Glucose/mmol L^{-1}	Glucose found/mmol L^{-1}
1	4.0	4.5
2	2.7	3.2
3	4.2	4.7
	Xylose/mmol L^{-1}	Xylose found/mmol L^{-1}
1	3.6	3.6
2	2.9	2.2
3	3.5	3.6
	Galactose/mmol L^{-1}	Galactose found/mmol L^{-1}
1	2.0	2.6
2	2.0	2.2
3	1.0	1.0
	Mannose/mmol L^{-1}	Mannose found/mmol L^{-1}
1	4.0	4.7
2	4.6	4.9
3	0.3	0.4

After optimizing its performance, the electronic tongue was assessed through studies on synthetic samples of sugars shown in Table 2, with three different sugar mixtures. As it can be seen results found are in good agreement with those expected.

4. Conclusions

In this work, the application of an electronic tongue formed by GCE/MWCNT/MetalsOOH nanoparticle modified electrodes is described for detection and quantification of carbohydrates in sugar test samples. The complex response obtained from the electronic tongue was successfully processed employing a multilayer ANN and wavelet compressed information which proved to be especially suited for building the response model. Therefore this electronic tongue has enormous potential to be applied in hydrolyzed samples from sugarcane bagasse. Merit of the proposed system is to achieve resolution of mixtures of carbohydrates, with performance equivalent to HPLC equipment, without need to use any biosensor component thus permitting more stable responses.

Acknowledgements

This work was financial supported by FAPESP (Proc. n° 2011/19289-5, BEPE 2014/15557-3 and 2012/00258-5) and by Spanish ministry MINECO (Project CTQ2013-41577-P). A.Cipri was supported by Research Executive Agency (REA) of the European Union under Grant Agreement number PITN-GA-2010-264772 (ITN CHEBANA). M del Valle acknowledges support by the Catalonia program ICREA Academia. The authors are very grateful to LMA-IQ for carrying out the SEM-FEG analysis.

Appendix A. Supplementary data

Supplementary data associated with this article can be found, in the online version, at http://dx.doi.org/10.1016/j.snb.2015.08.088.

References

[1] C.A. Cardona, J.A. Quintero, I.C. Paz, Production of bioethanol from sugarcane bagasse: Status and perspectives, Bioresour. Technol. 101 (2010) 4754–4766.
[2] J.B. Sluiter, R.O. Ruiz, C.J. Scarlata, A.D. Sluiter, D.W. Templeton, Compositional analysis of lignocellulosic feedstocks. 1. Review and description of methods, J. Agric. Food Chem. 58 (2010) 9043–9053.
[3] C.R. Soccol, L.P. Vandenberghe, A.B. Medeiros, S.G. Karp, M. Buckeridge, L.P. Ramos, A.P. Pitarelo, V. Ferreira-Leitao, L.M. Gottschalk, M.A. Ferrara, E.P. da Silva Bon, L.M. de Moraes, A. Araujo Jde, F.A. Torres, Bioethanol from lignocelluloses: Status and perspectives in Brazil, Bioresour. Technol. 101 (2010) 4820–4825.
[4] Y. Sun, J. Cheng, Hydrolysis of lignocellulosic materials for ethanol production: a review, Bioresour. Technol. 83 (2002) 1–11.
[5] A. Ebringerová, Z. Hromádková, T. Heinze, Hemicellulose, Adv. Polym. Sci. 186 (2005) 1–67.
[6] F.M. Girio, C. Fonseca, F. Carvalheiro, L.C. Duarte, S. Marques, R. Bogel-Lukasik, Hemicelluloses for fuel ethanol: A review, Bioresour. Technol. 101 (2010) 4775–4800.
[7] G. Wang, X. He, L. Wang, A. Gu, Y. Huang, B. Fang, B. Geng, X. Zhang, Non-enzymatic electrochemical sensing of glucose, Microchim. Acta 180 (2012) 161–186.
[8] K.E. Toghill, R.G. Compton, Electrochemical non-enzymatic glucose sensors: a perspective and an evaluation, Int. J. Electrochem. Sci. 5 (2010) 1246–1301.
[9] G. Karim-Nezhad, M. Hasanzadeh, L. Saghatforoush, N. Shadjou, S. Earshad, B. Khalilzadeh, Kinetic study of electrocatalytic oxidation of carbohydrates on cobalt hydroxide modified glassy carbon electrode, J. Brazil Chem. Soc. 20 (2009) 141–151.
[10] C. Batchelor-McAuley, G.G. Wildgoose, R.G. Compton, L. Shao, M.L.H. Green, Copper oxide nanoparticle impurities are responsible for the electroanalytical detection of glucose seen using multiwalled carbon nanotubes, Sens. Actuators B Chem. 132 (2008) 356–360.
[11] S. Zhou, X. Feng, H. Shi, J. Chen, F. Zhang, W. Song, Direct growth of vertically aligned arrays of $Cu(OH)_2$ nanotubes for the electrochemical sensing of glucose, Sens. Actuators B Chem. 177 (2013) 445–452.
[12] L.A. Hutton, M. Vidotti, A.N. Patel, M.E. Newton, P.R. Unwin, J.V. Macpherson, Electrodeposition of nickel hydroxide nanoparticles on boron-doped diamond

electrodes for oxidative electrocatalysis, J. Phys. Chem. C 115 (2011) 1649–1658.
[13] J. Wang, G. Chen, M. Wang, M.P. Chatrathi, Carbon-nanotube/copper composite electrodes for capillary electrophoresis microchip detection of carbohydrates, Analyst 129 (2004) 512.
[14] C. Batchelor-McAuley, Y. Du, G.G. Wildgoose, R.G. Compton, The use of copper(II) oxide nanorod bundles for the non-enzymatic voltammetric sensing of carbohydrates and hydrogen peroxide, Sens. Actuators B Chem. 135 (2008) 230–235.
[15] Y.-G. Zhou, S. Yang, Q.-Y. Qian, X.-H. Xia, Gold nanoparticles integrated in a nanotube array for electrochemical detection of glucose, Electrochem. Commun. 11 (2009) 216–219.
[16] X.-m. Chen, Z.-j. Lin, D.-J. Chen, T.-t. Jia, Z.-m. Cai, X.-r. Wang, X. Chen, G.-n. Chen, M. Oyama, Nonenzymatic amperometric sensing of glucose by using palladium nanoparticles supported on functional carbon nanotubes, Biosens. Bioelectron. 25 (2010) 1803–1808.
[17] Z.-x. Cai, C.-c. Liu, G.-h. Wu, X.-m. Chen, X. Chen, Palladium nanoparticles deposit on multi-walled carbon nanotubes and their catalytic applications for electrooxidation of ethanol and glucose, Electrochim. Acta 112 (2013) 756–762.
[18] F. Wolfart, A.L. Lorenzen, N. Nagata, M. Vidotti, Nickel/cobalt alloys modified electrodes: Synthesis, characterization and optimization of the electrocatalytical response, Sens. Actuators B Chem. 186 (2013) 528–535.
[19] V. Ganesh, S. Farzana, S. Berchmans, Nickel hydroxide deposited indium tin oxide electrodes as electrocatalysts for direct oxidation of carbohydrates in alkaline medium, J. Power Sources 196 (2011) 9890–9899.
[20] K. Dhara, T. Ramachandran, B.G. Nair, T.G. Satheesh Babu, Single step synthesis of Au–CuO nanoparticles decorated reduced graphene oxide for high performance disposable nonenzymatic glucose sensor, J. Electroanal. Chem. 743 (2015) 1–9.
[21] A.C. de Sa, L.L. Paim, N.R. Stradiotto, Sugars electrooxidation at glassy carbon electrode decorate with multi-walled carbon nanotubes with nickel oxy-hydroxide, Int. J. Electrochem. Soc. 9 (2014) 7746–7762.
[22] L.M.F. Gottschalk, R.A. Oliveira, E.P.d.S. Bon, Cellulases, xylanases, β-glucosidase and ferulic acid esterase produced by Trichoderma and Aspergillus act synergistically in the hydrolysis of sugarcane bagasse, Biochem. Eng. J. 51 (2010) 72–78.
[23] G. Jackson de Moraes Rocha, C. Martin, I.B. Soares, A.M. Souto Maior, H.M. Baudel, C.A. Moraes de Abreu, Dilute mixed-acid pretreatment of sugarcane bagasse for ethanol production, Biomass Bioenergy 35 (2011) 663–670.
[24] J.R.A. dos Santos, A.M. Souto-Maior, E.R. Gouveia, C. Martin, Comparison of shf and ssf processes from sugar cane bagasse for ethanol production by saccharotnyces cerevisiae, Quim Nova 33 (2010) 904–908.
[25] E.R. Gouveia, R.T. do Nascimento, A.M. Souto-Maior, G.J.D. Rocha, Validation of methodology for the chemical characterization of sugar cane bagasse, Quim Nova 32 (2009) 1500–1503.
[26] J. Gallardo, S. Alegret, R. Muñoz, L. Leija, P.Ro. Hernández, M. del Valle, Use of an electronic tongue based on all-solid-state potentiometric sensors for the quantitation of alkaline ions, Electroanalysis 17 (2005) 348–355.
[27] A. Gutés, F. Céspedes, M. del Valle, Electronic tongues in flow analysis, Anal. Chim. Acta 600 (2007) 90–96.
[28] X. Cetó, A.M. O' Mahony, J. Wang, M. del Valle, Simultaneous identification and quantification of nitro-containing explosives by advanced chemometric data treatment of cyclic voltammetry at screen-printed electrodes, Talanta 107 (2013) 270–276.
[29] X. Cetó, J.M. Gutiérrez, L. Moreno-Barón, S. Alegret, M. del Valle, Voltammetric electronic tongue in the analysis of cava wines, Electroanalysis 23 (2011) 72–78.
[30] M. del Valle, Electronic tongues employing electrochemical sensors, Electroanalysis (2010) 1539–1555.
[31] L. Nuñez, X. Cetó, M.I. Pividori, M.V.B. Zanoni, M. del Valle, Development and application of an electronic tongue for detection and monitoring of nitrate, nitrite and ammonium levels in waters, Microchem. J. 110 (2013) 273–279.
[32] Y. Vlasov, A. Legin, A. Rudnitskaya, C. Di Natale, A. D'Amico, Nonspecific sensor arrays ("electronic tongue") for chemical analysis of liquids (IUPAC Technical Report), Pure Appl. Chem. 77 (2005) 1965–1983.
[33] X. Cetó, A. González-Calabuig, J. Capdevila, A. Puig-Pujol, M. del Valle, Instrumental measurement of wine sensory descriptors using a voltammetric electronic tongue, Sens. Actuators B Chem. 207 (2015) 1053–1059.
[34] X. Cetó, J.M. Gutiérrez, M. Gutiérrez, F. Céspedes, J. Capdevila, S. Mínguez, C. Jiménez-Jorquera, M. del Valle, Determination of total polyphenol index in wines employing a voltammetric electronic tongue, Anal. Chim. Acta 732 (2012) 172–179.
[35] X. Cetó, J. Capdevila, A. Puig-Pujol, M. del Valle, Cava wine authentication employing a voltammetric electronic tongue, Electroanalysis 26 (2014) 1504–1512.
[36] G.Y.W. Taguchi, Introduction to off-line quality control, Central Japan Quality Control Assoc. (1979) 33–43.
[37] M. del Valle, R.M. Guerrero, J.M.G. Salgado (Eds.), Wavelets: Classification, Theory and Applications, Nova Science Pub Inc, New York, US, 2011.
[38] R.A. Johnson, D.W. Wichestein, Applied multivariate statistical analysis, Pearson Education, Harlow, GB, 2007.
[39] A. Cipri, M. del Valle, Pd nanoparticles/multiwalled carbon nanotubes electrode system for voltammetric sensing of tyrosine, J. Nanosci. Nanotechnol. 14 (2014) 6692–6698.
[40] Y. Shi, R. Yang, P.K. Yuet, Easy decoration of carbon nanotubes with well dispersed gold nanoparticles and the use of the material as an electrocatalyst, Carbon 47 (2009) 1146–1151.
[41] Z. Yang, J. Feng, J. Qiao, Y. Yan, Q. Yu, K. Sun, Copper oxide nanoleaves decorated multi-walled carbon nanotube as platform for glucose sensing, Anal. Methods 4 (2012) 1924.
[42] A. Salimi, H. Mamkhezri, R. Hallaj, S. Soltanian, Electrochemical detection of trace amount of arsenic(III) at glassy carbon electrode modified with cobalt oxide nanoparticles, Sens. Actuators B Chem. 129 (2008) 246–254.
[43] Q. Cheng, C. Wu, J. Chen, Y. Zhou, K. Wu, Electrochemical tuning the activity of nickel nanoparticle and application in sensitive detection of chemical oxygen demand, J. Phys. Chem. C 115 (2011) 22845–22850.
[44] N.J. Wittenberg, C.L. Haynes, Using nanoparticles to push the limits of detection. Wiley Interdisciplinary Reviews, Nanomed. Nanobiotechnol. 1 (2009) 237–254.
[45] C. Welch, R. Compton, The use of nanoparticles in electroanalysis: a review, Anal. Bioanal. Chem. 384 (2006) 601–619.
[46] C.C. Hu, T.C. Wen, Voltammetric investigation of palladium oxides.2. Their formation reduction behavior during glucose-oxidation in Naoh, Electrochim. Acta 39 (1994) 2763–2771.
[47] B.K. Jena, C.R. Raj, Enzyme-free amperometric sensing of glucose by using gold nanoparticles, Chem. A Eur. J. 12 (2006) 2702–2708.
[48] M. Pasta, F. La Mantia, Y. Cui, Mechanism of glucose electrochemical oxidation on gold surface, Electrochim. Acta 55 (2010) 5561–5568.
[49] J. Yang, W.-D. Zhang, S. Gunasekaran, An amperometric non-enzymatic glucose sensor by electrodepositing copper nanocubes onto vertically well-aligned multi-walled carbon nanotube arrays, Biosens. Bioelectron. 26 (2010) 279–284.
[50] A.A. Ensafi, M.M. Abarghoui, B. Rezaei, A new non-enzymatic glucose sensor based on copper/porous silicon nanocomposite, Electrochim. Acta 123 (2014) 219–226.
[51] T.R.I. Cataldi, I.G. Casella, E. Desimoni, T. Rotunno, Cobalt-based glassy-carbon chemically modified electrode for constant-potential amperometric detection of carbohydrates in flow-injection analysis and liquid-chromatography, Anal. Chim. Acta 270 (1992) 161–171.
[52] E. Richards, C. Bessant, S. Saini, Multivariate data analysis in electroanalytical chemistry, Electroanalysis 14 (2002) 1533–1542.

Biographies

Acelino Cardoso de Sá received his degree in Chemistry in 2007, received his Master in Condensed Matter Physics at Science Materials program at the Paulista State University-UNESP working on the themes: electroanalytical, copper nitroprusside, cobalt nitropursside, 3-aminopropyl silica gel and electrodes chemically modified. Ph.D. student in Analytical Chemistry. His main research field is the biofuels (second generation ethanol) at Institute of Chemistry–UNESP, Araraquara, Brazil. Ph.D. student at the Universitat Autònoma de Barcelona working in the analysis of sugars from cane sugar bagasse using electronic tongues.

Andrea Cipri studied Chemistry at the University of Sassari, Italy. He received his Master degree in 2011. At the beginning of 2012 he joined the group of Manel del Valle at the Universitat Autònoma de Barcelona (UAB), Spain, as a Marie Curie fellow for his PhD. He is currently a PhD fellow in Manel del Valle group and his research interests include the study of nano-materials and bio-materials for sensing applications and devices.

Andreu González-Calabuig received his M.Sc. degree in Chemistry in 2013 from the Universitat Autònoma de Barcelona, where he is at the moment completing his Ph.D. in Analytical Chemistry. His main research topics deal with the application of Electronic Tongues as a tool for security and food safety analysis.

Nelson Ramos Stradiotto graduated from the University of Sao Paulo, Brazil with a PhD degree in chemistry in 1980 for studies on "the kinetics and mechanism of tin reduction in aprotic media". He spent 2 years at The University of Southampton as a fellow researcher (1983–1984) and 2 years at The Loughborough University (1992–1994). Presently, he is a professor at the Institute of Chemistry—UNESP, Araraquara, Brazil. His research interests include Analytical Chemistry and Physical Chemistry in the specialties of Electrochemistry and Electroanalysis. The theme of current research is related to Sensors, Electrochemical Detectors coupled with chromatographic techniques and electroanalytical methods in Bioenergy, with emphasis on Biofuels, Bioproducts, Biomass and Biorefineries.

Manel del Valle received his Ph.D. in Chemistry in 1992 from the Universitat Autònoma de Barcelona, where he got a position of associate professor in Analytical Chemistry. He is a member of the Sensors & Biosensors Group where he is a specialist for instrumentation and electrochemical sensors. He has initiated there the research lines of sensor arrays and electronic tongues. Other interests of his work are the use of impedance measurements for sensor development, biosensors and the design of automated flow systems.

ANNEX

Article 3:

A novel bio-electronic tongue using different cellobiose dehydrogenases to resolve mixtures of various sugars and interfering analytes

A. Cipri, C. Schulz, R. Ludwig, Lo Gorton, M. del Valle

Biosensors and Bioelectronics, Manuscript submitted

A novel bio-electronic tongue using different cellobiose dehydrogenases to resolve mixtures of various sugars and interfering analytes

Andrea Cipri*[1]; Christopher Schulz*[2]; Roland Ludwig[3]; Lo Gorton[2]; Manel del Valle[1];

[1]Sensor & Biosensor Group, Chemistry Department, Universitat Autònoma de Barcelona, Barcelona, Spain;

[2]Department of AnalyticalChemistry/Biochemistry and Structural Biology, Lund University, Lund, Sweden;

[3]Department of Food Science and Technology BOKU – University of Natural Resources and Life Sciences, Muthgasse 18, 1190 Vienna, Austria

*Both authors contributed equally to this work

Abstract

A novel application of cellobiose dehydrogenase (CDH) as sensing element for an Electronic Tongue (ET) system has been tested. In this work CDH from various fungi, which exhibit different substrate specificities were used to discriminate between lactose and glucose in presence of the interfering matrix compound Ca^{2+} in various mixtures. This work exploits the advantage of an ET system with practically zero pre-treatment of samples and operation at low voltages in a direct electron transfer mode. The Artificial Neural Network (ANN) used in the ET system to interpret the voltammetric data was able to give a good prediction of the concentrations of the analytes considered. The correlation coefficients were high, especially for lactose (R^2 = 0.975) and Ca^{2+} (R^2 = 0.945). This ET application has a high potential especially for the food and dairy industry and also, in a future miniaturized system, for in situ food analysis.

1. Introduction

Electronic tongues (ETs) constitute a relatively new approach to solve problems in analytical chemistry. Even today it is difficult to find recognition elements for cheap and highly selective sensors or biosensors. Here ETs can come to our help. ETs are multi-sensor systems with cross-response that can process the signal using advanced mathematical methods based on pattern recognition and/or multivariate data analysis. These characteristics of the ET system are an advantage due to the possibility to make further interpretation of complex compositions of analytes, to solve mixtures, to differentiate primary species from interfering components or even to distinguish between false responses and true ones (del Valle 2010). ETs can be exploited to quantify a wide variety of compounds in different fields as food and beverage analysis (Cetó et al. 2013a), environment (Nunez et al. 2013; Raud and Kikas 2013) and medical fields (Lvova et al. 2009). They have also been applied in food industry to solve qualitative problems (Bagnasco et al. 2014; Cetó et al. 2013b). A wide variety of recognition elements, combinations thereof and sensor architectures are applied in ET systems and many examples are given in literature: for instance *"in bulk"* biosensors, where the enzymes or other biomolecules are inside the bulk of the electrode, *"inorganic"* sensors, as classic bare electrodes like glassy carbon, graphite or gold etc. and electrodes modified with metal nanoparticles, ion selective sensors (ISEs) covered with a PVC membrane or electrodes with catalysts (Cetó et al. 2012; Gutierrez et al. 2008; Wilson et al. 2015). In the range of surface modified electrodes the possibilities are almost infinite, from nanomaterials to biomolecules, e.g., carbon nanotubes, nanoparticles, enzymes, aptamers and a combination of these modifiers citing just a few (Cipri and del Valle 2014; Ocaña et al. 2014; Pacios et al. 2009). Most of such materials have been exploitable for ETs systems. Due to the nature of the ET there is no need for high selectivity. The key point is a good stability of the sensor response at least through a set of samples but also ideally through days. Also enzymes have been used as a detection element in ETs. Glucose oxidase was used for glucose determination in the presence of common interferents of the enzyme (A.Gutés 2006). Urease (and creatinine deiminase) was used for the determination of urea (or urea plus creatinine) in kidney related samples (Gutes et al. 2005; Gutierrez et al. 2007). Tyrosinase, peroxidases (Sapelnikova et al. 2003; Solna et al. 2005; Tønning et al. 2005) and also laccase were applied for resolution of phenol mixtures (Cetó et al. 2013a; Cetó et al. 2012). Acetylcholinesterases (Tønning et al. 2005) and cholinesterase (Sapelnikova et al. 2003; Solna et al. 2005) were applied to discriminate between different pesticides in their inhibition reaction

(Valdes-Ramirez et al. 2009). Such ET systems using biomolecules as enzymes for the detection have received the name Bioelectronic Tongues (BioETs) (Tønning et al. 2005) and were most recently reviewed by Peris and Escuder-Gilabert (Peris and Escuder-Gilabert 2013) and Ha and coworkers (Ha et al. 2015). It is known that enzymes are advantageous due to their inherent, higher specificity and the reduction of the activation energy necessary to drive a desired chemical reaction compared with non-enzymatically catalysed reactions (Berg et al. 2002). Both factors decrease (but do not abolish) the risk of interfering analytes being detected. Recently, there has been a lot of interest in redox enzymes and their applications for electrochemical biosensors, biofuel cells and bioelectrosynthesis (Katz and Willner 2004; Meredith and Minteer 2012; Osman et al. 2011; Rabaey and Rozendal 2010). One focus lies on the establishment of a direct electronic communication between electrodes and enzymes called direct electron transfer (DET) enabling biosensors or biofuel cell electrodes to operate at low or no overpotential with respect to the redox potential of the enzyme leading to increased cell voltages when applied to biofuel cells and when applied to biosensors, to mediator-less, third generation biosensors with decreased problems of interfering species being non-enzymatically detected. Furthermore often toxic and diffusive redox mediators shuttling electrons between enzymes and electrodes can be avoided when working with DET (Leech et al. 2012; Wang 2008). One of the enzymes for which a lot of interest has been shown in the field of biosensors and biofuel cells is cellobiose dehydrogenase (CDH) as it has been shown DET for a variety of substrates including analytically relevant sugars as glucose and lactose (Ludwig et al. 2013a).

CDH is an extracellular oxidoreductase secreted by wood degrading fungi. It is involved in the degradation process of cellulose being a structural part of wood. The natural substrate is cellobiose, which is a decomposition product from cellulose. (Henriksson et al. 2000; Ludwig et al. 2010; Zamocky et al. 2006) CDH oxidises cellobiose and reduces lytic polysaccharide monooxygenases (LPMOs), which in its reduced form supports the decomposition of cellulose as was recently found out (Beeson et al. 2011; Eibinger et al. 2014; Langston et al. 2011; Phillips et al. 2011).

CDH consists of two separate domains connected by a flexible polypeptide linker. These two domains consist of a larger, flavin adenine dinucleotide (FAD) containing flavodehydrogenase domain (DH_{CDH}) (Hallberg et al. 2002) and a smaller heme *b* containing cytochrome domain (CYT_{CDH}) (Hallberg et al. 2000). DH_{CDH} is catalytically active and responsible for the oxidation of the substrate leading to a fully reduced

FAD cofactor located in the DH_{CDH} (Jones and Wilson 1988). The electrons can be transferred by an internal electron transfer pathway (IET) to the CYT_{CDH} reducing the heme *b* cofactor (Igarashi et al. 2002). The CYT_{CDH} acts as an electron transfer protein between DH_{CDH} and the natural electron acceptor (LPMOs, see above) or an electrode surface (Ludwig et al. 2013a). CDHs are expressed by fungi from the dikaryotic phyla of Basidiomycota and Ascomycota and were phylogenetically classified into class I and class II respectively (Zamocky et al. 2006). Depending on the origin the biochemical properties, as size (usually between 80-100 kDA), isoelectric point (usually below pH 5) substrate spectrum and pH optimum, of CDHs can vary (Ludwig et al. 2010). All CDHs prefer cellodextrines and cellobiose as substrates, but also convert lactose (Zamocky et al. 2006). Some class II CDHs also show activity for glucose (Harreither et al. 2011; Henriksson et al. 1998; Zamocky et al. 2006). Next to differences in substrate specificities recently we found out that the activity of especially class II CDHs also depends on the presence of cations. Especially divalent cations as Ca^{2+} at millimolar concentrations were found to enhance the activity of CDH possibly by enhancing the rate limiting IET by screening negative charges being present at the interfaces of both domains decreasing the distance between the two domains. The activity of *Mt*CDH (class II) was found to be tunable most by Ca^{2+} with increases of around 5 times of its original activity at its optimal pH 5.5 when adding 50 mM Ca^{2+} (Kielb et al. 2015; Kracher et al. 2015; Larsson et al. 2000; Schulz et al. 2012).

The origin dependent different preferences for the substrate (lactose vs. glucose) and the varying dependence of the activity of CDH on cations make CDH a good candidate to build a sensor array to be exploited for a BioET system. CDH has already been applied in a BioET like setup, however in a rather selective manner using other enzymes as cholinesterase, tyrosinase and peroxidase to detect pesticides and phenols with low extend of cross-responses between the electrodes (Solna et al. 2005). However, the use of additional, unmodified electrodes and the rather high selectivity make both terms, Bio and ET questionable in this context. This work aims to show the feasibility of BioET using CDHs from different fungi as recognition elements. To make this possible we took advantage of the power of data analysis in ETs systems and the sensing and DET properties of CDH. To show how the system works two sugars (lactose and glucose) and one activity modulating cation (Ca^{2+}) were chosen as targets. A system like this can be potentially interesting for applications in the food and dairy industry, detecting levels of lactose in e. g. milk or lactose free milk. The Ca^{2+} and glucose content of milk might be of interest to detect possible adulteration of milk (Walstra et

al. 2014). In previous studies third-generation biosensors based on CDH to detect lactose in milk and in a dairy processing plant were shown to reliably measure levels of lactose with only dilution necessary as a sample preparation step (Glithero et al. 2013; Safina et al. 2010; Stoica et al. 2006; Yakovleva et al. 2012). Another advantage of this ET system is the non pre-treatment of the samples, giving an advantage for the producers to have a real time or in production line analysis.

2. Experimental

2.1 Reagents and Instruments

Sodium chloride (NaCl), 3-(N-morpholino)propanesulfonic acid (MOPS), lactose, D-glucose, ethanol (EtOH), sulphuric acid (H_2SO_4), hydrogen peroxide (H_2O_2) and 6-mercapto-1-hexanol 97% were purchased from Sigma Aldrich (St. Louis, MO, USA), calcium chloride ($CaCl_2$) was purchased from Merck KgaA (Darmstadt, Germany), dialysis membranes (Spectrapor, MWCO 12-14 kDA) were purchased from Spectrum Medical Industries (CA, USA). CDH from *Myriococcum thermophilum* (*Mt*CDH) (Zamocky et al. 2008) and a CDH variant from *Corynascus thermophilus* with enhanced activity for glucose (*Ct*CDH C291Y) (Harreither et al. 2012; Ludwig et al. 2013b) were recombinantly expressed in *Pichia pastoris*. CDH from *Neurospora crassa* (*Nc*CDH) was harvested and purified from the fungal culture (Harreither et al. 2011). The CDH preparations were used directly without further dilution and had concentrations of 7 mg/ml for *Mt*CDH, 18.8 mg/ml for *Ct*CDHC291Y and 8.4 mg/ml for *Nc*CDH. The concentrations of the enzymes were determined photometrically converting the absorption measured at 280 nm to a protein concentration by using the calculated absorption coefficients based on the amino acid sequences. The buffer used to perform the experiments was a 50 mM MOPS pH 6.7 adjusted to an ionic strength of 63 mM with NaCl. A pH of 6.7 and an ionic strength of 63 mM were chosen to potentially mimic the conditions present in cow's milk (Walstra et al. 2014).

The voltammetric analyses were performed with an EmStat2 PalmSens potentiostat using three modified gold electrodes as working electrodes (WE), a saturated calomel electrode (SCE) as a reference electrode and a platinum flag as an auxiliary electrode.

2.2 Preparation of the different CDH-biosensors

Polycrystalline gold electrodes (diameter=1.6 mm, BASi, West Lafayette, IN, USA) were cleaned by incubation in Piranha solution for 2 min (1:3 mixture of conc. H_2O_2 with H_2SO_4. (**Careful, the compounds react violently and highly exothermic with each other**), polished on polishing cloths with deagglomerated alumina slurry of a diameter of 1 µm (Struers, Ballerup, Danmark), sonicated in ultrapure water for 5 min and electrochemically cleaned in 0.5 M H_2SO_4 by cycling 30 times between 0.1 V and 1.7 V vs. SCE at a scan rate of 300 mV/s. The sensors were modified with a self-assembled monolayer (SAM) by immediately after rinsing with water, immersing the electrodes in a 10 mM ethanolic solution of 6-mercapto-1-hexanol overnight at room temperature. The electrodes were gently rinsed with ultrapure water and excess liquid was shaken off. On each of the three electrodes forming the ET 5 µL of a CDH solution, either *Mt*CDH, *Nc*CDH or *Ct*CDHC291Y was dropped on the SAM modified gold electrode surface and entrapped by covering it with a pre-soaked dialysis membrane, which was fixed with a rubber O-ring and Parafilm (Bemis, Neenah, WI, USA) as described by Haladjian and coworkers (Haladjian et al. 1994) and as shown in Fig. S1 (Supplementary material).

2.3 Measurement procedure

The voltammetric cell contained the three working electrodes (WEs) forming the sensor array, a reference and an auxiliary electrode. Each WE of the sensor array was measured independently and successively after each other connecting them to the single channel potentiostat. Stock solutions of lactose (5 mM), glucose (5 mM) and $CaCl_2$ (10 mM) were diluted with 50 mM MOPS/NaCl buffer, pH 6.7, to obtain solutions with varying concentrations of lactose, glucose and $CaCl_2$. For the characterisation and identification of the linear ranges of each of the biosensors used in the array calibration curves with concentrations between 0 and 7 mM for lactose, 0 and 7 mM for glucose and 0 and 50 mM for $CaCl_2$ were used. The concentrations for training and testing the ANN ranged from 0 to 250 µM for lactose and glucose and from 0 to 10 mM for Ca^{2+}. 27 samples were distributed in a simple 3-level factorial design[1] for training and 10 samples were randomly distributed along the experimental domain[2] for external test (Fig. 1).

[1] A 3-level factorial design is a design with points of interest organized in a cube 3x3x3.

[2] The experimental domain is the range of concentrations used to train the ANN and the test has to stay inside the domain otherwise they would be insignificant.

The cyclic voltammetric measurements were performed under nitrogen atmosphere at room temperature with samples being degased for 10 min with nitrogen prior to the measurement. The working potential was swept between -0.3 V and 0.15 V *vs.* SCE at a scan rate of 20 mV/s and a step potential of 2 mV.

2.4 Building the ANN model

The data analysis of the measurements was carried out using a multivariate calibration process. This process was based on an Artificial Neural Network (ANN) as response model. As explained in Section 2.2 a batch of 37 samples was prepared and divided in two groups (27+10), this division was made to train the model using the group of 27 and to test it with the group of 10. The test samples are useful to determine the prediction ability of the ANN. The samples were distributed randomly during the measurements to avoid any history effect.

The architecture definition of the ANN was configured and optimised based on our group's previous experience with ETs formed by amperometric sensors (Fig. 2). The optimisation included the number of neurons in the hidden layer in a range between 4 and 12, the number of output neurons was fixed to 3 (the number of target molecules) and 4 transfer functions (*logsig*: log-sigmoidal, *tansig*: hyperbolic tangent sigmoid, *purelin*: linear and *satlins*: saturated-linear) were assayed for each layer (input and output). Another optimisation step was provided from the pre-processing of the voltammetric data. The voltammograms were used in their full size unfolding them and joining the signals from every sensor to a "single-sensor-like" signal per every sample. Since this has generated tens of thousands of data points a pre-processing step consisting of wavelet compression was used. The pre-processing/compression step allowed the decrease of data to be managed from the software from 48 600 to 186 values, with a Daubechies wavelet function (*db4*) and a compression level of 3.

To evaluate the goodness of the fit of the ANN model the smallest value obtained from the test samples with an MSE (mean squared error) function was taken. The prediction abilities, instead, were evaluated through the linear regression of the comparison graphs of obtained (y) vs. expected (x) concentrations with slope of 1 and correlation coefficient close to 1 for the three target molecules.

2.5 Software

The voltammetric data were acquired by using PSTrace 4.4 (PalmSens, Utrecht, The Netherlands) software. Neural Network processing was developed by the authors by MATLAB 7.0 (Mathworks, Natick, MA, USA), using its Neural Network Toolbox (v. 3.0). The graphs were made with Sigma Plot 12 (Systat Software Inc., California, USA).

3. Results and discussion

3.1 Characterisation of each CDH biosensor

The sensor array used for the ET consisted of three different CDH modified gold/SAM electrodes – one was modified with *Mt*CDH, one with *Nc*CDH, and one with *Ct*CDHC291Y, expecting different substrate specificities depending on the enzyme origin. Before developing the ET application, the integrity and linear ranges for each of the biosensors versus each of the three analytes of interest, lactose, glucose and Ca^{2+} were determined. In Fig. 3 the cyclic voltammograms of the gold/SAM electrodes modified with either *Mt*CDH, *Nc*CDH or *Ct*CDHC291Y are shown. In the absence of substrate, clear redox waves originating from the oxidation and reduction of the heme *b* cofactor located in the CYT_{CDH} is visible. The midpoint potentials range between -153 mV vs. SCE for *Mt*CDH, -144 mV vs. SCE for *Nc*CDH and -148 mV vs. SCE for *Ct*CDHC291Y, which are close to literature values (Coman et al. 2007; Harreither et al. 2012; Sygmund et al. 2012). The additional oxidative redox wave present for *Nc*CDH at -210 mV vs. SCE might originate from the oxidation of the FAD cofactor located in the DH_{CDH} as found out to be possible recently (Schulz et al., in manuscript). The peak separations between the anodic and cathodic peak potentials vary between 42 mV and 52 mV and thus lay between a solution and a surface confined redox process typical for thin layer protein electrochemistry (Haladjian et al. 1994; Laviron 1979). When lactose as the standard substrate is added clear catalytic waves can be seen for all CDH modified electrodes proving they are catalytically active. For *Mt*CDH and *Ct*CDHC291Y, the catalytic waves start at potentials around the oxidation peak potential the CYT_{CDH} peak indicating DET from the CYT_{CDH} domain. For *Nc*CDH it seems that there are traces of catalysis at potentials already below the oxidation potential of the CYT_{CDH} peak indicating a potential DET from the DH_{CDH} as found out to be possible recently (Schulz et al., in manuscript). To determine the linear measuring ranges, the response of each CDH biosensor to varying analyte concentrations of lactose, glucose

and Ca^{2+} was determined, as shown in Fig. 4. The investigation with Ca^{2+} as analyte was performed in the presence of 7 mM lactose, since Ca^{2+} is not a substrate for CDH but only potentially increases the existing catalytic currents by affecting the interdomain electron transfer. As shown in Fig. 4 all CDH biosensors tested respond to lactose. The best responding biosensors are the ones modified with *Nc*CDH and *Ct*CDHC291Y, possibly because their pH optima for DET of 5.5 (Kovacs et al. 2012) and 7.5 (Harreither et al. 2012) respectively are close to the investigated pH of 6.7. The pH optimum for DET of *Mt*CDH is also at pH 5.5 (Harreither et al. 2007) but its decline of activity with increasing pH is steeper compared to that of *Nc*CDH (Harreither et al. 2007; Kovacs et al. 2012) possibly explaining the comparable low response of the *Mt*CDH biosensor to lactose. The upper linear measuring range for lactose can be estimated to reach 500 µM.

When looking into glucose as substrate (Fig. 4, middle row) clearly the *Ct*CDHC291Y variant designed for high activity with glucose responds best to glucose with a linear measuring range to up to 260 µM. When looking into Ca^{2+} as analyte the *Ct*CDHC291Y and *Mt*CDH modified biosensors are sensitive to additional Ca^{2+}. The absolute currents are higher for *Ct*CDHC291Y, since its activity in the absence of Ca^{2+} is already higher than that for *Mt*CDH. However, looking into the relative increases of the catalytic currents in the presence of 50 mM Ca^{2+} increases of around 6.3 times for *Ct*CDHC291Y and 4.5 times for *Mt*CDH show similar dependencies for both enzymes on additional concentrations of Ca^{2+}. The dependency of the activity of *Mt*CDH on additional [Ca^{2+}] is comparable to what has been found in other studies done at pH 5.5 and 7.5 (Kracher et al. 2015; Schulz et al. 2012). The activity of the glucose variant, *Ct*CDHC291Y, has not been studied before in the presence of Ca^{2+} but when comparing its activity with that of the wild-type *Ct*CDH in solution with cytochrome *c* as electron acceptor, the Ca^{2+} induced activity increase found here is around twice as high (Kracher et al. 2015). The nearly independence of the activity of *Nc*CDH on additional [Ca^{2+}] compares well with the literature, where no increase for *Nc*CDH was found when investigated in solution with cytochrome *c* as electron acceptor (Kracher et al. 2015). The linear ranges found here for the detection of Ca^{2+} range up to around 10 mM.

In summary, each investigated biosensor responds differently to the investigated analytes, which is a desired departure point for any ET design. This cross-response pattern was used to create a BioET with the help of an artificial neural network to resolve mixtures of all three analytes containing varying concentrations of

lactose and glucose between 0 and 250 μM and between 0 and 10 mM for Ca^{2+}. The BioET contained the three biosensors modified with *Mt*CDH, *Nc*CDH, or *Ct*CDHC291Y and an auxiliary and a reference electrode. The response of the ET to a set of 27 training samples and 10 test samples containing all three analytes was determined an analysed as input data for building the response model.

3.2 ANN response model

The training method used in the Artificial Neural Network was described in Section 2.4. To define the best architecture 144 different configurations were evaluated (product of the number of neurons in the hidden layer, the tested transfer functions in the hidden layer and the transfer functions in the output layer). The best result was as follows: 9 neurons in the hidden layer with the transform function *"logsig"* and 3 neurons in the output layer with a *"purelin"* as transform function. With this configuration the responses of the 10 test samples with known concentrations of lactose, glucose, and Ca^{2+} were then used to compare their calculated concentrations according to the ANN with their real concentrations. The correlations between predicted (by the ANN) and expected concentrations for all analytes are shown in Fig. 5, in this case for the external test set, the samples not intervening for the training process. Considering that the samples are mixtures of similar and/or interfering compounds and the typology of the sensors used satisfactory R^2 values were calculated especially for lactose (0.975) and Ca^{2+} (0.945). For glucose a rather low R^2 of 0.726 was obtained. Despite the R^2 value for glucose being rather low, the presence of the data related to glucose in the model supports the prediction of the other two targets, lactose and Ca^{2+}. This behaviour could be explained considering that in the array there is only one biosensor to detect glucose, which can lead to a little less accurate detection; moreover for the *Ct*CDH291Y modified electrodes, the enzyme is involved also in the conversion of lactose resulting in that the active site of the enzyme is partly occupied by the preferred substrate, giving a little lower sensitivity for glucose. To demonstrate how keeping the data related to glucose supported the prediction of lactose and Ca^{2+}, a few tests were run using 2 neurons for the output layer (data not shown), to predict only lactose and Ca^{2+} while keeping the rest of the configuration as it was for the original ANN. This resulted in significantly lower regression values showing that the ANN was less able to make a good prediction for lactose and Ca^{2+} when excluding the glucose related data. Also the prediction was completely

random, being different every time the software was run. This behaviour of the ANN led us to the conclusion that even if the glucose concentration predictions were poor, those data were essential for the complete prediction of the three analytes. As an example of the goodness of the prediction model the samples, used as external test to verify the ANN, are grouped in Table 1 showing the expected and predicted concentrations. The deviations between predicted and expected concentrations are on average +6.9% for lactose, +4.8% for Ca^{2+} and +12.3% for glucose, a highly reliable result, derived in this case from the different specificities shown by the different CDH enzymes used.

4. Conclusions

In this work we show the feasibility of a novel BioET system integrating bioinformatics for data treatment and bioelectrochemistry for smart analyte detection. In the present system we utilize the cross response of CDHs from different origins to the substrates lactose and glucose and the interfering compound Ca^{2+} to resolve mixtures of these analytes. The system operates in a DET mode allowing analyte detection at reduced potentials. After data treatment with an artificial neural network the BioET was able to successfully predict the concentrations especially for lactose and Ca^{2+} in artificial samples with an R^2 value of 0.975 and 0.945 respectively and a low deviation from the expected concentration values of +6.9% for lactose and +4.8% for Ca^{2+}. A BioET system like this, using the DET capabilities of CDH from different origins as sensor modifiers is a complete novelty. The great variety of CDHs may allow the system to be tailored to detect also other analytically relevant sugars as e.g. maltose or cellobiose. The findings are of potential interest for new biosensor applications for the food and dairy industry.

Acknowledgment

This research was supported by the Reasearch Executive Agency (REA) of the European Union under Grant Agreement number PITN-GA-2010-264772 (ITN CHEBANA), by the Catalonia Program ICREA Academia 2010, and by The Swedish Research Council (projects 2010-5031 and 2014-5908).

References and Notes

A.Gutés, A.B.I., M. del Valle, F. Céspedes, 2006. Electroanalysis 18, 82-88.

Bagnasco, L., Cosulich, M.E., Speranza, G., Medini, L., Oliveri, P., Lanteri, S., 2014. Food Chemistry 157, 421-428.

Beeson, W.T., Phillips, C.M., Cate, J.H.D., Marletta, M.A., 2011. Journal of the American Chemical Society 134, 890-892.

Berg, J.M., Tymoczko, J.L., Stryer, L., 2002. Biochemistry, Fifth Edition. W.H. Freeman, New York.

Cetó, X., Cespedes, F., del Valle, M., 2013a. Electroanalysis 25, 68-76.

Cetó, X., Cespedes, F., Pividori, M.I., Gutierrez, J.M., del Valle, M., 2012. Analyst 137, 349-356.

Cetó, X., Gutierrez-Capitan, M., Calvo, D., del Valle, M., 2013b. Food Chemistry 141, 2533-2540.

Cipri, A., del Valle, M., 2014. Journal of Nanoscience and Nanotechnology 14, 6692-6698.

Coman, V., Harreither, W., Ludwig, R., Haltrich, D., Gorton, L., 2007. Chemia Analityczna 52, 945-960.

del Valle, M., 2010. Electroanalysis 22, 1539-1555.

Eibinger, M., Ganner, T., Bubner, P., Rošker, S., Kracher, D., Haltrich, D., Ludwig, R., Plank, H., Nidetzky, B., 2014. Journal of Biological Chemistry 289, 35929-35938.

Glithero, N., Clark, C., Gorton, L., Schuhmann, W., Pasco, N., 2013. Analytical and Bioanalytical Chemistry 405, 3791-3799.

Gutes, A., Cespedes, F., Alegret, S., del Valle, M., 2005. Biosensors & Bioelectronics 20, 1668-1673.

Gutierrez, M., Alegret, S., del Valle, M., 2007. Biosensors & Bioelectronics 22, 2171-2178.

Gutierrez, M., Alegret, S., del Valle, M., 2008. Biosensors & Bioelectronics 23, 795-802.

Ha, D., Sun, Q., Su, K., Wan, H., Li, H., Xu, N., Sun, F., Zhuang, L., Hu, N., Wang, P., 2015. Sensors and Actuators B-Chemical 207, 1136-1146.

Haladjian, J., Bianco, P., Nunzi, F., Bruschi, M., 1994. Anal. Chim. Acta 289, 15-20.

Hallberg, B.M., Bergfors, T., Backbro, K., Pettersson, G., Henriksson, G., Divne, C., 2000. Structure 8, 79-88.

Hallberg, M.B., Henriksson, G., Pettersson, G., Divne, C., 2002. J. Mol. Biol. 315, 421-434.

Harreither, W., Coman, V., Ludwig, R., Haltrich, D., Gorton, L., 2007. Electroanalysis 19, 172-180.

Harreither, W., Felice, A.K.G., Paukner, R., Gorton, L., Ludwig, R., Sygmund, C., 2012. Biotechnology Journal 7, 1359-1366.

Harreither, W., Sygmund, C., Augustin, M., Narciso, M., Rabinovich, M.L., Gorton, L., Haltrich, D., Ludwig, R., 2011. Applied and Environmental Microbiology 77, 1804-1815.

Henriksson, G., Johansson, G., Pettersson, G., 2000. J. Biotechnol. 78, 93-113.

Henriksson, G., Sild, V., Szabo, I.J., Pettersson, G., Johansson, G., 1998. Biochim. Biophys. Acta 1383, 48-54.

Igarashi, K., Momohara, I., Nishino, T., Samejima, M., 2002. Biochem. J. 365, 521-526.

Jones, G.D., Wilson, M.T., 1988. Biochem. J. 256, 713-718.

Katz, E., Willner, I., 2004. Chemphyschem : a European journal of chemical physics and physical chemistry 5, 1084-1104.

Kielb, P., Sezer, M., Katz, S., Lopez, F., Schulz, C., Gorton, L., Ludwig, R., Wollenberger, U., Zebger, I., Weidinger, I.M., 2015. Chemphyschem 16, 1960-1968.

Kovacs, G., Ortiz, R., Coman, V., Harreither, W., Popescu, I.C., Ludwig, R., Gorton, L., 2012. Bioelectrochemistry 88, 84-91.

Kracher, D., Zahma, K., Schulz, C., Sygmund, C., Gorton, L., Ludwig, R., 2015. Febs Journal, in press; DOI: 10.1111/febs.13310.

Langston, J.A., Shaghasi, T., Abbate, E., Xu, F., Vlasenko, E., Sweeney, M.D., 2011. Applied and Environmental Microbiology 77, 7007-7015.

Larsson, T., Lindgren, A., Ruzgas, T., Lindquist, S.E., Gorton, L., 2000. J. Electroanal. Chem. 482, 1-10.

Laviron, E., 1979. Journal of Electroanalytical Chemistry 101, 19-28.

Leech, D., Kavanagh, P., Schuhmann, W., 2012. Electrochimica Acta 84, 223-234.

Ludwig, R., Harreither, W., Tasca, F., Gorton, L., 2010. Chemphyschem 11, 2674-2697.

Ludwig, R., Ortiz, R., Schulz, C., Harreither, W., Sygmund, C., Gorton, L., 2013a. Anal Bioanal Chem 405, 3637-3658.

Ludwig, R., Sygmund, C., Harreither, W., Kittl, R., Felice, A., 2013b. Mutated cellobiose dehydrogenase with increased substrate specificity. Google Patents.

Lvova, L., Martinelli, E., Dini, F., Bergamini, A., Paolesse, R., Di Natale, C., D'Amico, A., 2009. Talanta 77, 1097-1104.
Meredith, M.T., Minteer, S.D., 2012. Annual Review of Analytical Chemistry, Vol 5 5, 157-179.
Nunez, L., Ceto, X., Pividori, M.I., Zanoni, M.V.B., del Valle, M., 2013. Microchemical Journal 110, 273-279.
Ocaña, C., Arcay, E., del Valle, M., 2014. Sensors and Actuators B: Chemical 191, 860-865.
Osman, M.H., Shah, A.A., Walsh, F.C., 2011. Biosensors & Bioelectronics 26, 3087-3102.
Pacios, M., del Valle, M., Bartroli, J., Esplandiu, M.J., 2009. Journal of Nanoscience and Nanotechnology 9, 6132-6138.
Peris, M., Escuder-Gilabert, L., 2013. Analytica Chimica Acta 804, 29-36.
Phillips, C.M., Beeson, W.T., Cate, J.H., Marletta, M.A., 2011. Acs Chemical Biology 6, 1399-1406.
Rabaey, K., Rozendal, R.A., 2010. Nature Reviews Microbiology 8, 706-716.
Raud, M., Kikas, T., 2013. Water Research 47, 2555-2562.
Safina, G., Ludwig, R., Gorton, L., 2010. Electrochimica Acta 55, 7690-7695.
Sapelnikova, S., Dock, E., Solna, R., Skladal, P., Ruzgas, T., Emnéus, J., 2003. Analytical and Bioanalytical Chemistry 376, 1098-1103.
Schulz, C., Ludwig, R., Micheelsen, P.O., Silow, M., Toscano, M.D., Gorton, L., 2012. Electrochemistry Communications 17, 71-74.
Solna, R., Dock, E., Christenson, A., Winther-Nielsen, M., Carlsson, C., Emnéus, J., Ruzgas, T., Skladal, P., 2005. Analytica Chimica Acta 528, 9-19.
Stoica, L., Ludwig, R., Haltrich, D., Gorton, L., 2006. Analytical Chemistry 78, 393-398.
Sygmund, C., Kracher, D., Scheiblbrandner, S., Zahma, K., Felice, A.K., Harreither, W., Kittl, R., Ludwig, R., 2012. Applied and Environmental Microbiology 78, 6161-6171.
Tønning, E., Sapelnikova, S., Christensen, J., Carlsson, C., Winther-Nielsen, M., Dock, E., Solna, R., Skladal, P., Nørgaard, L., Ruzgas, T., Emnéus, J., 2005. Biosensors & Bioelectronics 21, 608-617.
Valdes-Ramirez, G., Gutierrez, M., del Valle, M., Ramirez-Silva, M.T., Fournier, D., Marty, J.L., 2009. Biosensors & Bioelectronics 24, 1103-1108.
Walstra, P., Wouters, J.T., Geurts, T.J., 2014. Dairy science and technology. CRC press, Boca Raton (FL).
Wang, J., 2008. Chemical Reviews 108, 814-825.
Wilson, D., Alegret, S., del Valle, M., 2015. Electroanalysis 27, 336-342.
Yakovleva, M., Buzas, O., Matsumura, H., Samejima, M., Igarashi, K., Larsson, P.-O., Gorton, L., Danielsson, B., 2012. Biosensors and Bioelectronics 31, 251-256.
Zamocky, M., Ludwig, R., Peterbauer, C., Hallberg, B.M., Divne, C., Nicholls, P., Haltrich, D., 2006. Current Protein & Peptide Science 7, 255-280.
Zamocky, M., Schumann, C., Sygmund, C., O'Callaghan, J., Dobson, A.D.W., Ludwig, R., Haltrich, D., Peterbauer, C.K., 2008. Protein Expression and Purification 59, 258-265.

Table 1. Comparison of expected and predicted concentrations of the external test samples for the three analytes.

Lactose (µM)		**Glucose (µM)**		**Ca^{2+} (mM)**	
Expected	*Predicted*	*Expected*	*Predicted*	*Expected*	*Predicted*
2.03E+02	2.25E+02	9.69E+01	6.57E+01	3.83E+03	4.85E+03
5.81E+01	7.40E+01	1.12E+02	1.81E+02	1.89E+03	1.53E+03
2.14E+02	2.25E+02	2.43E+02	2.53E+02	7.24E+03	8.11E+03
1.13E+02	1.05E+02	5.97E+01	4.01E+01	7.93E+03	8.98E+03
5.86E+01	6.49E+01	8.75E+01	1.43E+02	4.14E+03	5.73E+03
4.14E+01	6.22E+01	9.82E+01	1.54E+02	2.67E+03	3.72E+03
4.00E+01	7.00E+01	1.95E+02	2.90E+02	4.70E+02	1.18E+03
1.87E+02	2.22E+02	6.47E+01	2.35E+01	9.42E+03	9.68E+03
2.19E+02	2.33E+02	1.88E+02	1.76E+02	6.01E+03	5.41E+03

Figures and captions

Fig. 1. Distribution of the training (blue) and test (red) concentrations of lactose, glucose, and Ca^{2+} used to train and test the Artificial Neural Network (ANN).

Fig. 2. Scheme of the ANN architecture used. The numbers surrounded by the red circles are the numbers of neurons used in each layer.

Fig. 3. Cyclic voltammetric characterisation of the enzyme modified electrodes used for the construction of the electronic tongue. CDH was entrapped under a dialysis membrane on mercaptohexanol modified gold electrodes. From top to bottom it is possible to see the behaviour of *Mt*CDH, *Ct*CDHC291Y and *Nc*CDH in a 50 mM MOPS buffer solution at pH 6.7 in the absence (solid line) and in the presence of 250 µM lactose (dashed line). All experiments were performed at a scan rate of 20 mV/s with a SCE reference electrode and a Pt flag as counter electrode.

Fig. 4. Calibration graphs of the *Mt*CDH, *Ct*CDHC291Y and *Nc*CDH based biosensors obtained for the three analytes lactose (top), glucose (middle) and Ca^{2+} (bottom). In the left column the fully investigated concentration ranges are shown, in the right column only the linear concentration ranges are shown.

Fig. 5. Comparison graphics of the "expected vs. predicted" concentrations for the target analytes; lactose, glucose, and Ca^{2+} calculated by the ANN using the external test set samples with known, expected concentrations.

Fig. S1. 3D representation of the sensor configuration used in the electronic tongue system (ET). On the left a side view, on the right a top view.

Fig. 1

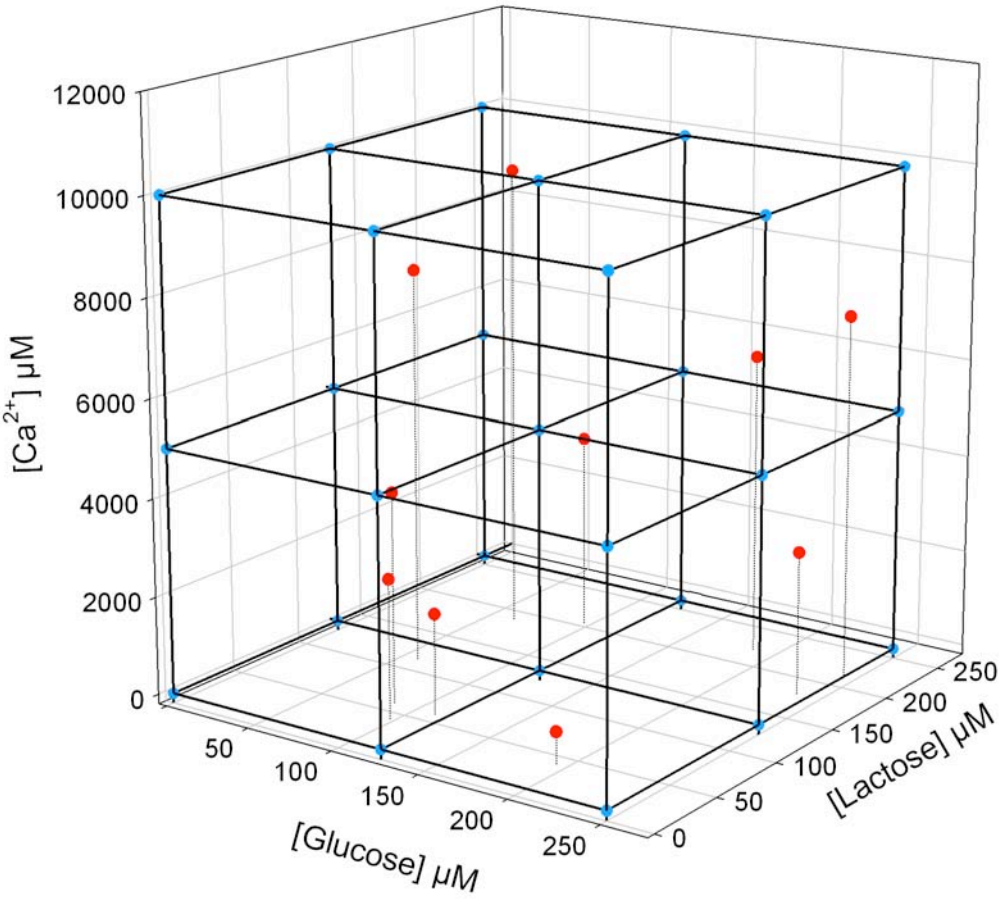
12000
10000
8000
6000
4000
2000
0
[Ca2+] µM
50
100
150
200
250
[Glucose] µM
0
50
100
150
200
250
[Lactose] µM

Fig. 2

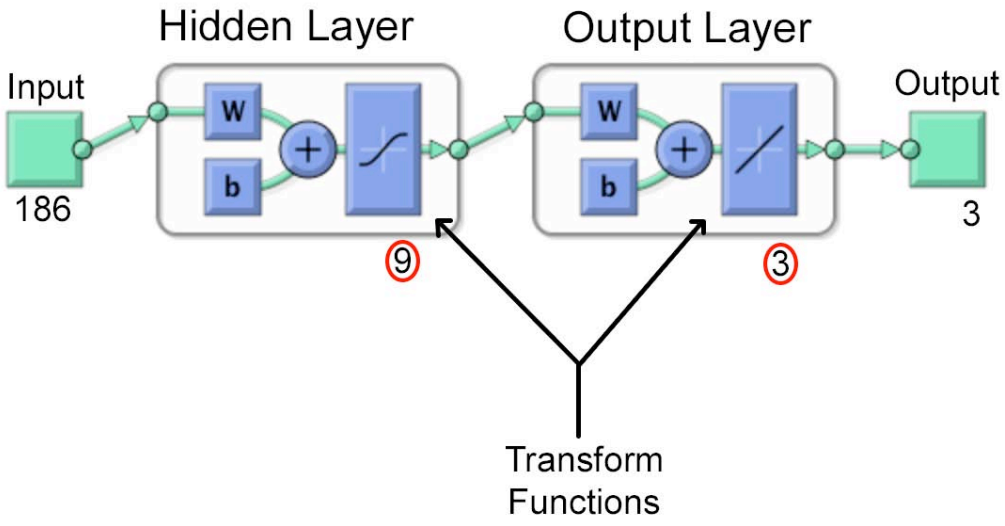
Hidden Layer
Output Layer
Input
186
W
b
9
W
b
3
Output
3
Transform
Functions

Fig. 3

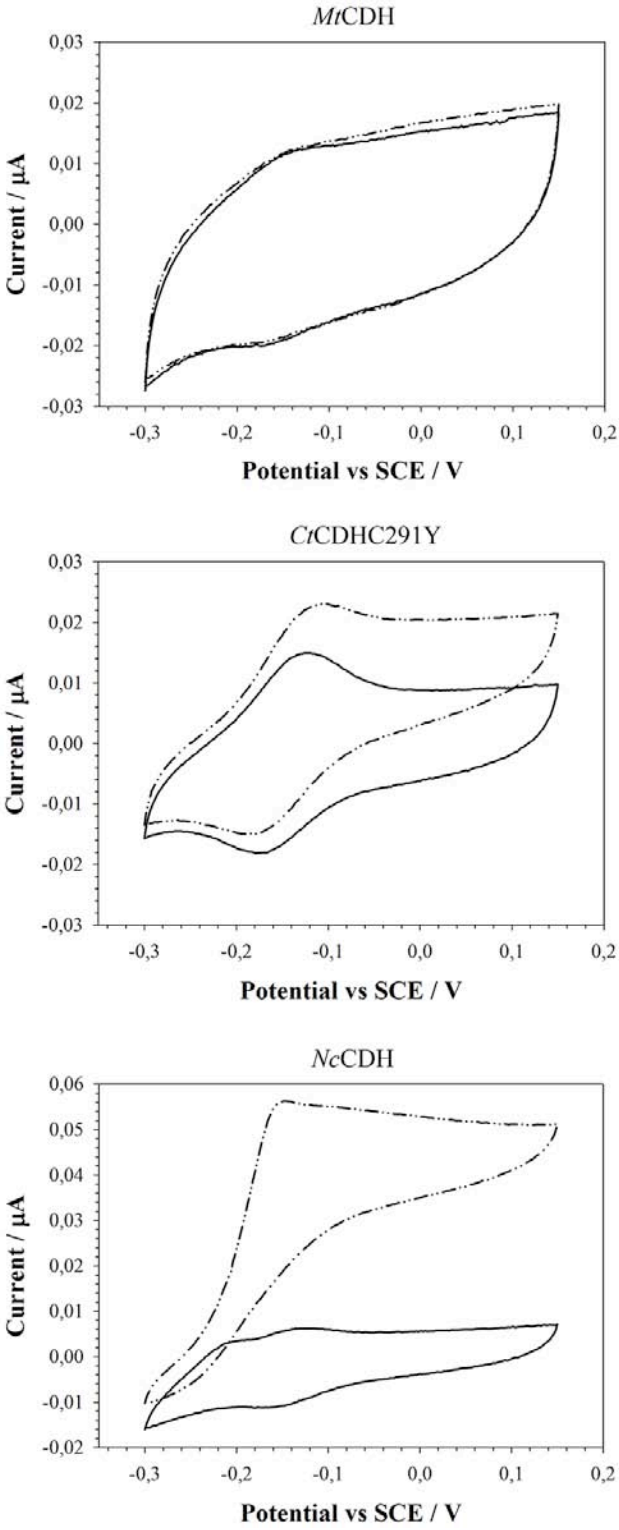
*Mt*CDH
Current / µA
Potential vs SCE / V
*Ct*CDHC291Y
Current / µA
Potential vs SCE / V
*Nc*CDH
Current / µA
Potential vs SCE / V

Fig. 4

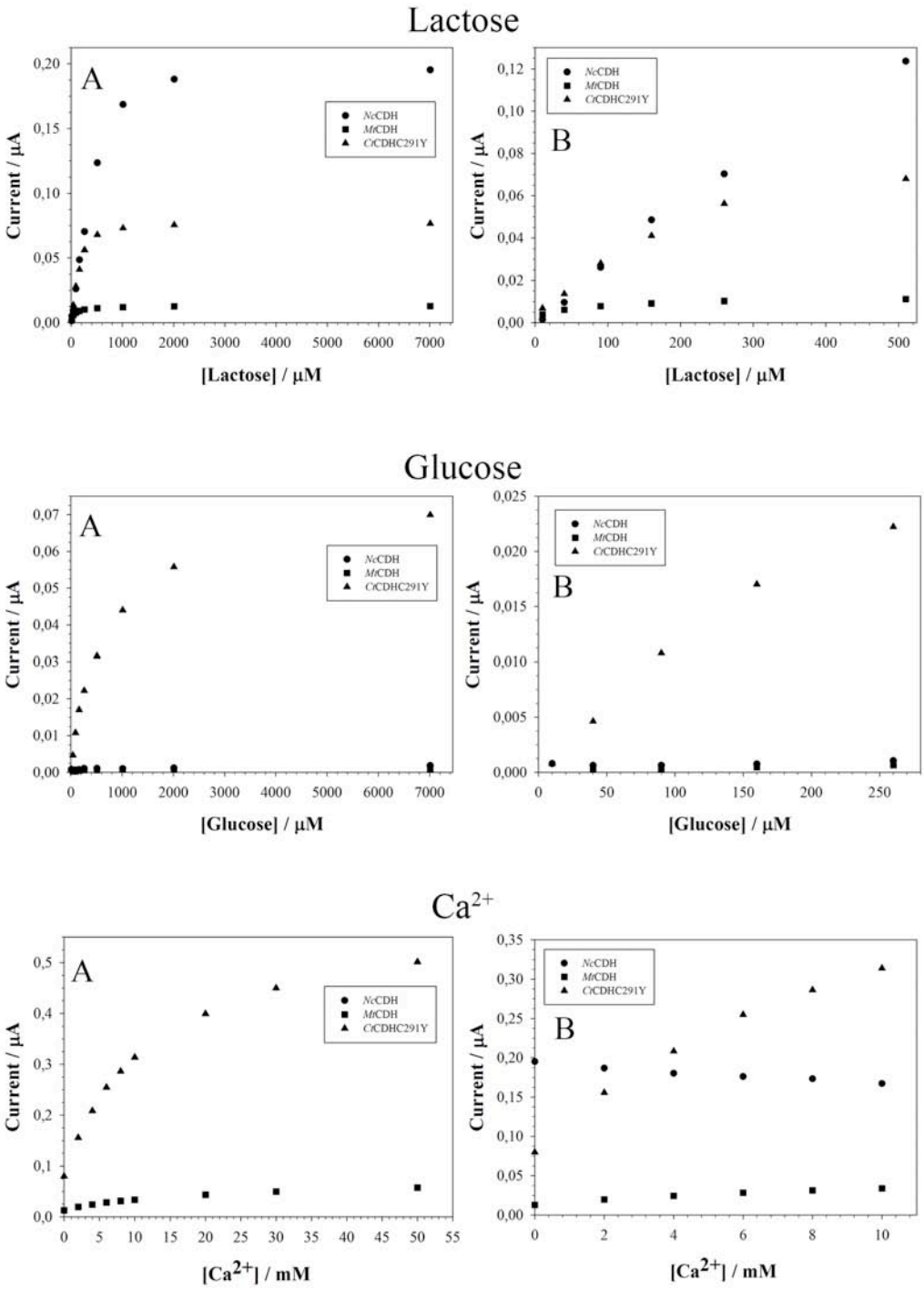
Lactose
A
B
NcCDH
MfCDH
CfCDHC291Y
Current / µA
[Lactose] / µM
Glucose
[Glucose] / µM
Ca2+
[Ca2+] / mM

Fig. 5

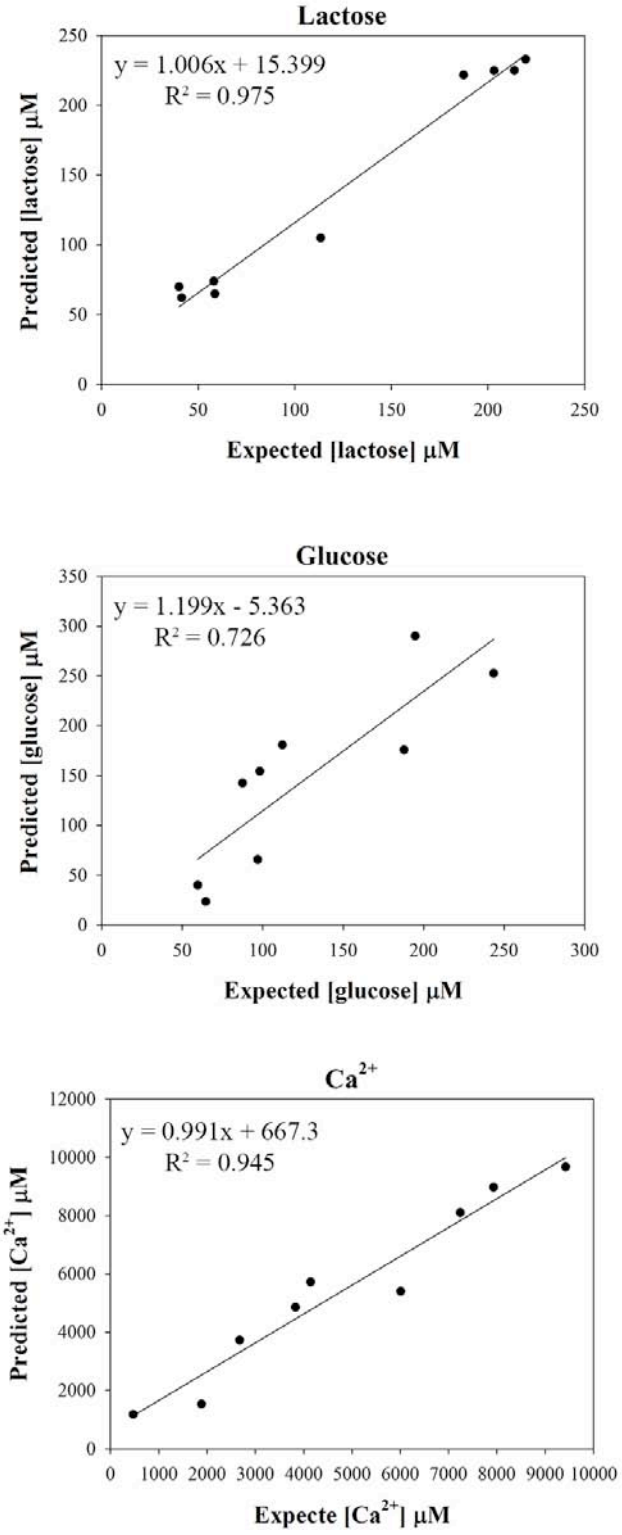
Lactose
y = 1.006x + 15.399
R² = 0.975
Predicted [lactose] µM
Expected [lactose] µM
0
50
100
150
200
250
Glucose
y = 1.199x - 5.363
R² = 0.726
Predicted [glucose] µM
Expected [glucose] µM
0
50
100
150
200
250
300
350
Ca2+
y = 0.991x + 667.3
R² = 0.945
Predicted [Ca2+] µM
Expecte [Ca2+] µM
0
2000
4000
6000
8000
10000
12000
1000
3000
5000
7000
9000

Fig. S1

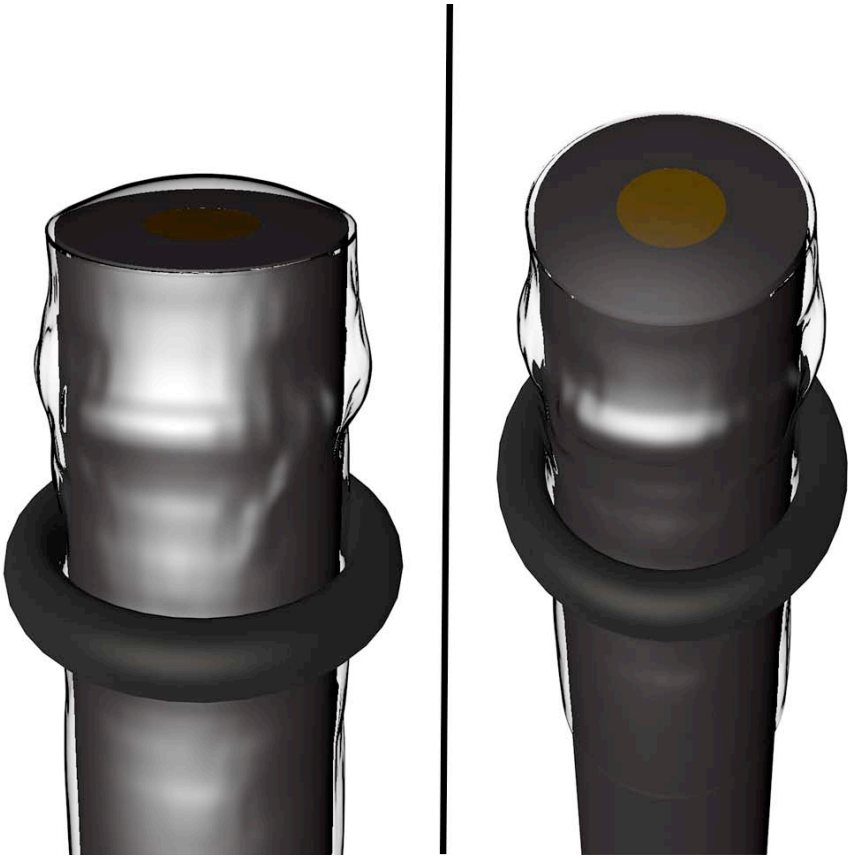

Aknowledgments

Well I am definitely not good at this, first because I don't like to write and second because sometimes I prefer to thank people practically with my help, support and/or being to their side then with only words, but anyway here I am.

Of course the first people I would like to thank are my family, mom and dad for their help and support in every way they could and my brother to have always been there for me.

Ferdia and Delfina, my "*family abroad*". You guys are my Irish brother and Portuguese sister now and always. We shared a lot of great moments having fun and also supporting each other since we all were in the same situation, away from our families and our comfort zone. This made our relationship stronger than a normal friendship, and it is the reason why I feel to call you both my brothers'… thank you guys.

Serena… what can I say… you have been of such a great support and you still are every day. Thank you for everything, all the fun and laughs, all the moments we had, all the times that we talked and you said some word in your dialect and after my puzzled face you just said "*isn't that Italian?*" I'm looking so very forward for the months to come.

My lab mates, Cristina, Andreu, Julio, Berta, Xavi, thank you very much for all the help when I came and for all the fun time that we had in the lab… including mojito's time… for making my time in Barcelona such a great experience… you are great.

The friends from my secondment in Sweden, Christopher that received and helped me with all the bureaucracy there and making me feel comfortable in the lab, of course Valentina, incredible lab mate there in Lund, always laughing, talking and having fun. The Italian group I met there, Daniele, Stefano, Marta, Valeria and so on, would be a very long list if I name all of them, such great time with barbecues and party nights.

My long time friends, Michele, Roberta, Marco, Anna, Roberto, Noemi, Letizia, Luca, Antonio, Gaetano, that make me feel like I never left every time I come back home, thank you for being like you are… great guys.

Of course there is no order or priority in this list, I just wrote it as everything was coming to my mind, and a last but not least "thank you" goes to all the people I met during this amazing experience that was my PhD, from the people of the Marie Curie network to the people during the Swedish secondment until the people here in Barcelona, at the university and around the city… thank you all.